

SCHOOL OF ENGINEERING AND ARCHITECTURE
INDUSTRIAL ENGINEERING DEPARTMENT
MASTER DEGREE COURSE IN MECHANICAL ENGINEERING

MASTER DEGREE THESIS

in

Modeling and Control of Internal Combustion Engines and Hybrid Propulsion Systems

**Optimization of a high performance engine GDI Wet System and
its control via virtual analysis and experimental tests**

CANDIDATE

Martina Bernardinello

ADVISOR

Nicolò Cavina, Full Professor

CO-ADVISORS

Davide Moro, Full Professor

Enrico Corti, Associate Professor

COMPANY ADVISORS

Klajdi Mustafaj, Eng.

Paolo Scarpato, Eng.

Academic year 2020/21

Session III

Dedicated to my parents

Index

- ABSTRACT 12**
- 1 14**
- Introduction 14**
- 2 16**
- GDI technology 16**
 - 2.1 Strengths and weaknesses 16**
 - 2.2 Main parameters 17**
 - 2.3 Injection 18**
- 3 22**
- Components..... 22**
 - 3.1 GDI high pressure pump 23**
- 4 26**
- GDI Wet System sizing..... 26**
 - 4.1 Goals..... 26**
 - 4.2 Activity description 26**
 - 4.3 Data analysis with MATLAB 32**
- 5 46**
- 1-D Modeling using GT-Power..... 46**
 - 5.1 GT – Power software 46**
 - 5.2 GT-ISE elements 51**
 - 5.3 Test plan..... 54**
 - 5.4 Goals..... 55**
 - 5.5 Conclusions 79**
- 6 80**

Control of the GDI pump in MIL environment.....	80
6.1 Model based design	80
6.2 MIL, SIL and HIL	81
6.3 Simulink software	82
6.4 Goals.....	82
6.5 Control algorithm	83
6.6 Modeling phase.....	83
6.7 Validation phase.....	91
6.8 Co-simulation phase in MIL environment.....	93
6.9 Conclusions.....	99
7.....	100
Conclusions.....	100
APPENDIX.....	102
BIBLIOGRAPHY.....	112
RINGRAZIAMENTI	114

Figure index

Figure 1 Bosh components (Source: Bosh GmbH).....	18
Figure 2 Injection system scheme	22
Figure 3 GDI high pressure pump	23
Figure 4 GDI pump operation	24
Figure 5 Engine map points	27
Figure 6 Rail Pressure Map	28
Figure 7 SOI Map	28
Figure 8 ET Map	29
Figure 9 Short pipe configuration	30
Figure 10 Long pipe configuration	31
Figure 11 Trigger wheel	33
Figure 12 Rail pressure corresponding to injector active phase	34
Figure 13 Speed regressive graphic - Short Pipe	36
Figure 14 Speed regressive graphic - Long Pipe	36
Figure 15 Rail pressure regressive graphic - Short Pipe	37
Figure 16 Rail pressure regressive graphic - Long Pipe	37
Figure 17 ET regressive graphic – Short Pipe	38
Figure 18 ET regressive graphic – Long Pipe	38
Figure 19 SOI regressive graphic – Short Pipe	39
Figure 20 SOI regressive graphic - Long Pipe	39
Figure 21 Volumetric flow regressive graphic – Short Pipe	40
Figure 22 Volumetric flow regressive graphic – Long Pipe	40
Figure 23 CoV graphic for Ref Rail + 20% – Ref Restr – Pipe Short configuration	42
Figure 24 CoV graphic for Ref Rail + 20% – Ref Restr – Pipe Long configuration	43
Figure 25 Rail pressure, piston displacement and injectors current at engine speed= 0.4, rl= 0.9, long pipe	44
Figure 26 Complete injection system in GT-ISE – Long pipe	51
Figure 27 Pressure waves at 1500 RPM – Short pipe	57
Figure 28 Pressure waves at 1500 RPM – Long pipe	57
Figure 29 Mass flow rate at 1500 RPM – Short pipe	58

Figure 30 Mass flow rate at 1500 RPM – Long pipe	58
Figure 31 Pressure waves at 2000 RPM – Short pipe	59
Figure 32 Pressure waves at 2000 RPM – Long pipe	59
Figure 33 Mass flow rate at 2000 RPM – Short pipe	60
Figure 34 Mass flow rate at 2000 RPM – Long pipe	60
Figure 35 Pressure waves at 2500 RPM – Short pipe	61
Figure 36 Pressure waves at 2500 RPM – Long pipe	61
Figure 37 Mass flow rate at 2500 RPM – Short pipe	62
Figure 38 Mass flow rate at 2500 RPM – Long pipe	62
Figure 39 Pressure waves at 3000 RPM – Short pipe	63
Figure 40 Pressure waves at 3000 RPM – Long pipe	63
Figure 41 Mass flow rate at 3000 RPM – Short pipe	64
Figure 42 Mass flow rate at 3000 RPM – Long pipe	64
Figure 43 Pressure waves at 4000 RPM – Short pipe	65
Figure 44 Pressure waves at 4000 RPM – Long pipe	65
Figure 45 Mass flow rate at 4000 RPM – Short pipe	66
Figure 46 Mass flow rate at 4000 RPM – Long pipe	66
Figure 47 Pressure waves at 5000 RPM – Short pipe	67
Figure 48 Pressure waves at 5000 RPM – Long pipe	67
Figure 49 Mass flow rate at 5000 RPM – Short pipe	68
Figure 50 Mass flow rate at 5000 RPM – Long pipe	68
Figure 51 Pressure waves at 6000 RPM – Short pipe	69
Figure 52 Pressure waves at 6000 RPM – Long pipe	69
Figure 53 Mass flow rate at 6000 RPM – Short pipe	70
Figure 54 Mass flow rate at 6000 RPM – Long pipe	70
Figure 55 Pressure waves at 7000 RPM – Short pipe	71
Figure 56 Pressure waves at 7000 RPM – Long pipe	71
Figure 57 Mass flow rate at 7000 RPM – Short pipe	72
Figure 58 Mass flow rate at 7000 RPM – Long pipe	72
Figure 59 Pressure waves at 8000 RPM – Short pipe	73
Figure 60 Pressure waves at 8000 RPM – Long pipe	73
Figure 61 Mass flow rate at 8000 RPM – Short pipe	74
Figure 62 Mass flow rate at 8000 RPM – Long pipe	74
Figure 63 Pressure waves at 9000 RPM – Short pipe	75

Figure 64 Pressure waves at 9000 RPM – Long pipe	75
Figure 65 Mass flow rate at 9000 RPM – Short pipe	76
Figure 66 Mass flow rate at 9000 RPM – Long pipe	76
Figure 67 Pressure waves at MAX SPEED RPM – Short pipe	77
Figure 68 Pressure waves at MAX SPEED RPM – Long pipe	77
Figure 69 Mass flow rate at MAX SPEED RPM – Short pipe	78
Figure 70 Mass flow rate at MAX SPEED RPM – Long pipe	78
Figure 71 MIL-SIL-HIL cycle	81
Figure 72 Scheme of the GDI pump control model	84
Figure 73 Fuel system scheme	85
Figure 74 Rail pressure target calculation	86
Figure 75 PI controller scheme	87
Figure 76 Pre – Control Injected Volume per stroke calculation	88
Figure 77 MSV actuator control	89
Figure 78 Fuel Rail Temperature Model	90
Figure 79 Angle before pump TDC at which there is inlet valve closure	92
Figure 80 Pre-control volume	92
Figure 81 Pump volume PI	93
Figure 82 RPM 1000	94
Figure 83 RPM 2000	94
Figure 84 RPM 3000	95
Figure 85 RPM 4000	95
Figure 86 RPM 5000	96
Figure 87 RPM 6000	96
Figure 88 RPM 7000	97
Figure 89 RPM 8000	97
Figure 90 RPM 9000	98
Figure 91 RPM MAX SPEED	98

Abbreviations

CCV= Cycle to Cycle Variation;

CoV= Coefficient of Variation;

Deg = Degrees;

ECU= Engine Control Unit;

FMV = Fuel Metering Valve;

GDI = Gasoline Direct Injection;

HIL= Hardware In the Loop;

HP= High Pressure;

MIL= Model In the Loop;

MSV= Metering Solenoid Valve;

SIL= Software In the Loop;

TDC = Top Dead Centre.

ABSTRACT

The presented work, carried on in collaboration with Automobili Lamborghini S.p.A. at NAIS S.r.l., is focused on the study of the injection system of a gasoline direct injection engine (GDI) designed at Automobili Lamborghini S.p.A.

GDI engines are considered to be one of the most effective system that car manufacturers can implement in order to meet stricter CO₂ production and pollutant emissions regulations. Furthermore, GDI engine is accounted to be the ideal thermal part of hybrid powertrains which will play an increasing significant role to meet future CO₂ and emissions standards. Therefore, in the last years significant research efforts are being applied to the development of GDI technology to optimize its performance in terms of specific fuel consumption and emission control capabilities.

These engines require an extremely reliable high pressure fuel injection system, allowing advanced combustion strategies and improving the fuel atomization process together with the air–fuel mixing.

However, in these installations intense fuel pressure oscillations may occur due to continuous pumping and injection events, possibly causing low precision in the fuel metering from cylinder to cylinder and relatively poor spray quality. For this reason the injection system design must be supported by accurate computational models able to predict the actual injector flow and the whole fuel system behaviour.

This thesis describes a combined 1-D numerical and experimental analysis of a complete GDI injection system.

The aim is to design the GDI injection system in order to have the minimum injection variability between injectors. This is possible analysing the rail pressure waves that affect the injections.

Thanks to a numerical code created on MATLAB the results coming from a first calibration attempt were compared with experimental data, mainly engine speed, rail pressure, SOI, ET and volumetric flow to verify the reliability of the acquired results. They were calculated after specific tests made on the hydraulic test bench (named Wet-System) developed at Automobili Lamborghini S.p.A., which consists of a high pressure pump, pipes, a fuel rail and injectors so to simulate the complete injection system operation. Different configurations were studied changing the system geometry, such as rail internal diameter, high pressure pipe length, high

pressure pipe inlet position inside the rail and flow-restrictor diameter at the end of high pressure pipe. Eight different configurations were analysed and the one that showed the lowest CoV of injection was proposed as a final design, i.e. minimum injection variability.

Then a 1-D numerical analysis of the GDI injection system was developed on the chosen configuration with the aim of predicting pressure waves propagation phenomena and the injected mass flow rate.

The focus of the 1-D analysis is to verify through the comparison between simulated values and experimental ones if the model predicts accurately the physics of the system, in order to use it on a wider range of operating points. For example not-tested points or new configurations can be studied.

Once the configuration was selected, the following step consisted in controlling the GDI pump in MIL environment through a co-simulation between high pressure system model built in GT-ISE and control model made with the software Simulink. The high pressure control model was developed and validated. The aim was to have a closed loop control of the rail pressure using the same ECU control strategy. The main task of the control is to actuate the angle, respect to pump top dead centre, the MSV valve had to be closed in order to make the actual pressure follow the target one. The control model and the simulation in MIL environment are very useful since they help on the pre-calibration of ECU functions, reducing drastically testing activities.

1

Introduction

The demand for a drastic reduction of the specific CO₂ production posed by legislation drives the current scenario for the automotive powertrain development along with the decreasing trend for the allowed pollutant emission levels.

In this scenario, the shift from the homogeneous charge, in-direct injection scheme, to the stratified charge, direct injection combustion system, is the most effective way to improve spark ignition engine thermal efficiency. Hence, GDI engines are considerably increasing their market share, often in combination with turbo-charging of small and medium displacement units, in order to exploit the potential of such shaped engines to improve thermal efficiency in fundamental operating conditions such as low load and cold start.

The quick development of direct injection in spark ignition engines implies a higher importance of the injection system performances in terms of combustion and emissions control. In fact, along with the theoretical advantages, the development of stratified charge in direct injection systems implies a number of issues that must be faced. The fuel metering accuracy, the rate of fuel introduction in the combustion chamber and the consequent spray evolution, fuel atomization and mixing with surrounding air directly control the combustion development. Hence, the injection system, in a wide range of operating conditions, directly affects engine performance and efficiency, pollutant emissions and noise. As a consequence, a deep knowledge of the actual injection rate is crucial for designing new generation injection systems,

particularly in the operating conditions in which advanced injection strategies are to be applied to govern the combustion process.

A typical direct injection system consists of a low pressure pump feeding a cam-actuated high pressure pump, a pipe connecting the pump to the rail and the injectors delivering the fuel in the combustion chamber. In the aim of increasing the injection system metering accuracy, the stand-alone injector analysis maybe not adequate. In fact, the injector performances are affected by many boundary parameters, such as pressure time-history upstream the injector, backpressure, fluid and injector nozzle temperature. In particular, the upstream pressure time-history is largely influenced by the injection system layout and by its actuation frequency. As well known, fast opening and closing of injectors and alternate motion of the high pressure pump piston produce considerable pressure oscillations in the fuel system, possibly resulting in an injector behaviour in terms of fuel metering and injection rate profiles that can be significantly different from what is predicted by a stand-alone injector characterization. Further, pressure fluctuations can cause noise and the damaging of some components. Hence, the ability in evaluating, numerically and experimentally, the actual operating conditions for the entire injection system is crucial to obtain robust results. The Wet System approach is commonly used in order to replicate, in a research test bench, the overall injection system and to control its working parameters. At Automobili Lamborghini S.p.A a GDI Wet System test bench was set-up for the analysis of the complete GDI system and to support the development of numerical tools for the computational analysis. This thesis describes a combined 1-D numerical and experimental approach aimed at sizing and optimizing the GDI Wet System. Further, the validation of the physical model built in GT-ISE and the control of the GDI pump through a co-simulation GT-Power – Simulink in MIL environment in order to pre-calibrate in simulation.

2

GDI technology

2.1 Strengths and weaknesses

Engines with an indirect injection work with pre-mixed combustion: it occurs a mixture with a title that is always near the stoichiometric to guarantee the ignition. In-direct injection engines, unlike what said before, is aspirated only air, injecting fuel directly inside the cylinder.

The possibility of injecting in the combustion chamber allows, in theory, to stratify the mixture (injecting in the compression phase at partial loads) in order to be able to delate pumping losses. Having the injector directly inside the combustion chamber, it can be created a stoichiometric mixture only under the candle, guarantying the ignition, but also to operate overall with lean mixture to limit consumptions and emissions (there are reduced pumping losses and heat exchange though the wall).

Unfortunately, today this technology is not wide spread due to the post-treatment problem, which is linked to some exhaust gas components released when the engine works in the stratified way.

The attention is paid in particular over NO_x (nitrous oxides), that the trivalent catalyst is not able to break down in environment with the presence of oxygen (lean mixtures).

At last, three mixture preparation strategies can be used:

- stratified charge;

- homogeneous charge;
- mix made of homogeneous and stratified charge.

The first one is optimal in consumptions and emissions, the second in performances.

2.2 Main parameters

Engine speed : physical quantity that measures the revolutions per minute in rpm.

Rail pressure : pressure, measured in Bar, inside the rail (chamber that connects injectors to the pump through the HP pipe).

SOI : start of injection, measured in angular terms, consists in the beginning of injection with respect to cylinder TDC.

EOI : end of injection, measured in angular terms, consists in the end of injection with respect to cylinder TDC.

ET : energizing time, measured in ms, is the injection time calculated as the difference between SOI and EOI.

Volumetric flow : quantity of fluid that passes through the injectors in one second, measured in m^3/s .

2.3 Injection

2.3.1 Injector position



Figure 1 Bosh components (Source: Bosh GmbH)

1) NARROW SPACING (Close to spark)

Injector located in central position.

Advantages:

- larger spray pattern options;
- lowest counter-interaction with intake tumble flow;
- better CAT-Heating conditions (CoV reduction).

Disadvantages:

- spark is moved closer to intake side determining less homogeneous condition at ignition time in the cylinder;

- larger thermo-mechanical stresses since many components (injectors, valves and spark) are installed very close to each other.

2) WIDE SPACING (Far from spark)

2.1 Injector is located at **intake side** because of lower thermal loads than in the case of installation at exhaust side.

Advantages:

- easier installation and lower thermal mechanical loads;
- spark can be installed in central position determining well homogeneous condition at ignition time in the cylinder.

Disadvantages:

- reduced spray pattern option (just 180° are available and valve interference must be also considered);
- spray momentum counter acts tumble momentum;
- worse CoV during CAT-Heating.

2) WIDE SPACING (Far from spark)

2.2 Injector located at **exhaust side** cannot be installed in series engine because of the too large thermal load that might cause deposit formation and mechanical failure.

Advantages:

- easier installation;
- spark can be installed in central position determining well homogeneous condition at ignition time;
- large spray pattern options since there are almost no interference with intake valve opening;
- spray momentum promotes tumble momentum.

Disadvantages:

- high thermal loads (deposits, mechanical failure).

2.3.2 Air-fuel mixing mechanism - Fuel metering

There are three air-fuel mixing mechanisms.

Spray-Guided:

The spray momentum drives the fuel liquid and the vapor distribution: spray pattern and injection pressure will determine the mixture formation.

This condition occurs in actual engines at partial load and CAT-Heating operations where air momentum and boost pressure (in-cylinder density) are lower.

Wall-Guided:

The spray momentum together with piston bowl shapes drives the fuel liquid and the vapor distribution. Spray pattern, piston shape, injection pressure and timing will determine the mixture formation.

This condition occurs when mixture stratification is searched.

Air-Guided:

The air (Tumble mainly or Swirl) momentum drives the fuel liquid and the vapor distribution determining the mixture formation. Spray pattern and injection pressure play a lower role.

This condition occurs in actual engines at full load when air flow momentum and in-cylinder density are very high.

2.3.3 Targeting

Targeting means defining the number of holes, their directions and their own mass flow rate in order to achieve, together with air interaction, a proper air-fuel mixing in order to:

- avoid or reduce spray liquid wall impact;
- avoid rich mixture pockets;

- achieve the target homogeneous (stratified) mixture;
- reduce the engine CCV resulting low CoV;
- promote CAT-Heating (low CoV);
- avoid nozzle tip diffusion flames.

2.3.4 Spray pattern

Spray pattern should be optimized in spray/wall guided operation in CAT-Heating point and at low load/engine speed (lower in-cylinder density, slower air flow).

At full load and especially at target power the air-fuel mixing is air guided. Thus, spray pattern is less effective, unless specific injector optimizations are made.

Tumble flow helps in mixing the fuel with air homogeneously keeping low the CoV.

2.3.5 Injection strategy

Single pulse

General considerations on SOI:

- larger advance promotes a more homogeneous mixing and a larger amount of the liquid fuel will impact the piston.

General consideration on EOI:

- 580/590 c.a. deg. after TDC are taken as a reference at full load / power to avoid poor air-fuel mixing.

3

Components

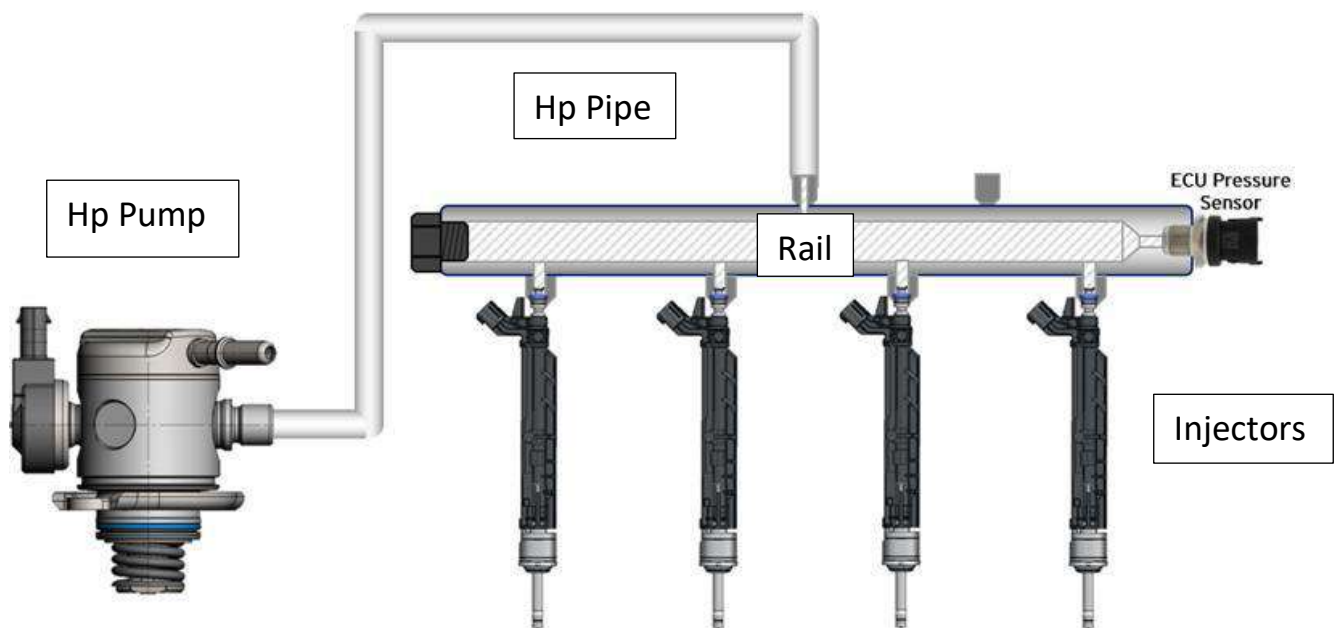


Figure 2 Injection system scheme

Figure 2 represents the injection system scheme. It consists of four main components: a high pressure pump (on the left), a high pressure pipe, a fuel rail and some injectors.

GDI pump components and operation phases are explained in detail below.

3.1 GDI high pressure pump

GDI pump consists of the following assembly groups: Flow control valve (MSV), inlet valve, outlet valve, piston and seal, pressure relief valve, pressure damper, fuel filter as well as hydraulic, mechanical and electrical interfaces.

The MSV actuator group is controlled by electrical activation of the solenoid by the ECU so that the flow volume can be regulated between zero and maximum delivery within the specified ranges of speed and system pressure. This is achieved by regulating the start point of the MSV control signal (MSV delivery angle). The MSV actuation closes the inlet valve, then the fuel in the delivery chamber is compressed by the piston lift and the fuel is finally delivered to the high pressure circuit as the outlet valve is opened by pressure difference.

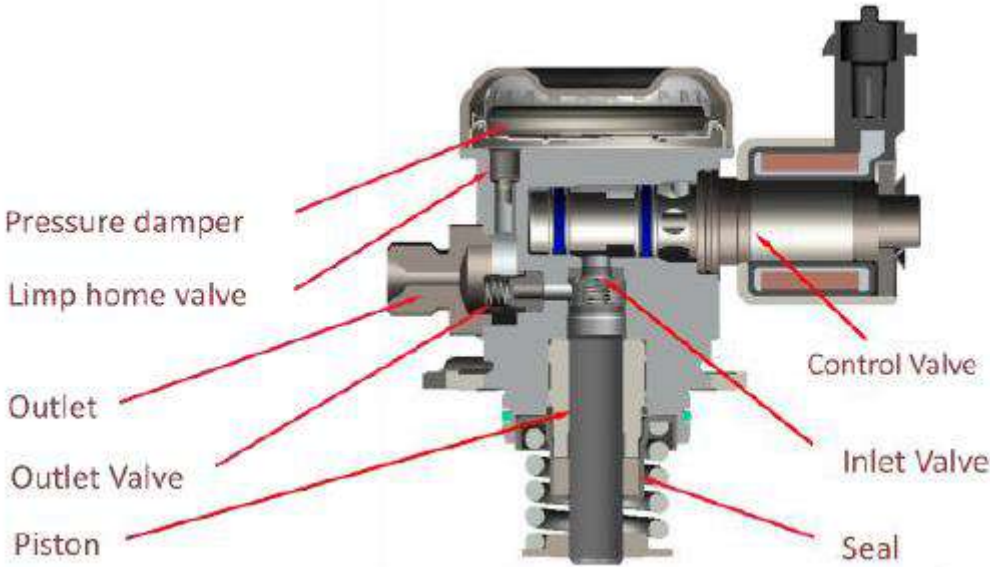


Figure 3 GDI high pressure pump

GDI pump operation can be described in 4 phases:

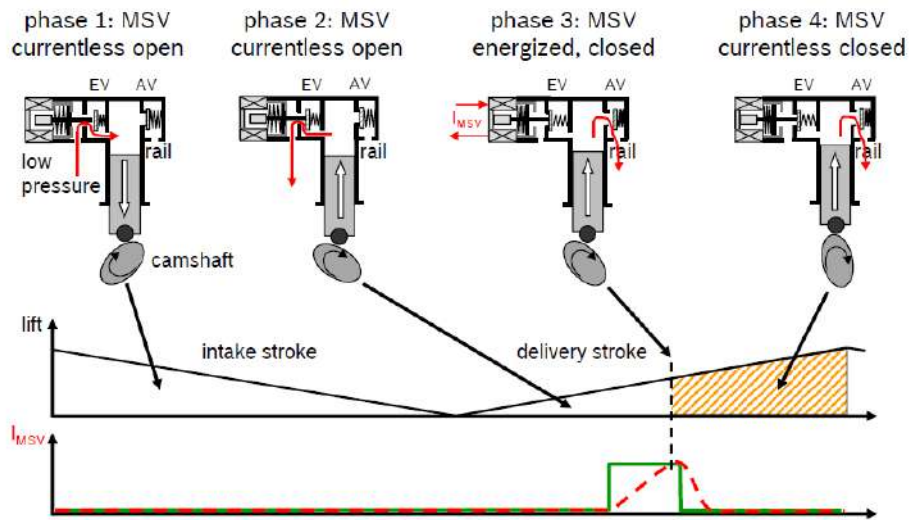


Figure 4 GDI pump operation

Phase 1 : suction phase (expansion of the chamber volume as the lift is decreasing), with the MSV open the fuel is flowing into the pump chamber.

Phase 2 : compression phase (lift is increasing), according to the fuel demand the MSV is not closed yet, therefore fuel is flowing back to the low pressure line.

Phase 3 : pressure generation inside the pump chamber as the MSV is closed by the ECU.

Phase 4 : fuel is delivered into the rail as soon as the outlet valve opens by the pressure difference between the pump chamber and the rail line (pumping phase).

Once the piston reaches its TDC, the expansion phase starts again and the MSV valve opens by the pressure difference between chamber pressure and low pressure line.

4

GDI Wet System sizing

4.1 Goals

The aim of a GDI Wet System sizing is in general to minimize the variation of the injected quantity of fuel between injectors. In order to do this, pressure pulsations inside the rail have to be optimized because the injected quantity is directly linked to rail instantaneous pressure in the moment the injection is made by injector. To fulfill this scope, a Wet system equivalent to the one of the engine was set up in Automobili Lamborghini S.p.A. and the instantaneous pressure inside the rail was analysed using fast pressure sensors. The final purpose of this thesis is to achieve reliable instantaneous pressure values with which it is possible to estimate the injection variation between injectors.

Another target is to avoid resonance making a frequency analysis but this is not the thesis aim.

4.2 Activity description

GDI System sizing activity consists in simulation and testing activities, analysing different configurations in order to minimize the injector CoV and as a consequence the pressure pulsations inside the rail. The rail pressure pulsations occur under stationary conditions: speed, rail target pressure, injection time, SOI and ET are constant. Engine map is composed by all the needed data for the engine operation. The mapping is divided into tables, each one containing

the information of all the sensors and electrical devices connected to it. Tables are stored inside the ECU. Each point of the engine map is obtained combining different values of speed and load. All these points are to be spread over the entire engine operation range. *Figure 5* represents a scatter plot in function of engine speed (x-axis) and normalized rl, i.e. load (y-axis). The 54 blue dots are the engine map points tested. In *Figure 6, 7, 8* are represented the contour plots of rail pressure map, SOI map and ET map obtained from a first pre-calibration. Pre-calibration has been taken from simulations and from experience gained from other Automobili Lamborghini S.p.A. engines. To each engine speed and load combination corresponds an exact value of rail pressure, SOI and ET.

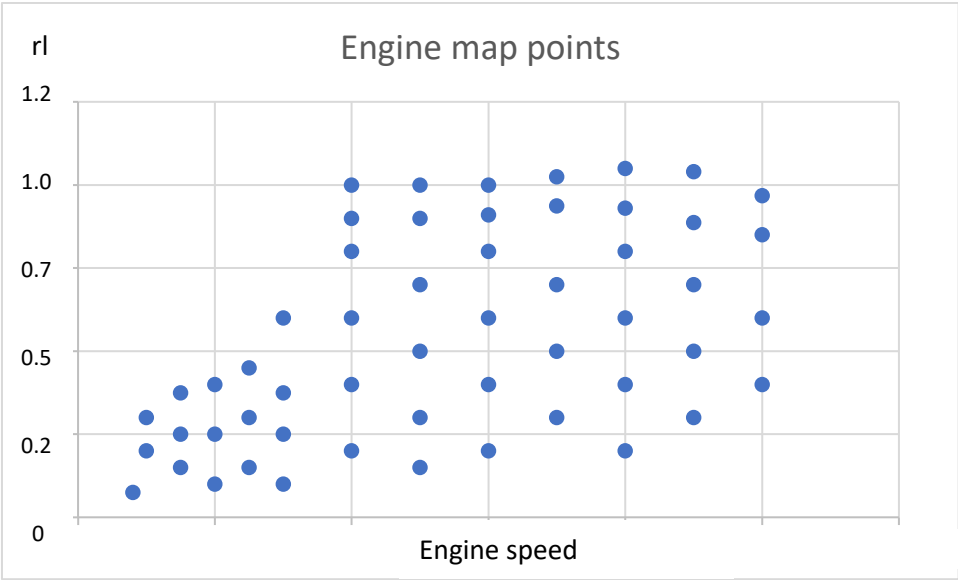


Figure 5 Engine map points

Rail Pressure Map (bar)

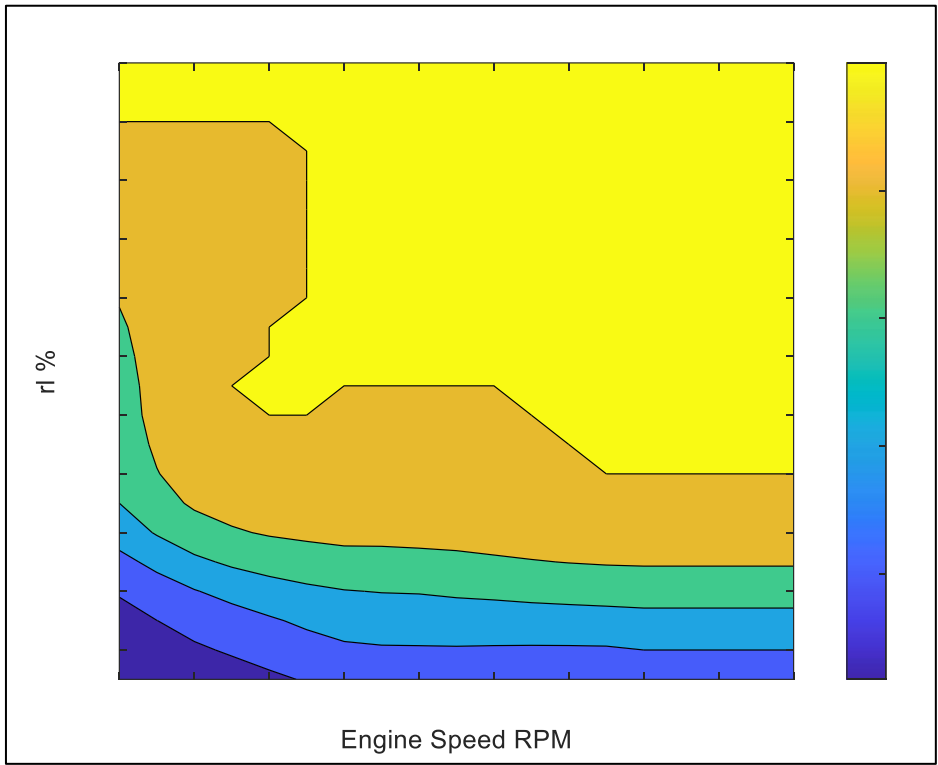


Figure 6 Rail Pressure Map

SOI Map (Crank Angle bTDCf)

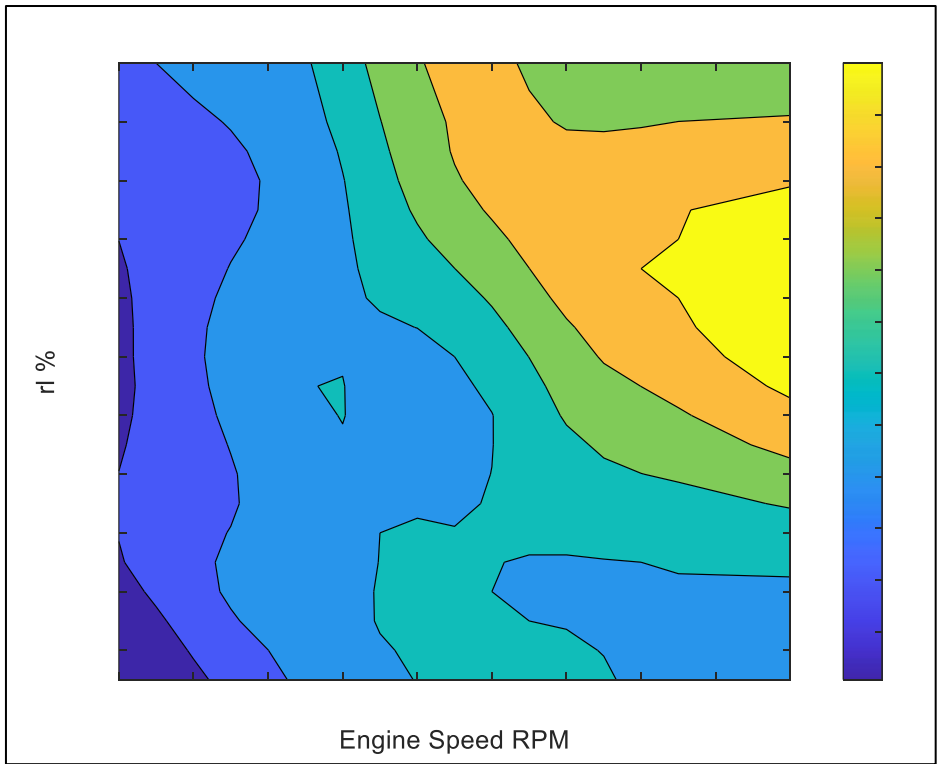


Figure 7 SOI Map

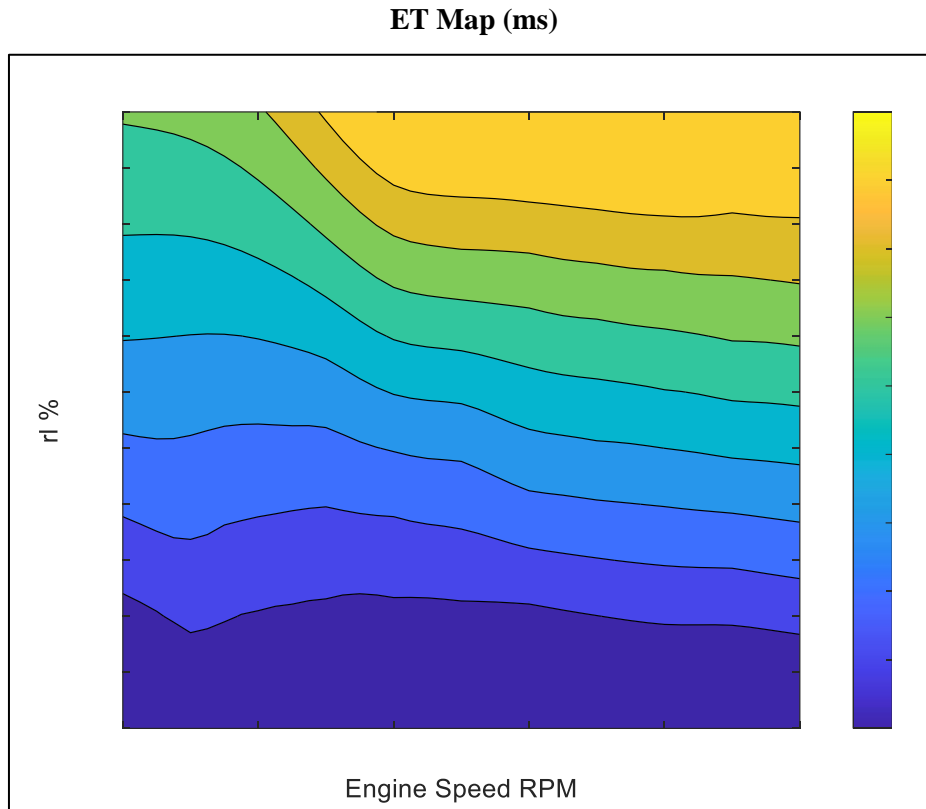


Figure 8 ET Map

4.2.1 Design parameters

During the design phase, three parameters have been evaluated:

- Rail gallery diameter determines the total rail volume. A larger volume is better for having a low injection-injection variability, but it generates a high inertia for pressure build-up in cranking and transients.
- Inlet orifice dimension determines the pressure drop between pump outlet and rail during pumping phase. A smaller diameter would damp the pulsation inside the rail during the pumping phase, but it limits the fuel flow and increases the pressure at pump outlet, which could damage the pump or fuel line. A larger diameter would increase the amplitude of pressure waves and can also lead to unwanted resonances.
- Rail inlet position: if placed in the middle of the rail it would guarantee a better distribution of the flow towards the injectors, but the fuel line will be longer, which can affect wave dynamics and packaging. A shorter pipe reduces the wave transfer time from the pump to the rail.

Two different configurations of rail inlet position were studied.

Short pipe

In this configuration the pipe inlet is located on the side of the rail.

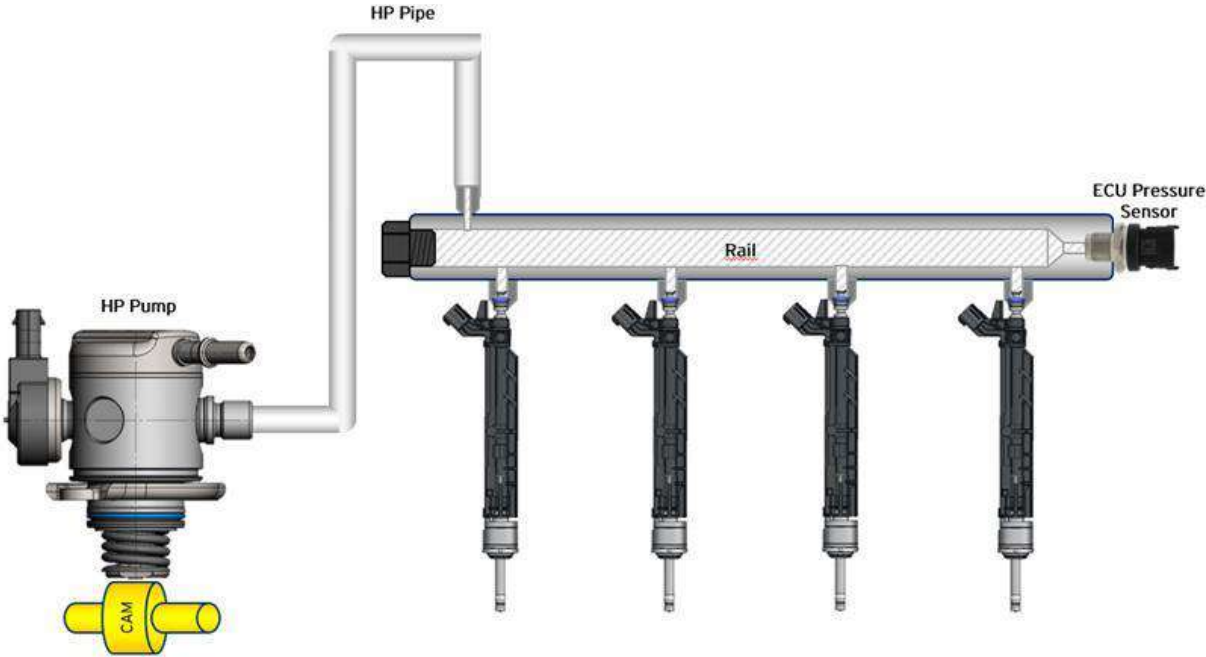


Figure 9 Short pipe configuration

Long pipe

In this configuration the pipe inlet location is at the center of the rail.

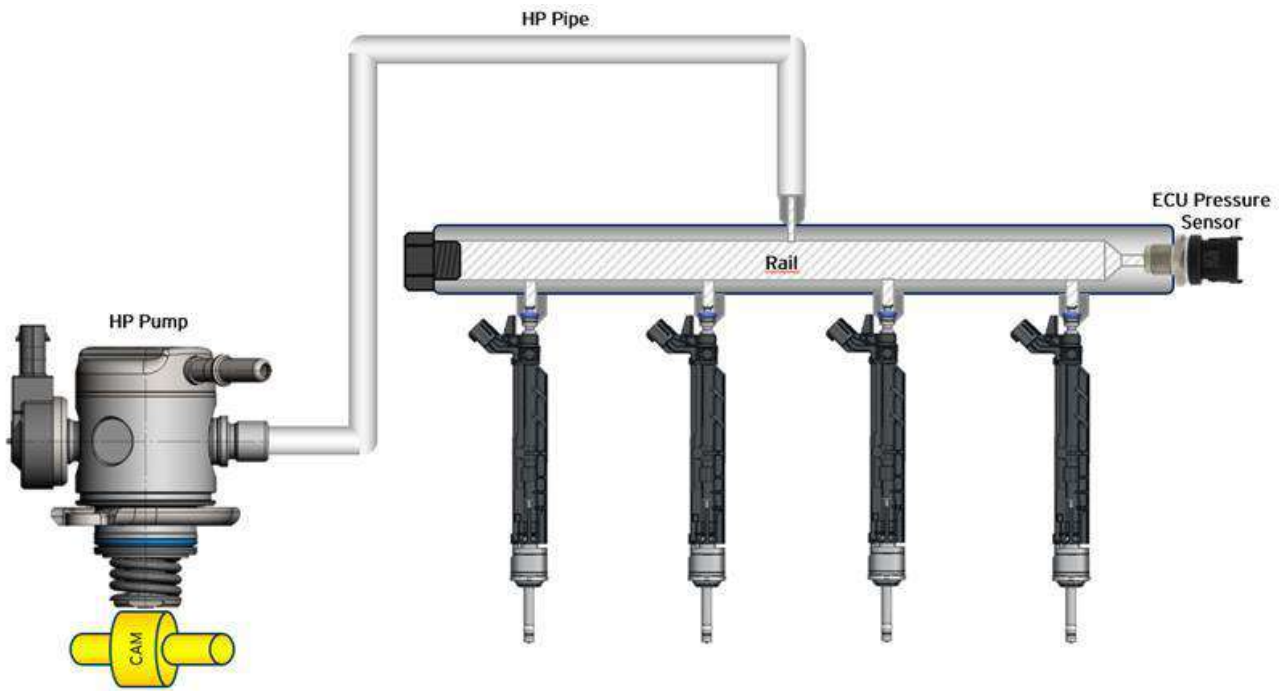


Figure 10 Long pipe configuration

4.2.2 Configurations

Eight configurations have been tested:

- reference rail diameter, reference inlet orifice dimension, short pipe;
- reference rail diameter, reference inlet orifice dimension, long pipe;
- reference diameter, reference inlet orifice dimension plus 15%, short pipe ;
- reference diameter, reference inlet orifice dimension plus 15%, long pipe ;
- reference diameter plus 20%, reference inlet orifice dimension, short pipe ;
- reference diameter plus 20%, reference inlet orifice dimension, long pipe ;
- reference diameter plus 20%, reference inlet orifice dimension plus 15%, short pipe ;
- reference diameter plus 20%, reference inlet orifice dimension plus 15%, long pipe.

All 54 points have been performed for each of the 8 different configurations.

4.3 Data analysis with MATLAB

4.3.1 MATLAB software

MATLAB (an abbreviation of "MATrix LABoratory") is a proprietary multi-paradigm programming language and numeric computing environment developed by MathWorks. MATLAB allows matrix manipulations, plotting of functions and data, implementation of algorithms, creation of user interfaces, and interfacing with programs written in other languages.

4.3.2 Goals

In this work Matlab was used in order to create two scripts (reported in appendix) with two different aims.

The first one was made in order to verify that the tested points, experimental values acquired at the test bench, were consistent with the values coming from the first calibration attempt. This was done to make sure that the tests were performed correctly.

The second one, once verified that experimental data are consistent with referring tests, has the scope to estimate the injection variation between injectors. In this thesis CoV has been chosen to estimate this parameter.

4.3.3 Injection issues and CoV

The peculiarity of this engine is that there is a non-synchronous behaviour between the pump shaft and the engine crankshaft.

For this reason there is an offset between the pump TDC and the cylinder TDC.

Therefore, the pump TDCs cannot be determined in an univocal way just basing on the Cylinder TDC. A dedicated position sensor is used in order to find the pump position.

Pump Camshaft

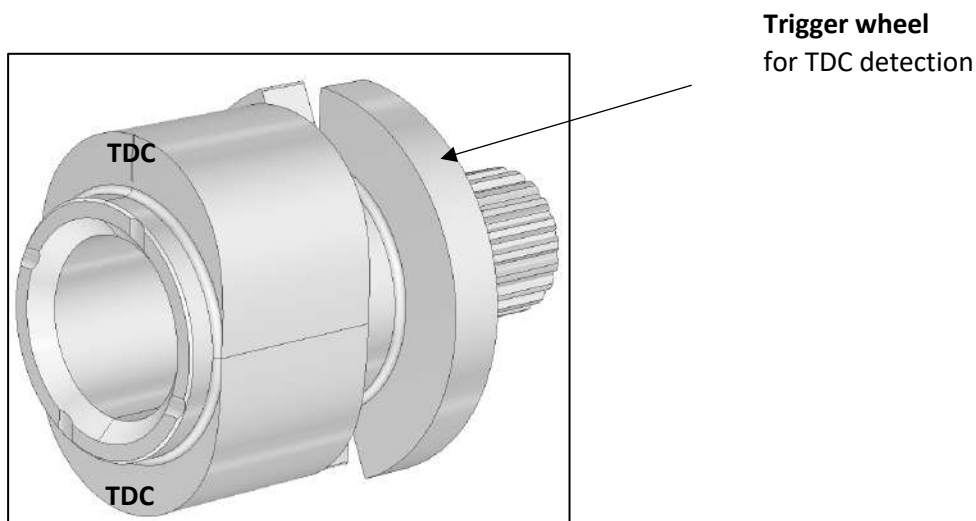


Figure 11 Trigger wheel

As a direct consequence, the injections could not be phased with the pump lift phases, generating pressure pulsations inside the rail. The injections thus will happen at different instantaneous pressures. Furthermore not only the injection pressures will be different basing on the considered cylinder, but also the same cylinder will have this problem during consequent engine cycles.

The injection duration defines the amount of fuel injected for each injection pulse.

The amount of fuel provided when the injector is open is a specific injector characteristic and it is proportional to the injection pressure.

In standard condition the delivered quantity measured at an injection pressure of 100 bar (P_{test}) is defined as “Qstat” (volumetric flow in cm^3/s).

If the aim is to estimate the amount of flow at different injection pressures, the following formula can be used:

$$\text{Flow rate} = \sqrt{\frac{P_{\text{actual}}}{P_{\text{test}}}} * Q_{\text{stat}}$$

The fuel injected for each pulsation can be calculated as:

$$q_{inj} = ET * \text{Flow rate}$$

In *Figure 12* two plots are represented: the upper one shows rail pressure wave and the bottom one injection current both in angle domain.

When the injector current is higher than zero, the considered injector is open and the injection is happening. Rail pressure is selected for each of the active phases of the injectors that correspond to the intervals delimited by the coloured lines. Hence, the calculations of the flow rate and the fuel injected for each pulsation.

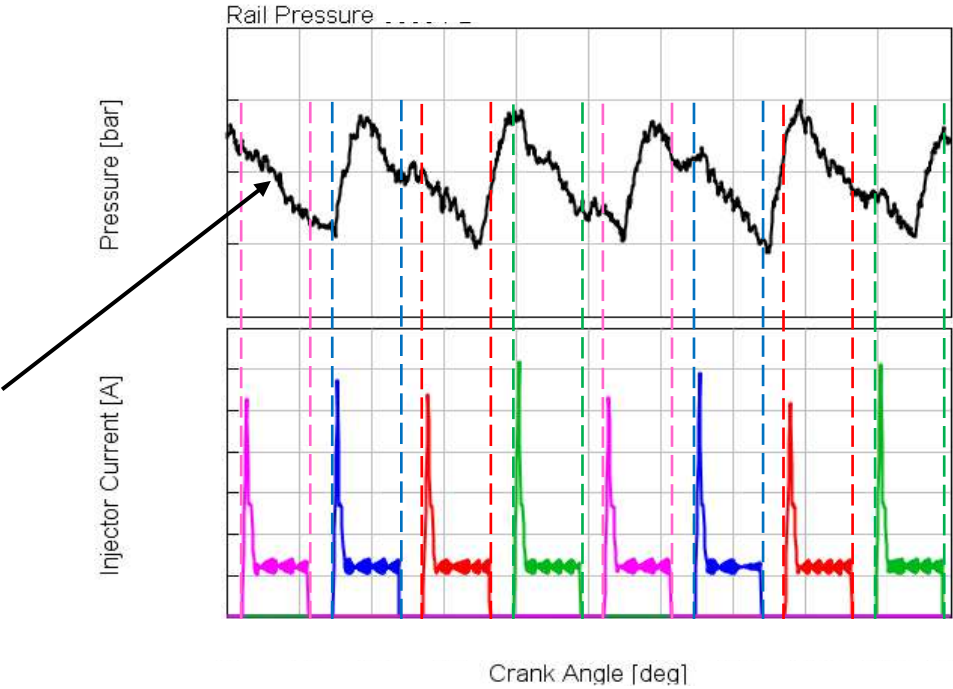


Figure 12 Rail pressure corresponding to injector active phase

The rail pressure has a direct impact on the injection. The instantaneous pressure on the injector during the injection phase will add variability to the injected mass. It is possible to estimate this variability between the injections of each injector for the minimum number of engine revolutions in which there will be repeatability of the trend.

The CoV (coefficient of variation) is used in percentage through this formula:

$$CoV [\%] = \frac{\text{Standard deviation } (\sigma)}{\text{Average } (\bar{x})} * 100$$

$$\sigma = \frac{\sum(x - \bar{x})^2}{n}$$

The best configuration will be the one with the smallest CoV, i.e. the less injection variability.

4.3.4 MATLAB regressive plots

The first objective, mentioned in section 4.3.2, is completed thanks to regressive graphics. More the experimental values are similar to the ones given by a first pre-calibration much the curve trend fits the first-third bisector.

Out trend values are not to be considered because they don't reflect indicated data.

Speed, rail pressure, ET, SOI and volumetric flow are shown for the configurations with reference diameter plus 20%, reference inlet orifice dimension and short/long pipe.

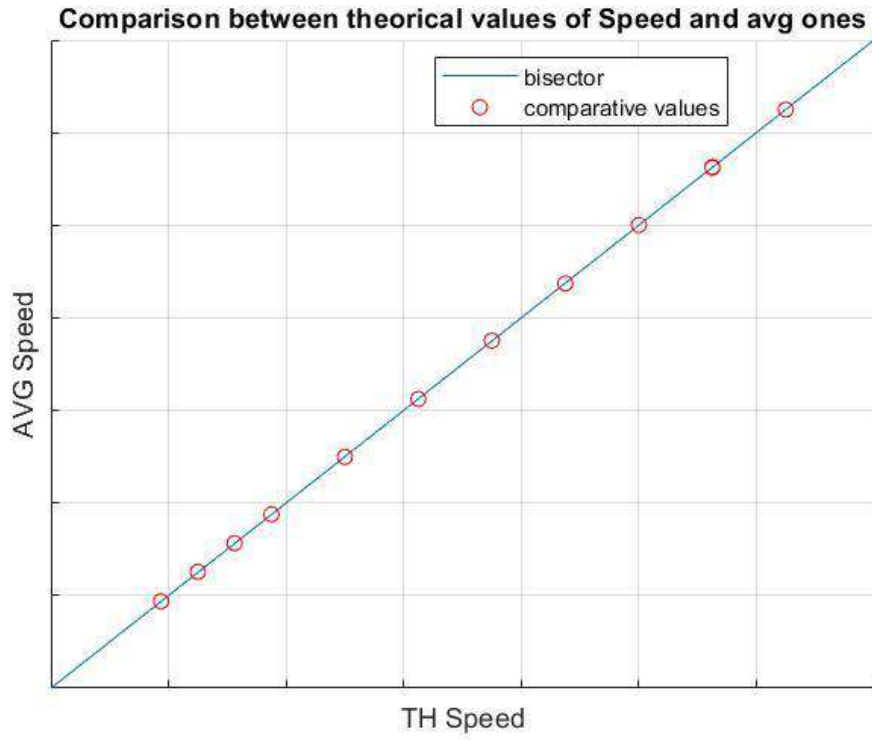


Figure 13 Speed regressive graphic - Short Pipe

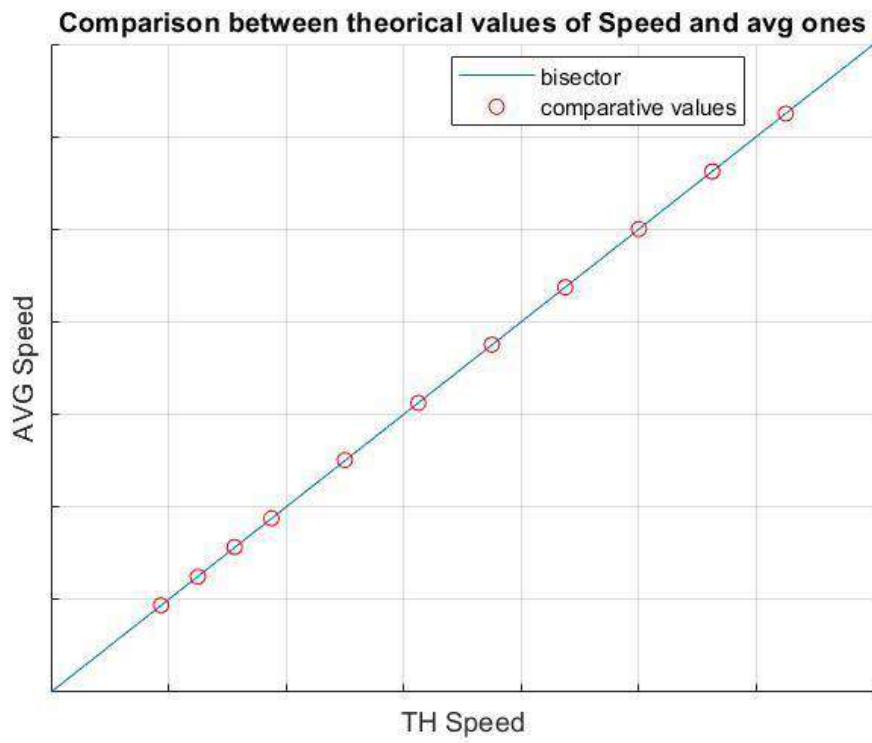


Figure 14 Speed regressive graphic - Long Pipe

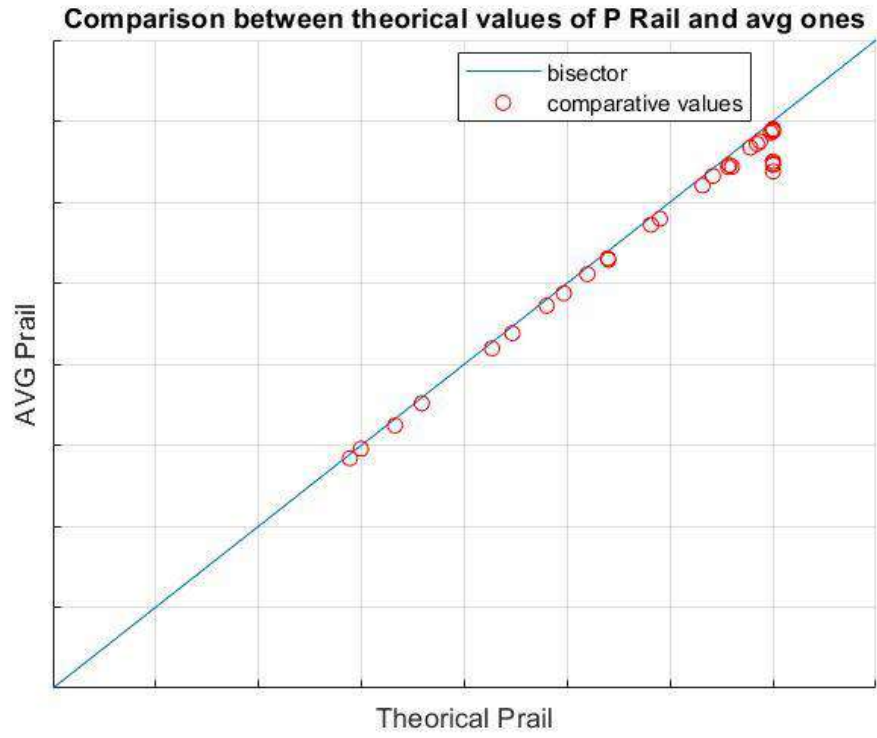


Figure 15 Rail pressure regressive graphic - Short Pipe

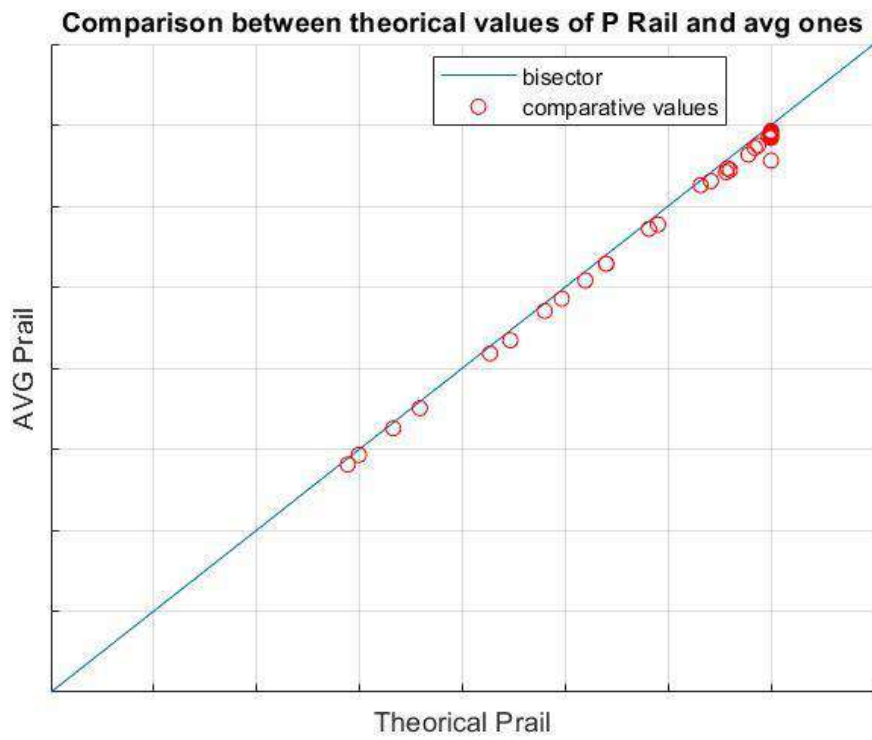


Figure 16 Rail pressure regressive graphic - Long Pipe

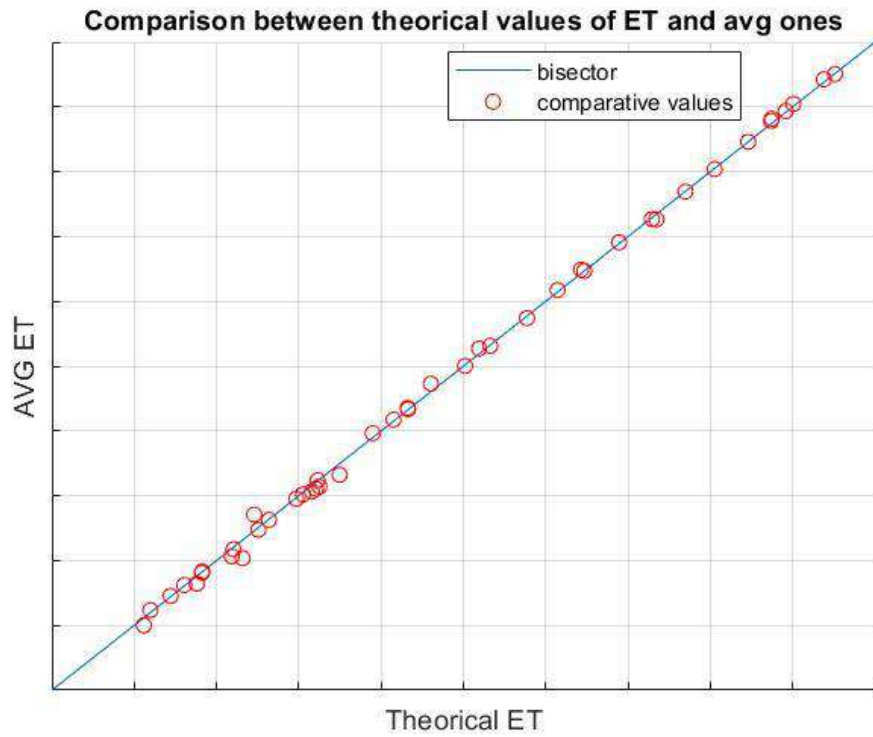


Figure 17 ET regressive graphic – Short Pipe

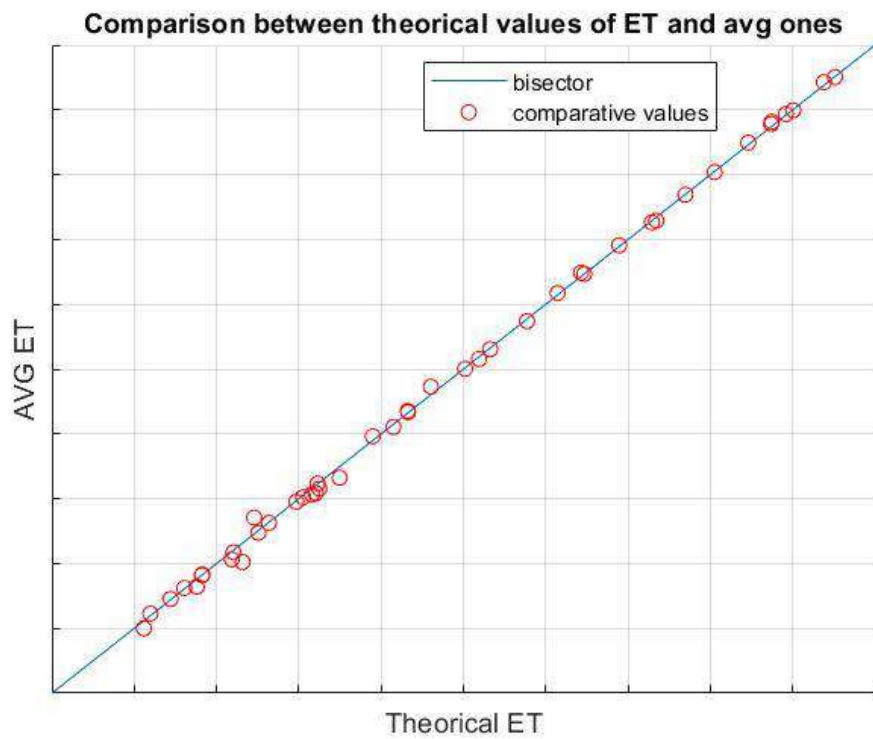


Figure 18 ET regressive graphic – Long Pipe

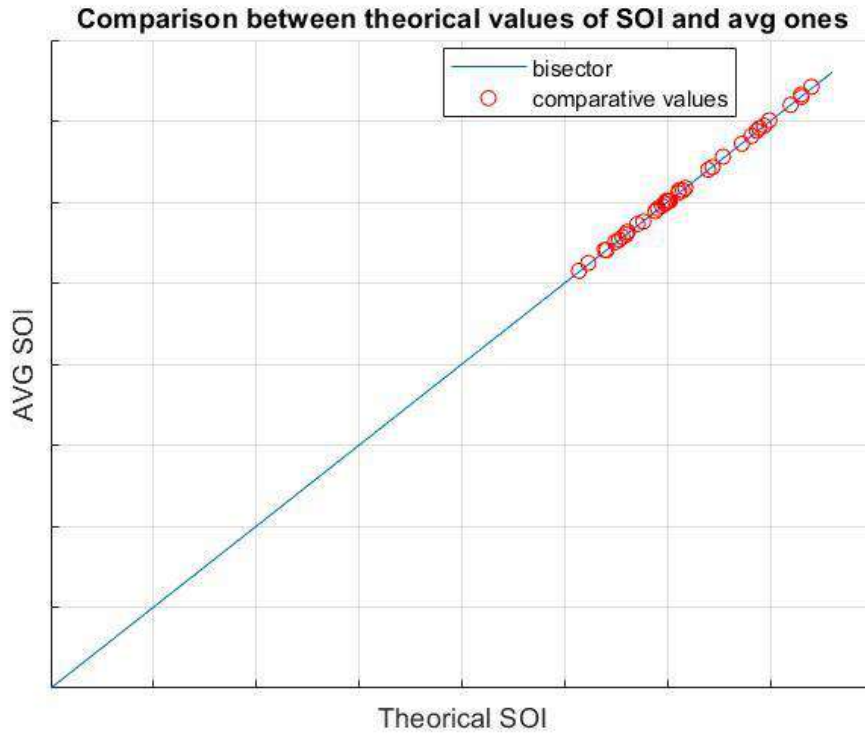


Figure 19 SOI regressive graphic – Short Pipe

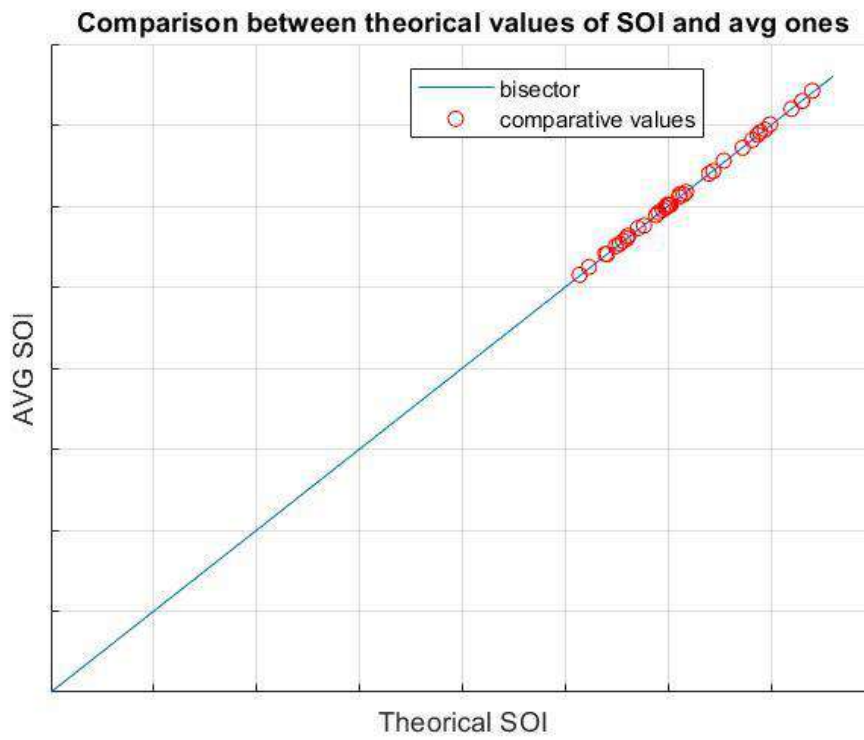


Figure 20 SOI regressive graphic - Long Pipe

Comparison between theoretical values of volumetric flow and avg ones

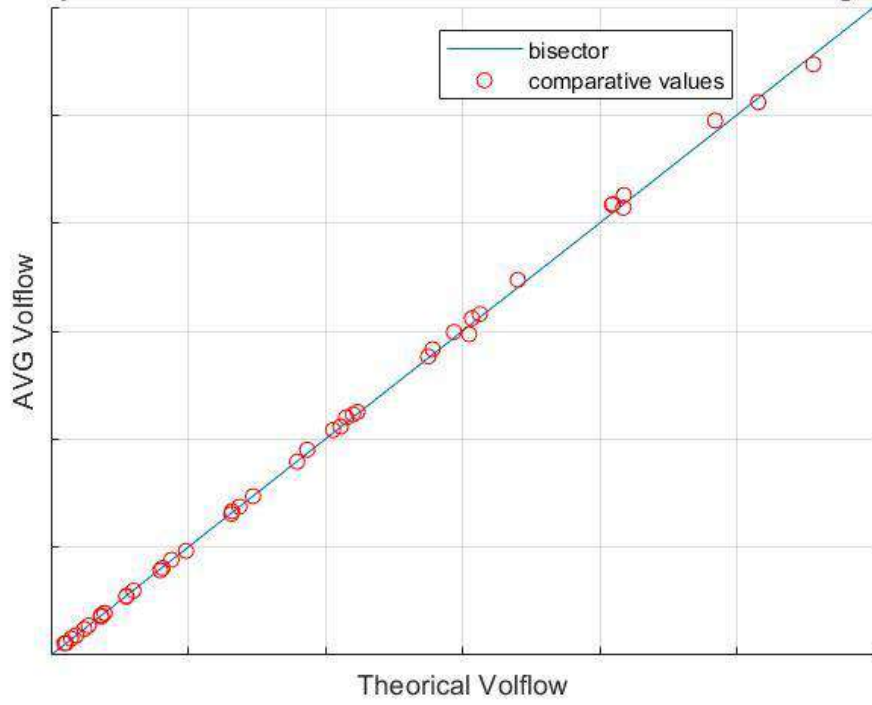


Figure 21 Volumetric flow regressive graphic – Short Pipe

Comparison between theoretical values of volumetric flow and avg ones

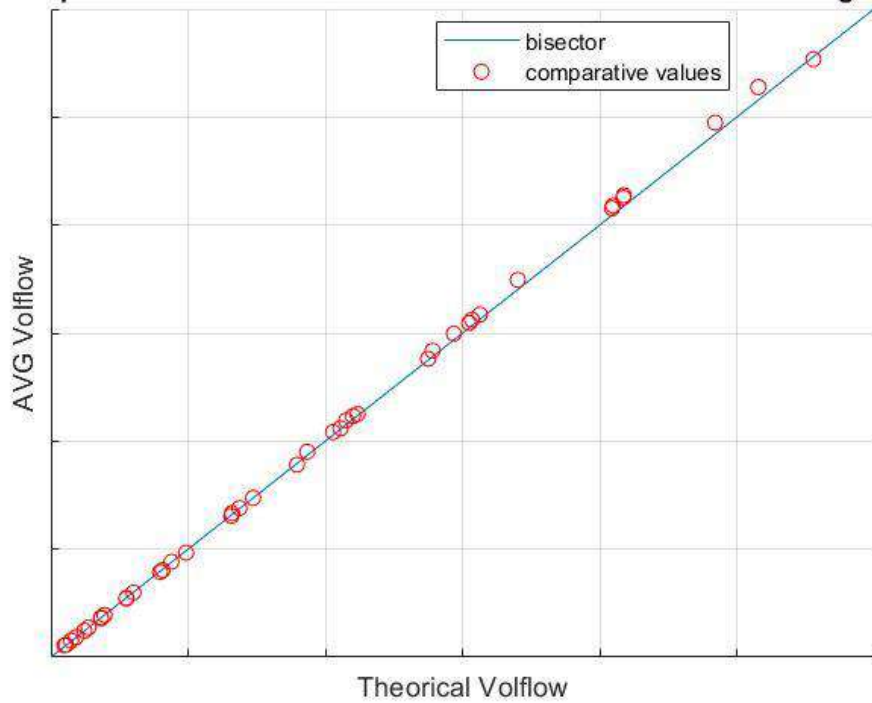


Figure 22 Volumetric flow regressive graphic – Long Pipe

4.3.4.1 Conclusion

The aim has been reached, the experimental values and the ones coming from the pre-calibration are largely superimposed. Experimental data are reliable.

4.3.5 COV graphics

The second aim is completed thanks to CoV contour plots. They are in function of engine speed in rpm (x-axis) and load (y-axis). All axes are normalized.

For sake of brevity not all the CoV plots will be reported but only a table containing the average and the maximum values.

Configurations	CoV Estim	
	CoV avg	CoV max
Ref Rail – Ref Restr – Pipe Short	0.40%	0.62%
Ref Rail – Ref Restr – Pipe Long	0.39%	0.58%
Ref Rail – Ref Restr + 15% – Pipe Short	0.40%	0.60%
Ref Rail – Ref Restr + 15% – Pipe Long	0.40%	0.58%
Ref Rail + 20% – Ref Restr – Pipe Short	0.31%	0.48%
Ref Rail + 20% – Ref Restr – Pipe Long	0.31%	0.47%
Ref Rail + 20% – Ref Restr + 15% – Pipe Short	0.32%	0.47%
Ref Rail + 20% – Ref Restr + 15% – Pipe Long	0.33%	0.47%

The best configurations in terms of average and maximum values are *Ref Rail + 20% – Ref Restr – Pipe Short* and *Ref Rail + 20% – Ref Restr – Pipe Long* because they minimize the injection variability having the smallest combinations of average and maximum CoVs.

In *Figures 23, 24* are reported the contour graphics of the two configurations chosen.

Ref Rail + 20% – Ref Restr – Pipe Short

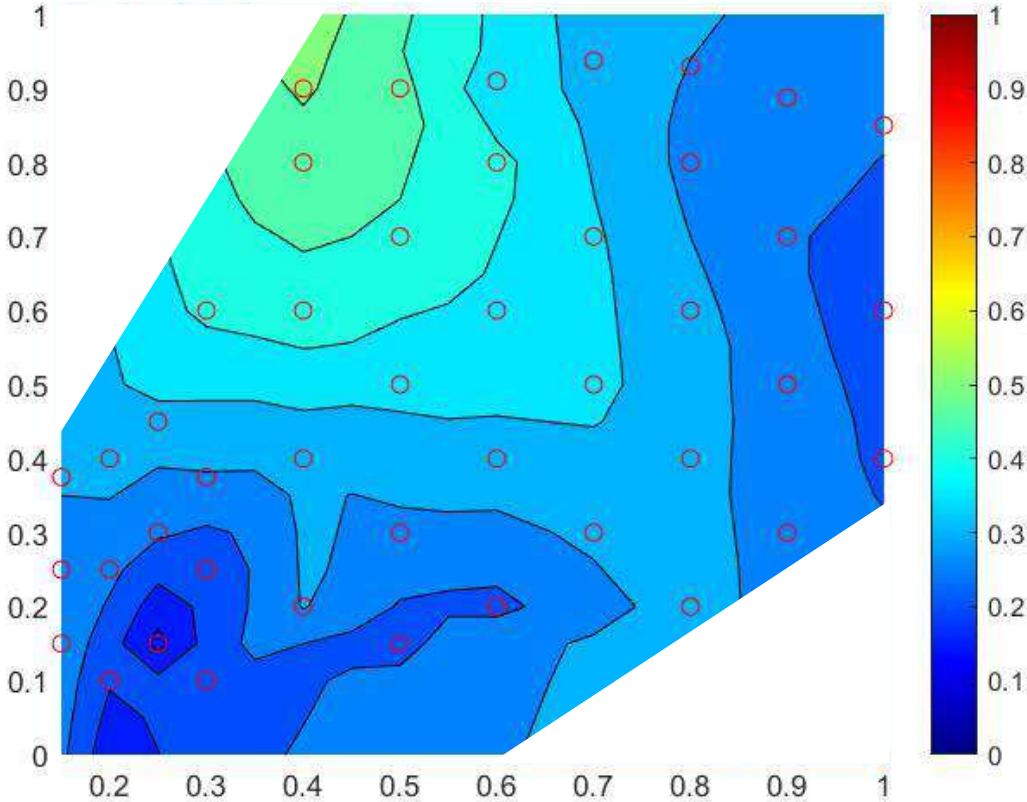


Figure 23 CoV graphic for Ref Rail + 20% – Ref Restr – Pipe Short configuration

Ref Rail + 20% – Ref Restr – Pipe Long

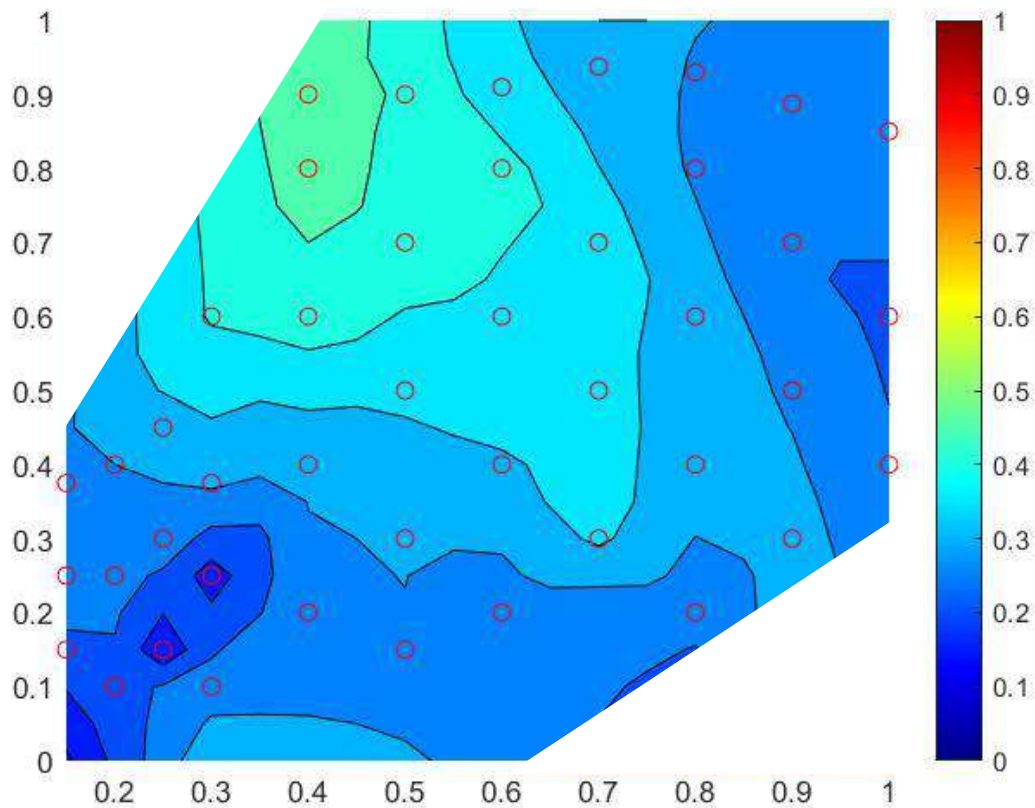


Figure 24 CoV graphic for Ref Rail + 20% – Ref Restr – Pipe Long configuration

Analysing the graphics the most critical part is the green one with a CoV value that is about 0.5. The points inside this area are:

- engine speed= 0.4, rl= 0.9 for short pipe;
- engine speed= 0.4, rl= 0.8-0.9 for long pipe.

The high CoV values are caused by the fact that injections and pumping phases are completely in contra-phase generating a variation in the injected quantities.

For example in *Figure 25* rail pressure, piston displacement and injectors current are shown at engine speed= 0.4, rl= 0.9, long pipe.

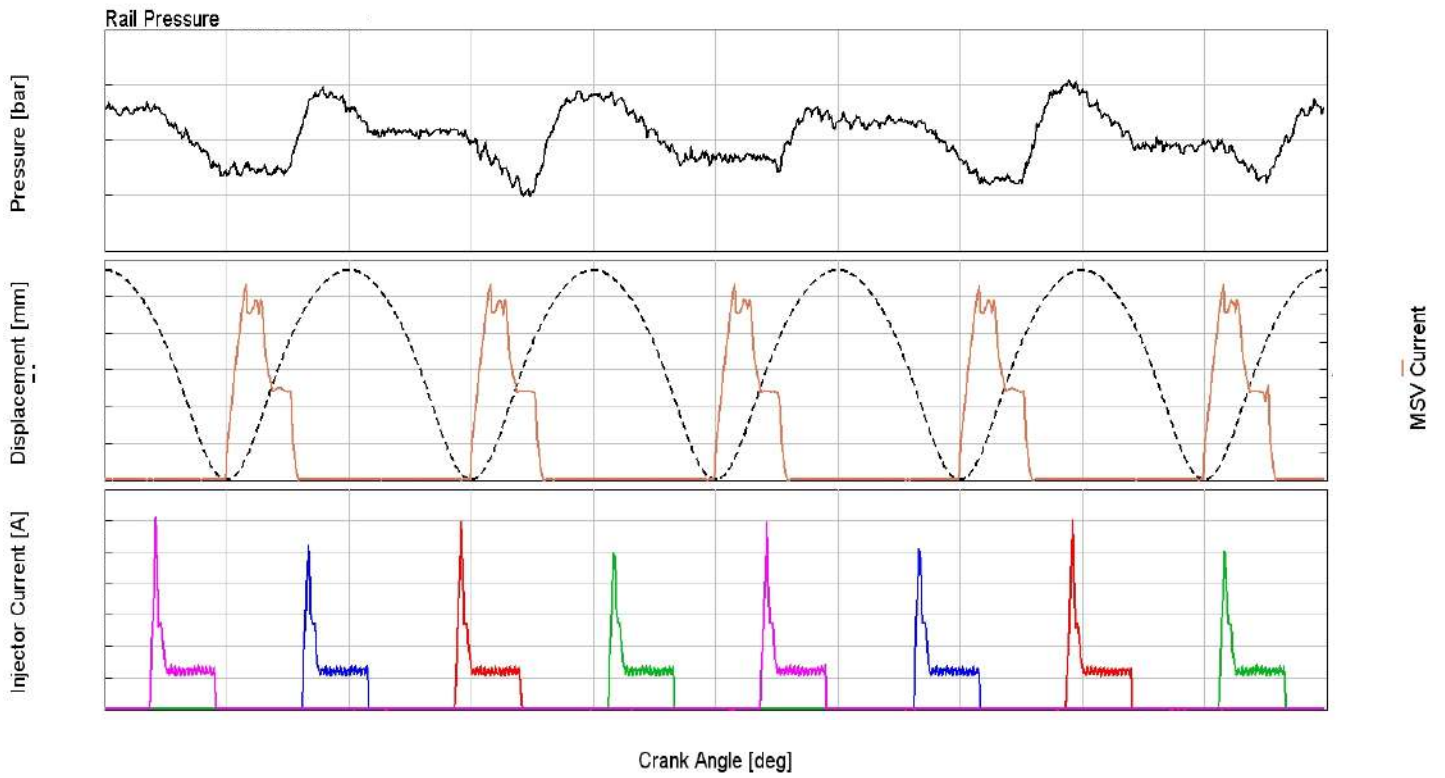


Figure 25 Rail pressure, piston displacement and injectors current at engine speed= 0.4, $rl= 0.9$, long pipe

4.3.5.1 Conclusion

Long pipe configuration has a slightly smaller maximum CoV and for this reason it is taken as the best solution.

5

1-D Modeling using GT-Power

5.1 GT – Power software

As it has been anticipated previously, the commercial software GT-Power was used for the development of the high pressure system model; this code, produced by Gamma Technologies LLC, is part of the “suite” GT-SUITE, that is a software package for the simulation of multi-physics systems that can be met typically in automotive industries as for example for the study of lubrication systems, engine thermic management and for the dynamics of acoustic mechanical systems. In particular GT-Power is devoted to internal combustion engines simulations and it solves with numerical schemes gas-dynamic equations, that govern fluid motions, in sub-volumes in which the model has been discretized. It is able to define fluid properties (pressure and temperature) in inlet and outlet of the different parts of the engine and in particular the air condition and the fuel at the entrance of the cylinder; after that with proper combustion models (predictive, semi-predictive and non-predictive) the software is able to model the chemical energy of the fuel released in pressure and temperature and it is able to calculate the indicated average pressure (PMI) from which, subtracting the frictions and the auxiliar absorptions, it is possible to estimate average effective pressure (PME), torque, power and other quantities of interest.

The software is composed by the subsequent parts:

- *GT-Isr*: the pre-processor that is the graphic interface that allows to model the high pressure system and its components through the use of parts/objects libraries and the definitions of the relative properties and characteristics;
- *GT-Solver*: the true solver that contains the numerical schemes and executes the calculations;
- *GT-Post*: the post processor that allows to visualize calculations results and generate graphics, tables and diagrams to represent them.

The numerical mono-dimensional simulation codes are today largely used in automotive field in order to predict the greater part of engine performance parameters and the pollutant emissions at the exhaust. These powerful instruments are very useful in evaluating the impact that different strategies, calibrations or components could have on the main engine quantities.

At the end the use of these tools can very often allow to predict some quantities that are hardly detectable experimentally guaranteeing a great saving in the numbers of experimental tests and as a consequence in their cost.

5.1.1 The calculation code GT-Power

GT-Power is a library present inside the fluid-dynamic simulation tool GT-Suite, developed by Gamma Technologies and it is centred on the analysis of internal combustion engines performances, indifferently with spontaneous ignition and compression ignition. It has been enriched in the last years, extending its potential and giving the possibility to realize traversal analysis regarding the combustions process, the exhaust emissions, acoustic and thermic analysis, vehicular analysis and the coupling with other mechanical systems.

5.1.2 Equations and discretization

The calculation code GT-Power is based on the resolution of the *Navier-Stokes equations* : continuity equation (mass conservation), momentum conservation equation and energy equation.

The entire engine injection system, including its components and the principal circuits, is modelled inside the software through dedicated templates, that are blocks reflecting the physical aspect of a component. These blocks show lengths, volumes, roughness and every other property that is necessary in order to characterize completely the system. Entire scheme is discretized in a lot of little sub-volumes which are connected one to each other through boundaries, that are fictitious surfaces that connect adjacent sub-volumes.

Scalar quantities (pressure, temperature, species concentration) are calculated in correspondence of the centre of each sub-volume, that is also its centre of gravity, and they are considered uniform over the entire volume. Vectorial quantities (velocity, mass flow, etc.) are calculated in correspondence of the boundaries. A discretization of this type is defined as *Staggered Grid*. The fluid-dynamic equations, resolved inside GT-Power environment, are summarized below:

- mass conservation equation;
- energy conservation equation;
- enthalpy conservation equation.

The solution is calculated making the integration of these equations both in time and space. The integration can be done using an implicit method, an explicit one or almost stationary. The fluid-dynamic mono-dimensional simulation codes typically use the explicit solution rather than a numeric solution based on an iterative process. Briefly, the equations are used, in a first moment, discretized respect to time using a Taylor series development. Subsequently the derivatives are approximated respect to time and space with an incremental ratio calculated in the centre of the volume. The solution is calculated for every time-step which value is taken by the previous one using the mass conservation equation, the momentum conservation equation and the energy conservation equation.

In order to make the solution sufficiently accurate and stable, an adequate time-step has to be chosen to make the condition of Courant satisfied: it is a characteristic number that defines the existent relationship between discretization length (corresponding to each sub-volume lengths) and time-step.

5.1.3 Courant condition

Obviously it is necessary to choose a discretization level adapt to simulation accuracy and time requested for the calculation.

If time steps are too small, it is required a big computational strength, compared to an improvement in the solution accuracy not enough relevant.

There are two levels in which the system has been discretized:

- 1) *Macro level* : the original element is manually subdivided from the operator in presence of discontinuity, curves, different materials and junctions.
- 2) *Micro level* : the single parts are divided in a lot of sub-volumes following a certain discretization length Δx , defined by the user. For the performance analysis, the discretization lengths suggested are:
 - Δx related to aspiration ducts: 40% of engine bore;
 - Δx related to exhaust ducts: 55% of engine bore.

The differences regarding discretization lengths are linked, guaranteeing the Courant condition.

Because of temperatures at the exhaust major than the others, the sound speed is rising and it is necessary to increase the discretization length inside the exhaust ducts to make the Courant condition be respected in order to guarantee a time-step almost uniform for all the systems.

5.1.4 GT-Power structure

GT-Power library presents itself to the user with a graphic interface structured like a tree in which can be seen:

- templates: predefined elements in which there are different attributes that allow to define a specific “object” ;
- objects: elements that derive from the template in which it is possible to assign the value for each attribute that characterizes the template (length, diameter, material, etc.);

- parts: a copy of the object defined above, that is inserted from the user inside the project map.

Inside GT-Power library are preloaded three template typologies, each one with different characteristics and functionalities:

- components: they allow to model the physic entities characterized generally with a mass or a volume (cylinder, tree, turbine, compressor, etc.);
- connections: elements used to link two or more objects (injectors, aspiration and exhaust valves, etc.);
- references: a data set inserted inside specific objects (valves lift profiles, geometric characteristics, etc.).

5.2 GT-ISE elements

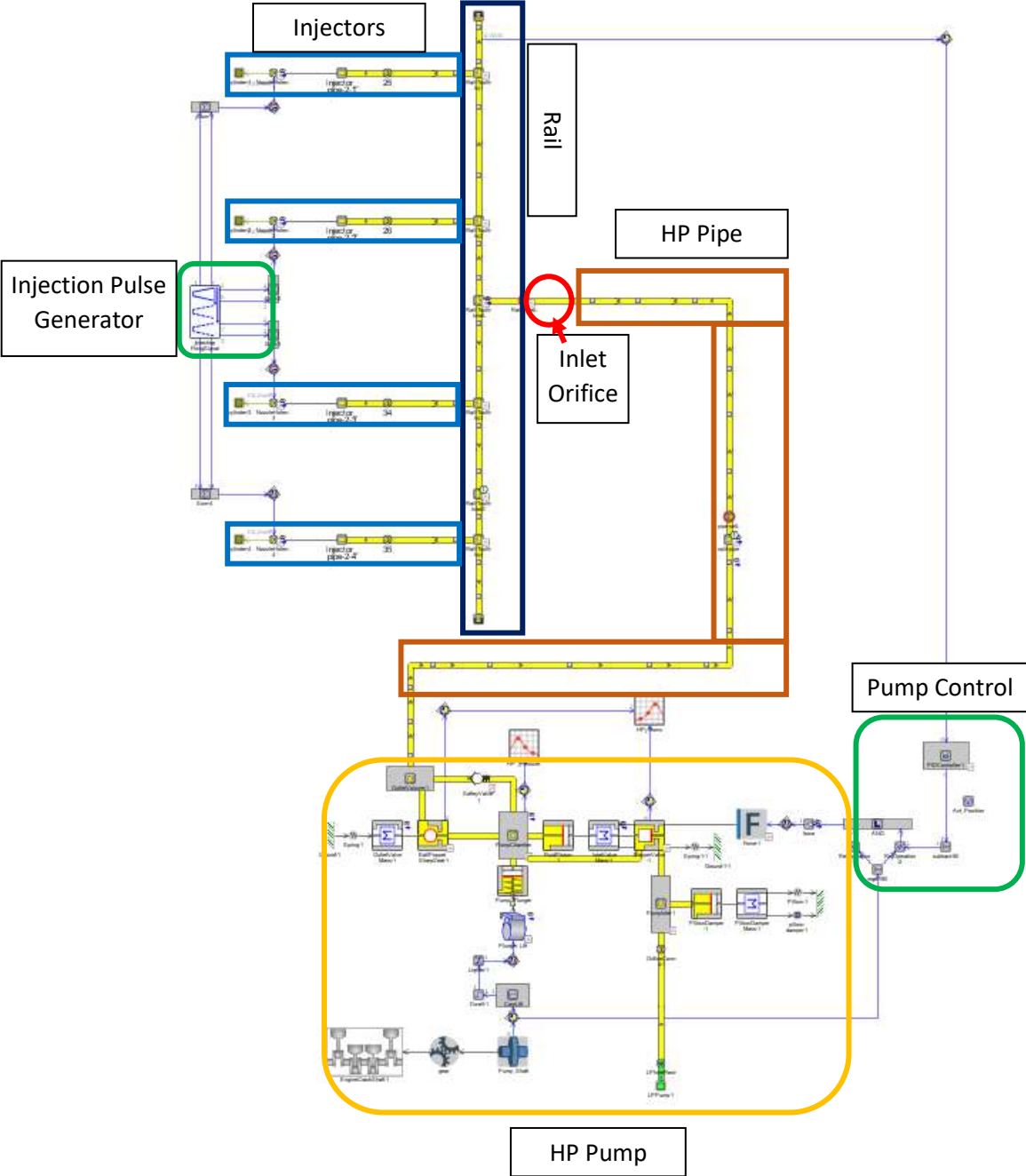


Figure 26 Complete injection system in GT-ISE – Long pipe

GT model has been previously developed in Automobili Lamborghini S.p.A. but an accurate analysis of the components functions has been made in order to know in depth how it works and therefore being able to verify model answer. Follows what emerged from this study.

Thanks to GT-ISE software, the high pressure flow path, that is made of the elements already seen and connected to the pump model, has been built for both the configurations chosen. In *Figure 26* the long pipe configuration is represented.

5.2.1 Model description

The system has been modelled in GT-ISE environment. This tool is often used to simulate hydraulic systems according to a 1-D approach, allowing a powerful analysis in time and frequency domains. Linear analysis in fact plays a crucial role during the design process detecting system's natural frequencies and associating them to specific components.

Each sub-part of the fuel supply system has been modelled by means of an assembly of elementary components coming from different available libraries, building the "super components".

Modeling every single part separately allowed a deep validation of the system components step by step. The advantages of this approach are several; from one side it is helpful to easily understand how to improve the entire model validation, from the other side, it offers the chance to use every validated sub-model in other future applications sensibly reducing the time required to realize a new mathematical model. Furthermore, a combined study of the fuel system using both experimental and simulated results is even decisive, offering the chance to properly evaluate all the parameters which are difficult to be directly measured.

5.2.2 Fuel pump

High pressure pump has been modelled in detail to investigate its operation effects on the global injection system. In particular, all the key components have been modelled separately in GT-ISE in order to achieve a good level of reliability, including the inlet valve, the electromechanical actuator, the pumping element connected to the cam and the outlet valve.

Pump model includes also an overpressure valve and a damper at the inlet of the pump to limit pressure fluctuations on the supply circuit, reproducing the experimental Wet System bench setup. As regards the PID controller, a simplified model replicating the real logical architecture of both the complete ECU control and the Wet System bench was created in GT-Power. In particular, it consists in a closed loop control continuously comparing the measured rail pressure and the target value and updating the opening and closing timing of the electromechanical actuator connected to the inlet valve. A validation of the 1-D model of the injection system was performed comparing simulation results with the experimental data coming from dedicated efficiency tests, at different engine speed and load, performed at Automobili Lamborghini S.p.A. hydraulic test bench.

5.2.3 Injectors

Injector target is to ensure the amount of fuel delivery requested with the right timing and spray quality. The injectors have been modelled in detail to analyse their behaviour depending on rail pressure oscillations. To this aim, peculiar attention was devoted to mechanical and hydraulic modelling, since evaluating the correct volume inside the injector is crucial to obtain a meaningful response for the pressure pulsations.

Ballistic issue

Ballistic problem is linked to injection duration. A GDI engine operates in two zones differing each other for a net slope change. A ballistic zone, for small ETs, where the needle is not fully raised and a linear zone where the injected quantity becomes proportional to the command duration. The ballistic zone and the minimum ET required to open the injector are shifted toward higher ETs increasing rail pressure, because the injector needs a longer energizing time to overcome the higher pressure force on injector control valve. On the other hand, the linear zone slope increases with rail pressure because, once the needle is completely raised up, higher upstream pressure determines a higher injection rate.

5.2.4 Rail and pipes

Common experience demonstrates that the modelling phase of all high pressure and low pressure lines is crucial in the study of a complete injection system. Every connection was studied separately in accordance to its position and design, in order to find the right compromise between model accuracy and acceptable computational times.

5.3 Test plan

Being the present research focused on the analysis of the rail pressure fluctuations effects on the injectors operation, a parametric investigation of different hydraulic circuit designs was carried out.

Different configurations were used in order to study the effect of several parameters on the complete injection system hydraulic response.

In detail, different lengths for the pump–rail pipe, different rail diameter and the influence exerted by the introduction of a flow restrictor at the rail inlet were investigated.

Finally, two different layouts were used; the first one with a side connection of the pump–rail pipe, the second one with a top connection.

The above described system layouts were used for the Wet System analysis according to the experimental test plan carried out on the GDI Wet System bench at Automobili Lamborghini S.p.A.

After the basic injector characterization, for each layout, the system was tested at different load levels and speeds to simulate different engine operating conditions.

Experimental data were used to assess the reliability of the developed 1D model of the complete Wet System.

5.3.1 System dynamics experimental analysis

During the dynamic analysis tests, the fluid-dynamic behaviour of the overall Wet System was analysed, mainly in terms of pressure waveforms; angle-based acquisitions were performed recording data over entire pump shaft revolutions to appreciate the pressure waveforms phasing related to the pumping system operation.

A combined approach coupling both experimental tests and simulations was adopted in order to fully understand the influence of every single system parameter and accurately validate the numerical model.

Wet System was experimentally tested following the plan reported. Each hydraulic configuration was analysed in different load conditions (low, medium and high) and speeds corresponding to the experimental tests in order to investigate a wide engine operating range. The effect of the high pressure pipe design, in terms of internal diameter and length, flow-restrictor, rail inlet position and also rail diameter were studied.

High pressure pipe oscillations amplitude is always higher than rail pressure one, due to the bigger rail internal volume and the flow restrictor effect.

5.3.2 Numerical results and model validation

A parallel simulation was run for each experiment with the purpose of tuning the 1-D model and enhancing its accuracy. The validation was achieved using rail and high pressure pipe pressures acquisitions. Results were compared in angle domain, achieving consistent outcome in all test conditions.

Numerical results (green curves) are depicted overlapped to the correspondent experimental values (red curves) for all engine speeds and loads. A good agreement among experimental and numerical results has been obtained in terms of pressure peaks intensity and mass flow rate respect to injection phase.

5.4 Goals

Summarizing, the aims of GT analysis are to:

- test the model answer on experimental data acquired in the cell.

It is done making a comparison in GT-POST between simulated values and experimental ones for:

1. rail pressure and pressures acquired thanks to fast sensors inside high pressure pipe. The first one is closer to high pressure pump and the second is closer to rail inlet;
2. injections linked to injectors. In particular the attention is put on the correct phasing between green curve and red curve because the values are obviously different. This is

due to the fact that the green curve represents the injected mass rate instead of the red one that represents injector current when the injector is active.

- use the model, once verified that it responds adequately, also out of the tested points in order to explore not tested areas or to test different configurations.

Long pipe configuration physical model is used in the next chapter to make a co-simulation in MIL environment in order to control high pressure pump replacing the PID with the ECU control model created in Simulink.

The graphics shown below regard the chosen configurations *Ref Rail + 20% – Ref Restr – Short/Long pipe*. For sake of brevity only full load plots are reported.

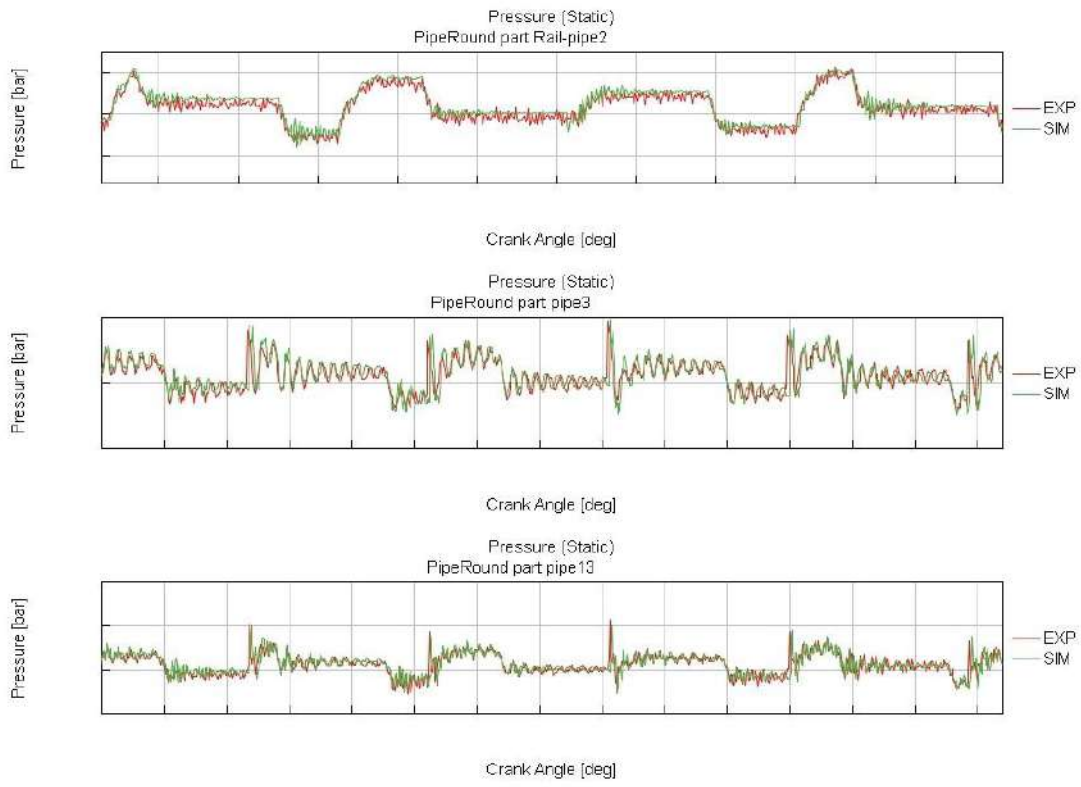


Figure 27 Pressure waves at 1500 RPM – Short pipe

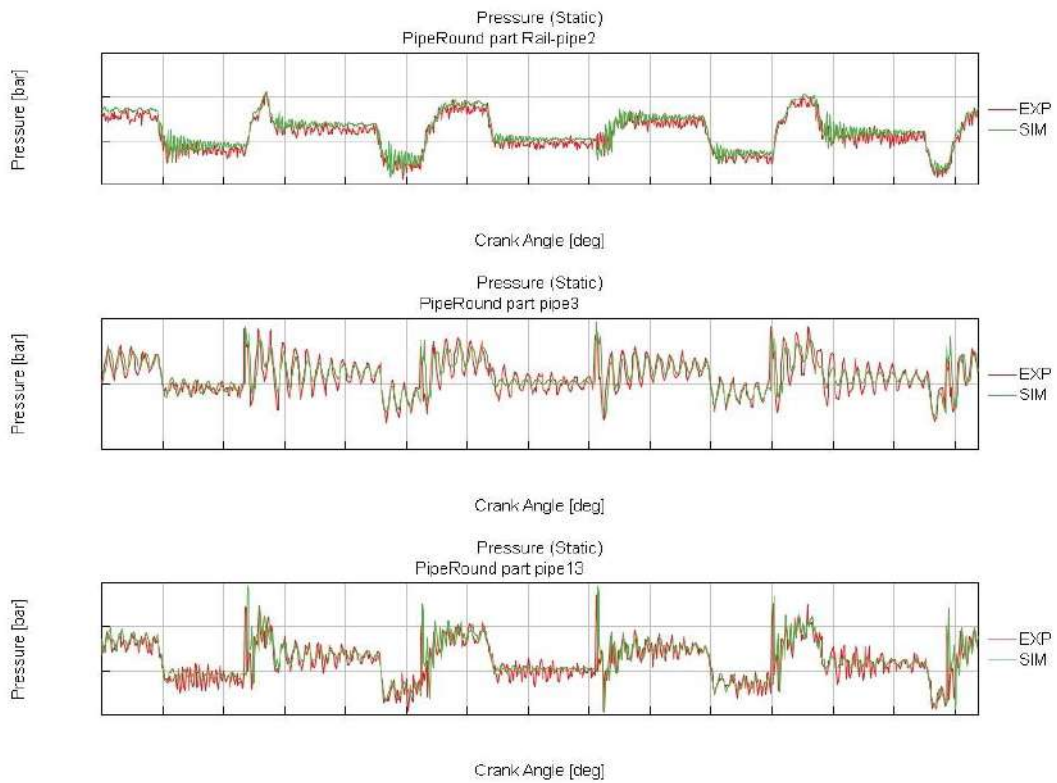


Figure 28 Pressure waves at 1500 RPM – Long pipe

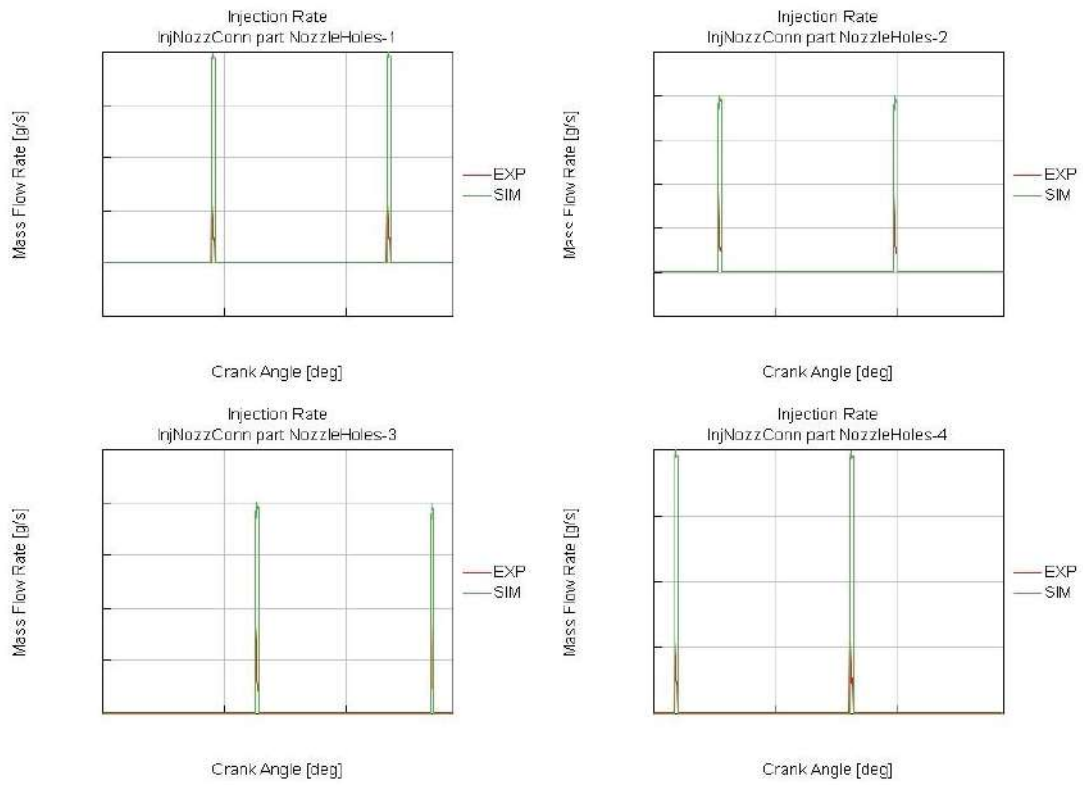


Figure 29 Mass flow rate at 1500 RPM – Short pipe

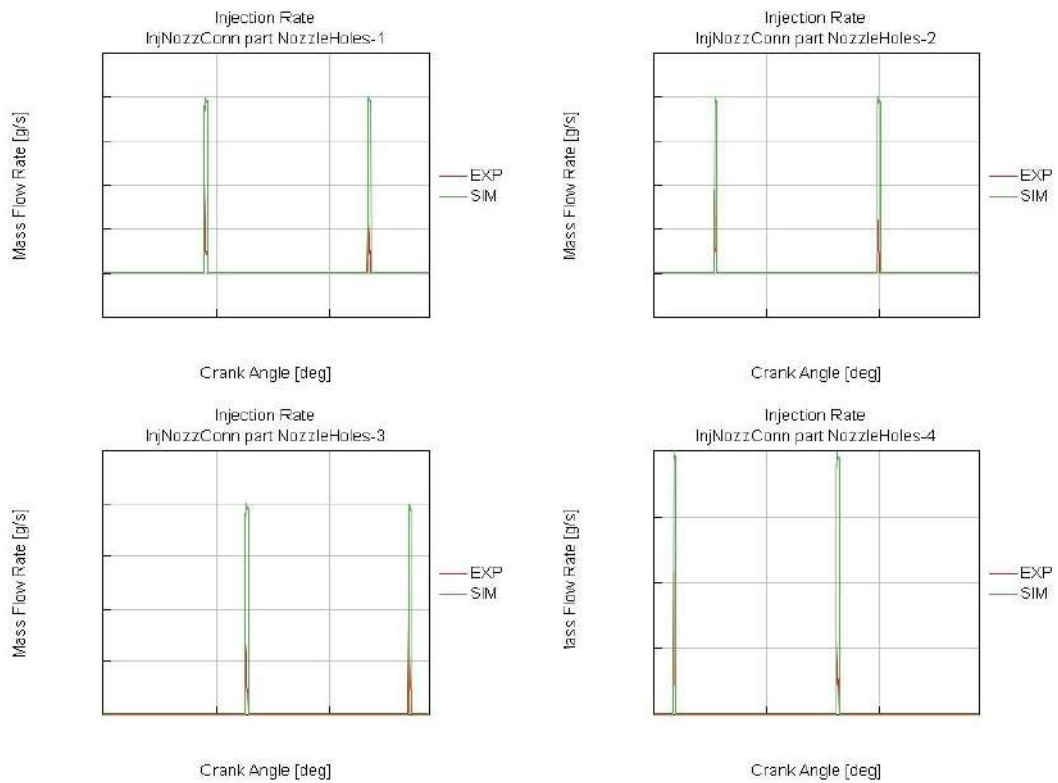


Figure 30 Mass flow rate at 1500 RPM – Long pipe

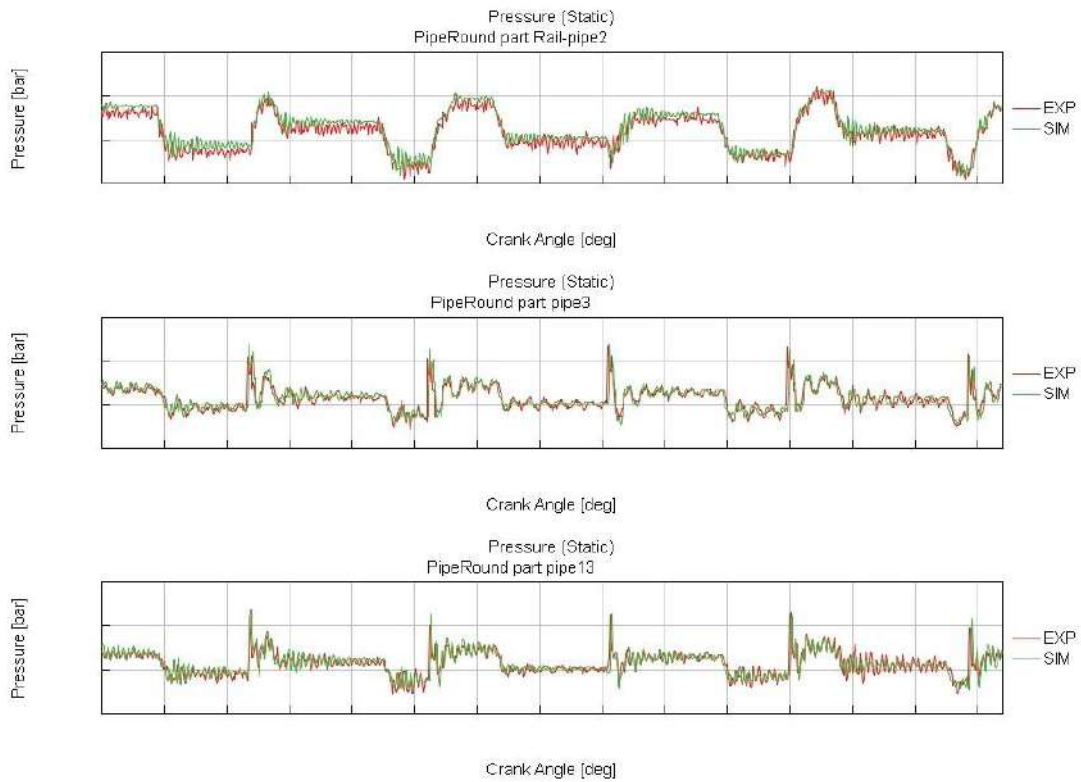


Figure 31 Pressure waves at 2000 RPM – Short pipe

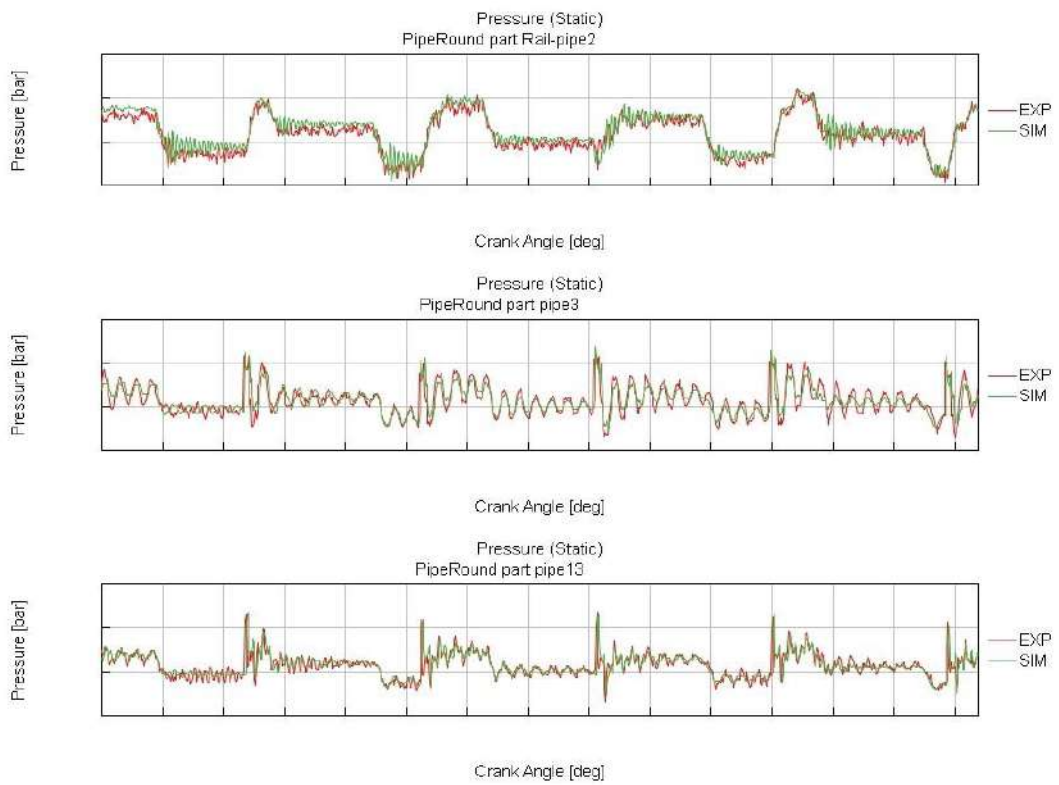


Figure 32 Pressure waves at 2000 RPM – Long pipe

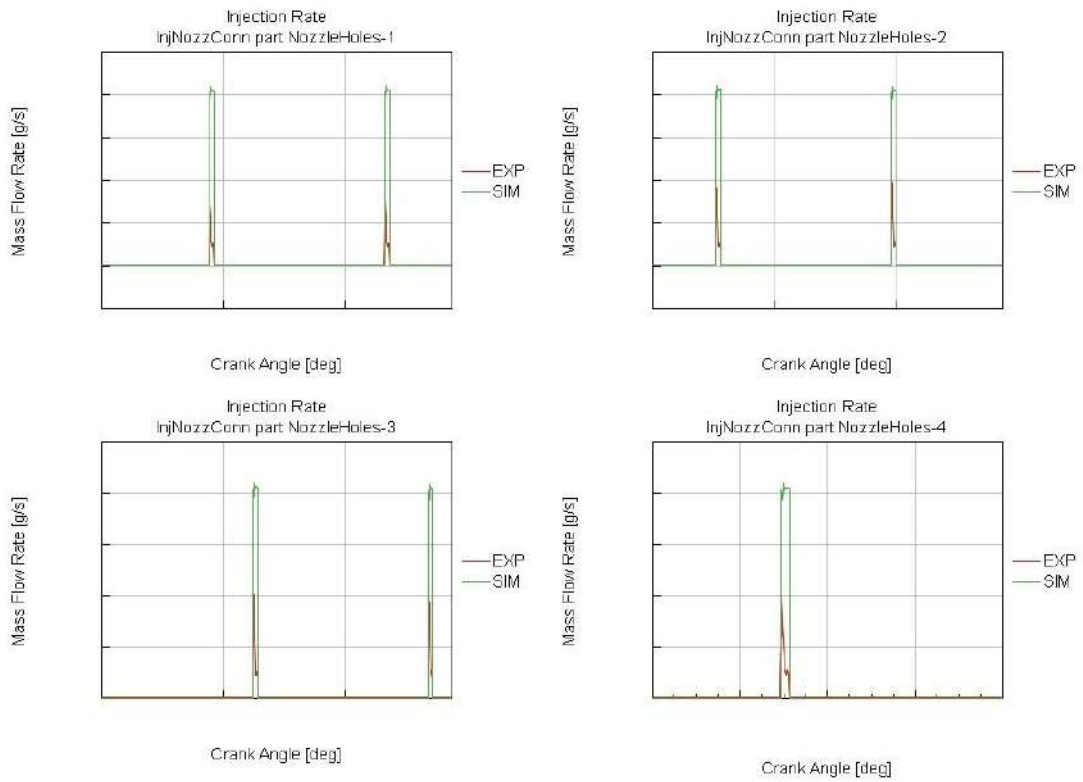


Figure 33 Mass flow rate at 2000 RPM – Short pipe

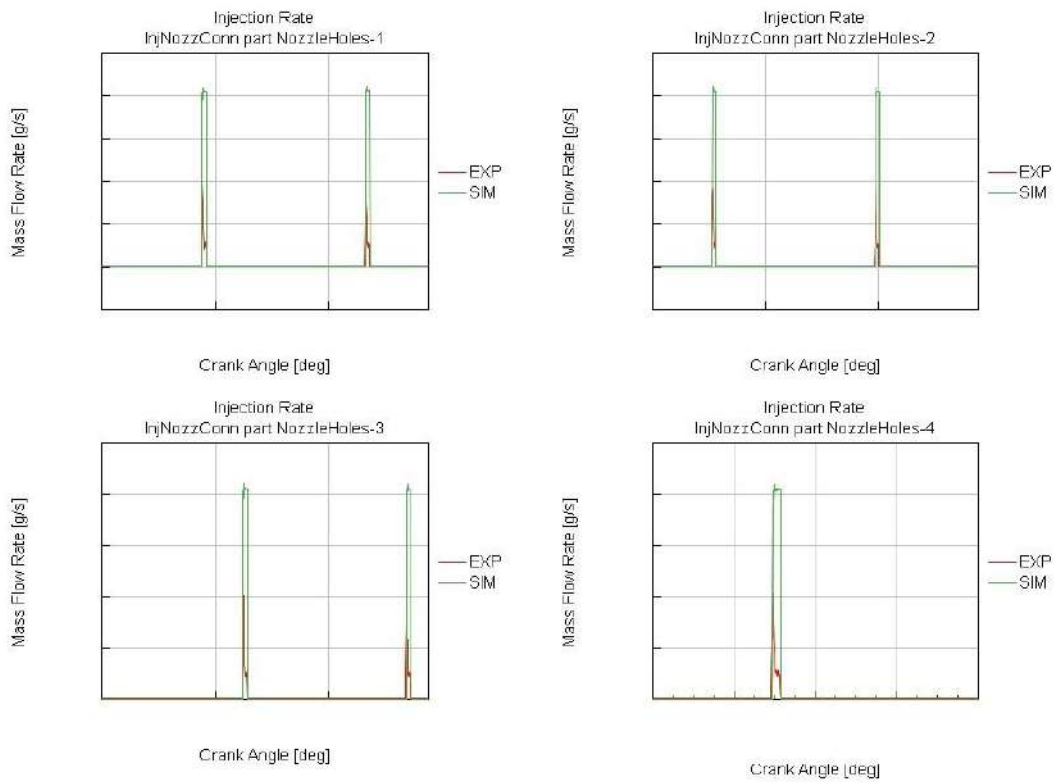


Figure 34 Mass flow rate at 2000 RPM – Long pipe

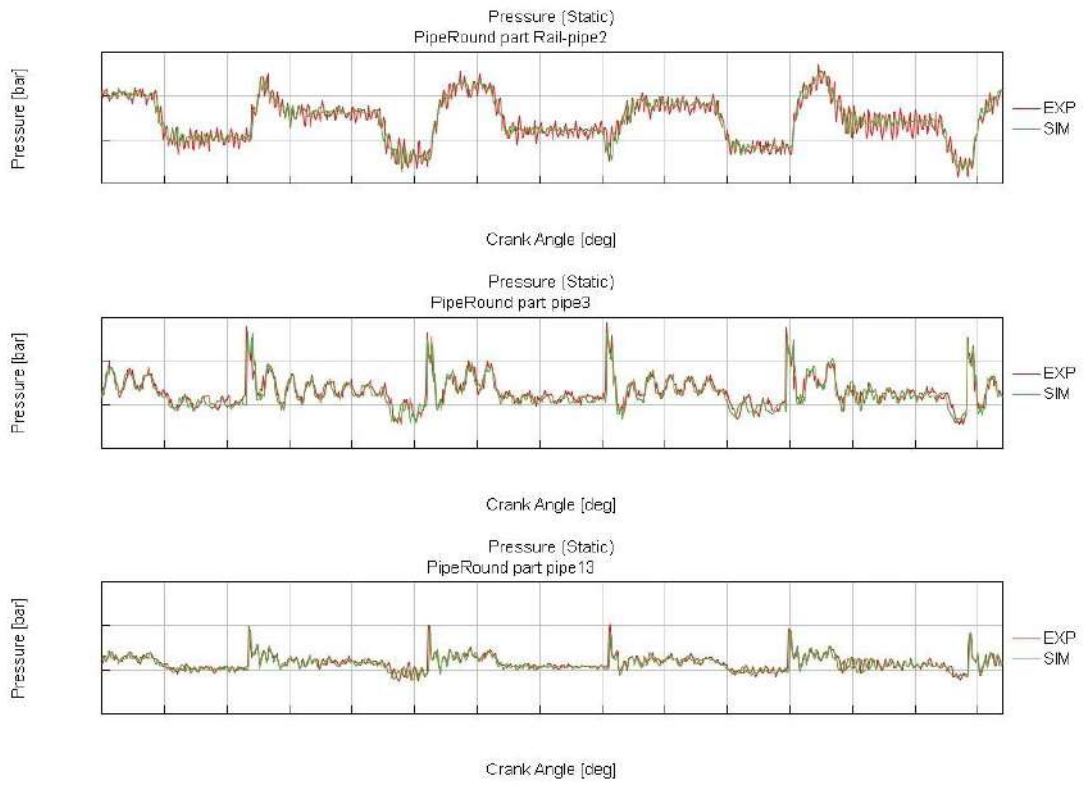


Figure 35 Pressure waves at 2500 RPM – Short pipe

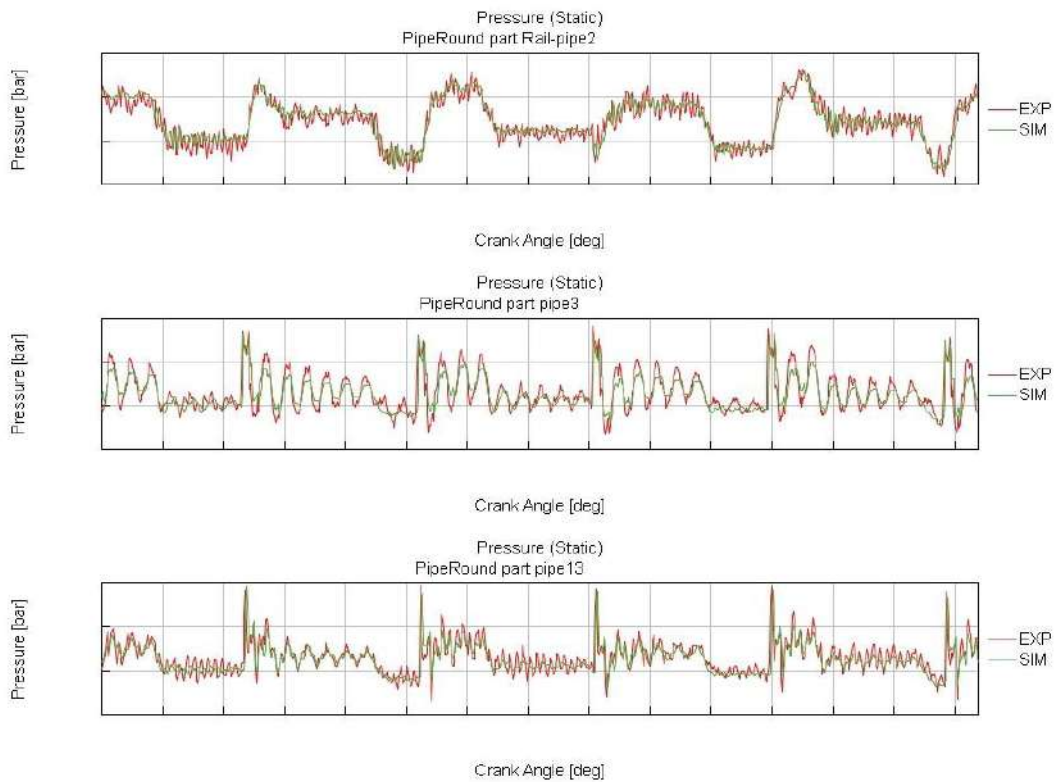


Figure 36 Pressure waves at 2500 RPM – Long pipe

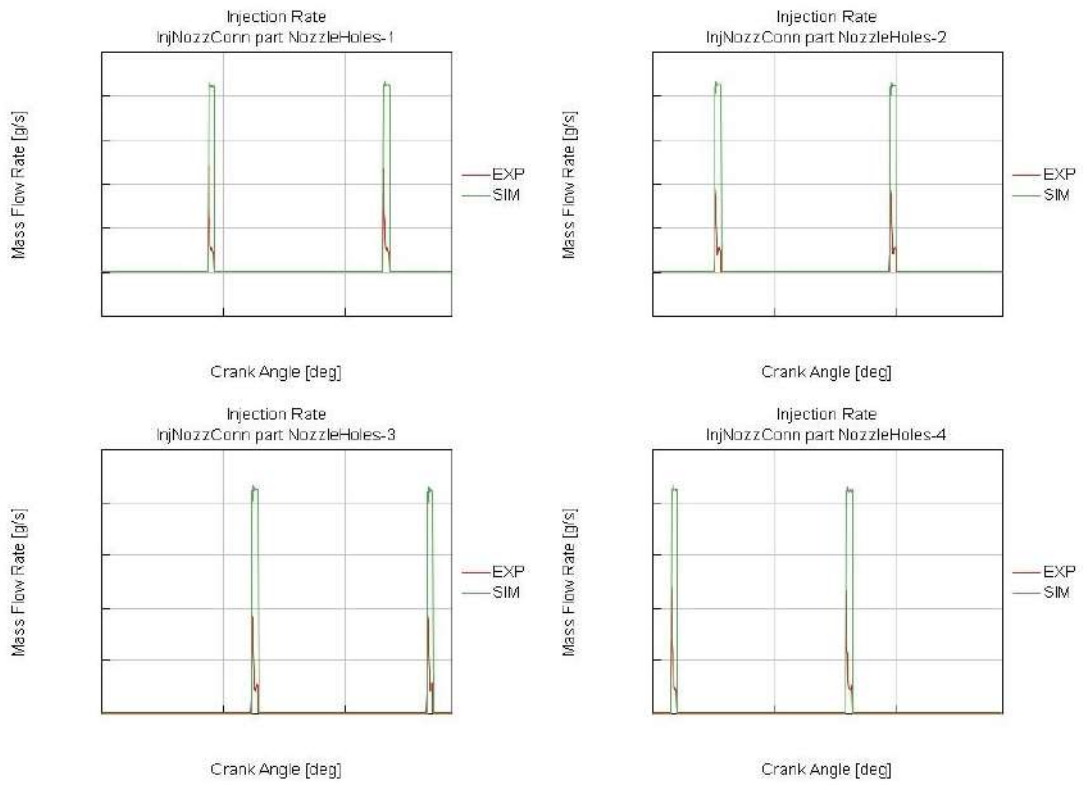


Figure 37 Mass flow rate at 2500 RPM – Short pipe

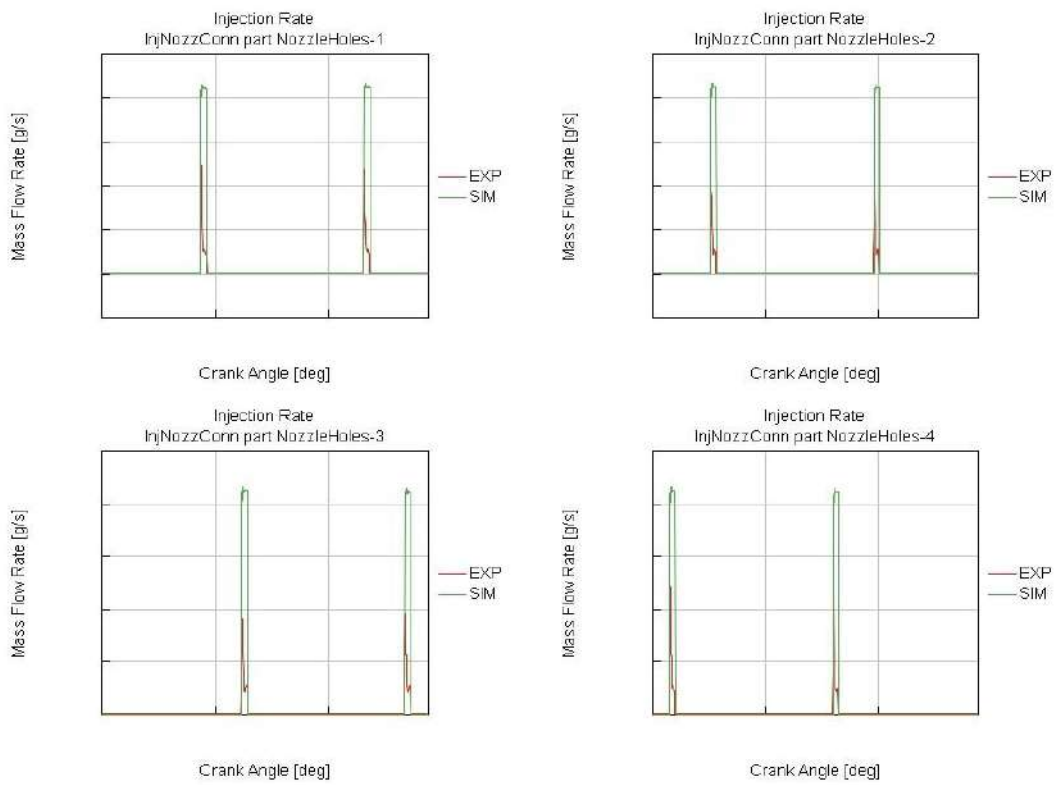


Figure 38 Mass flow rate at 2500 RPM – Long pipe

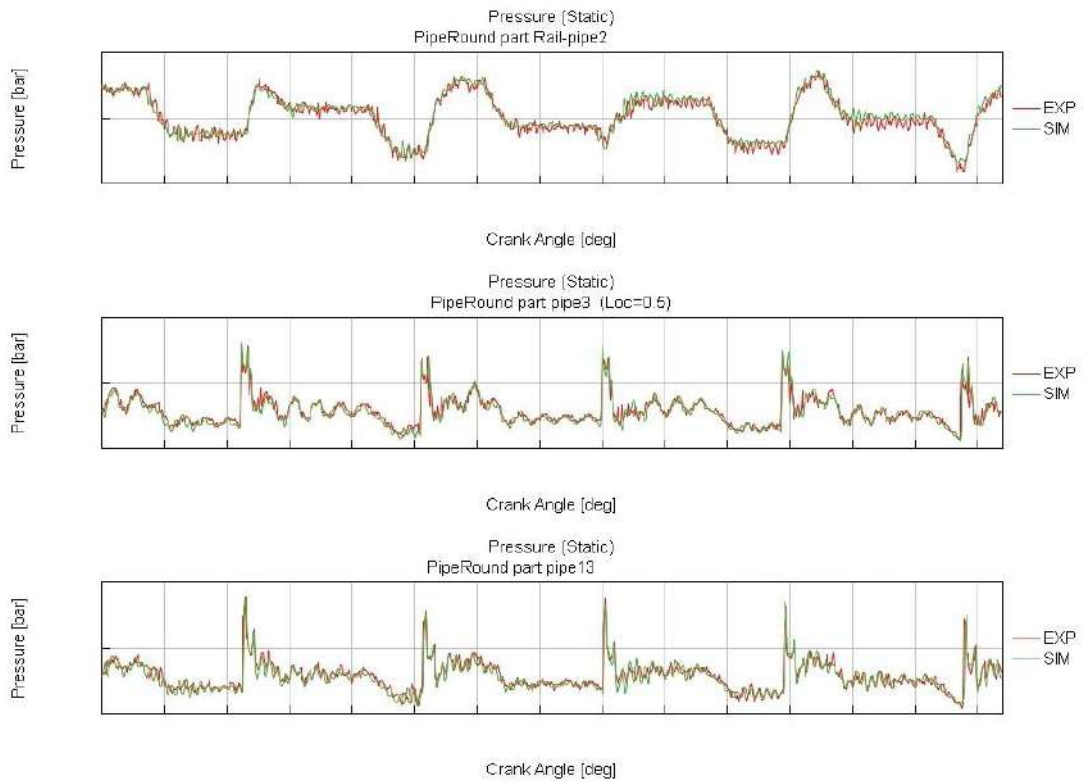


Figure 39 Pressure waves at 3000 RPM – Short pipe

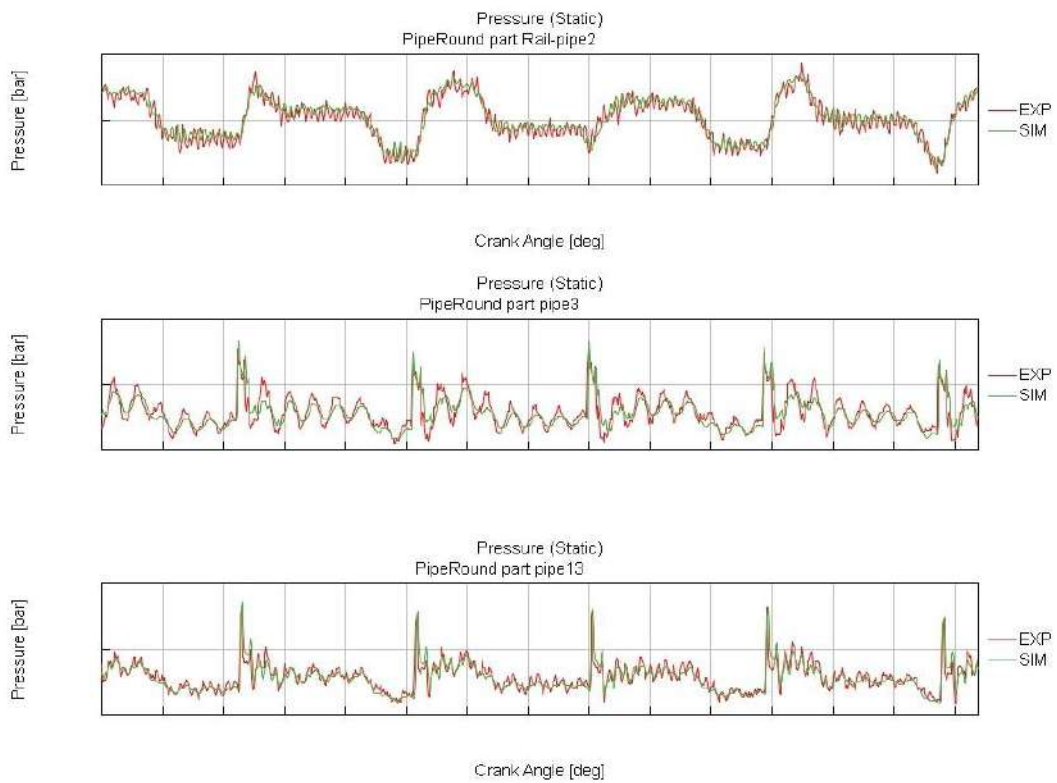


Figure 40 Pressure waves at 3000 RPM – Long pipe

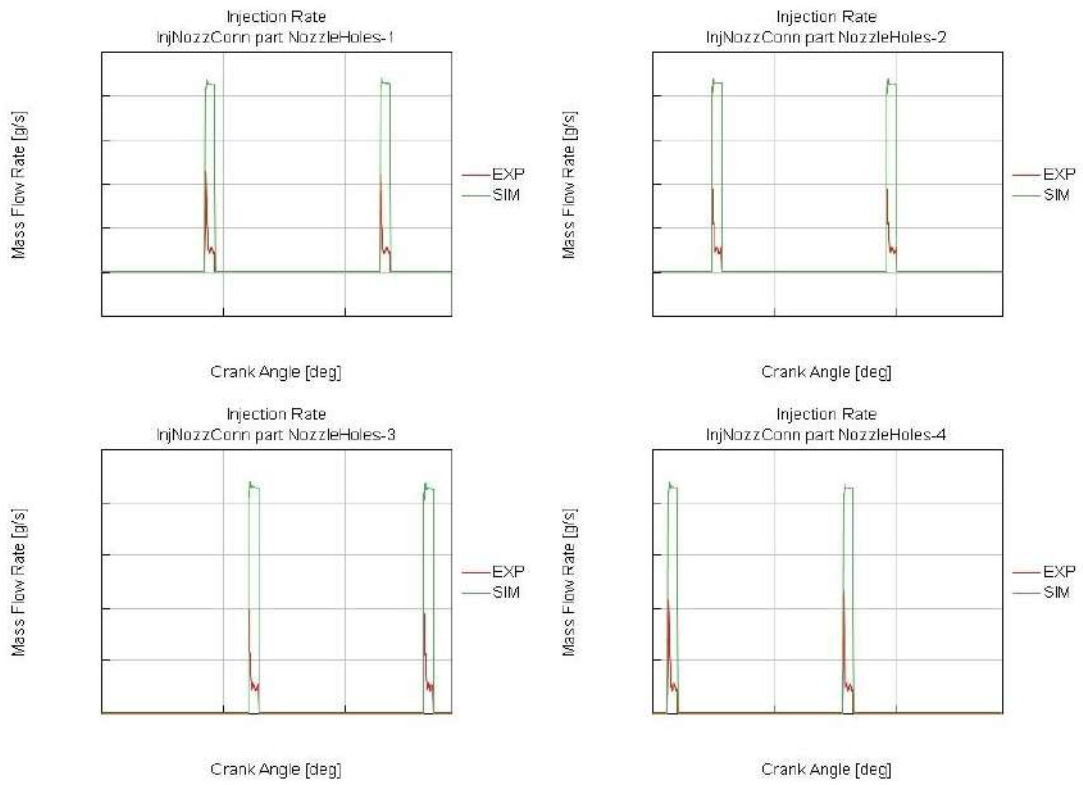


Figure 41 Mass flow rate at 3000 RPM – Short pipe

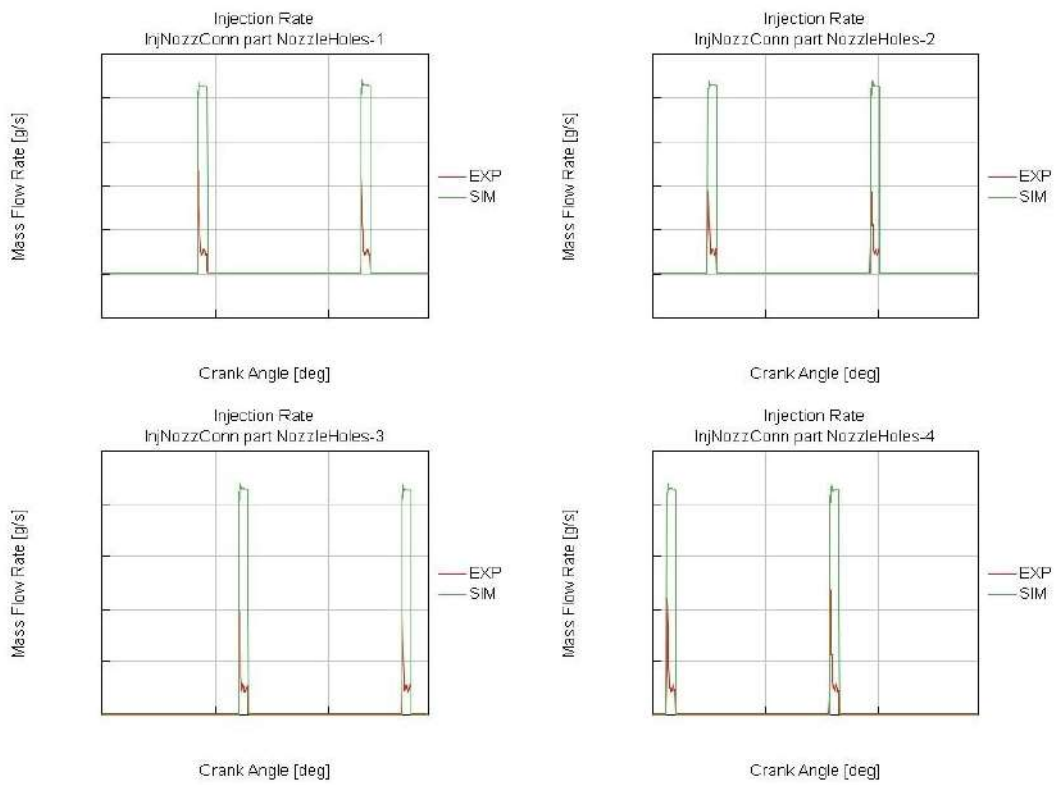


Figure 42 Mass flow rate at 3000 RPM – Long pipe

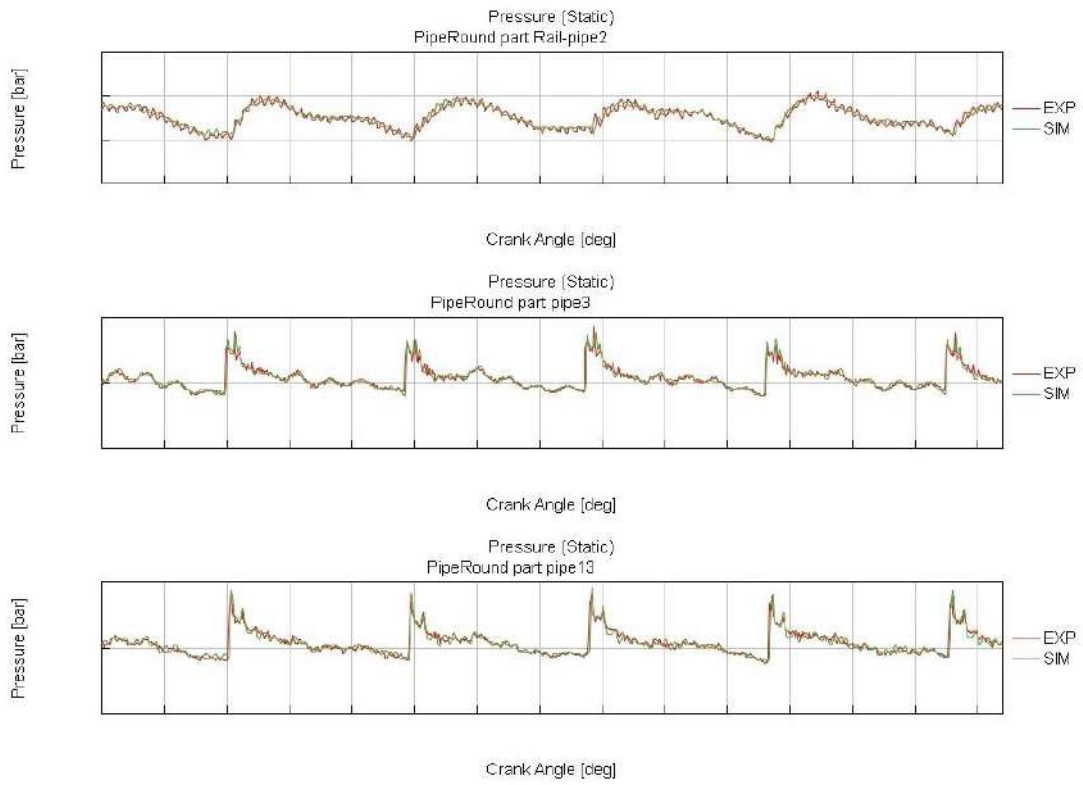


Figure 43 Pressure waves at 4000 RPM – Short pipe

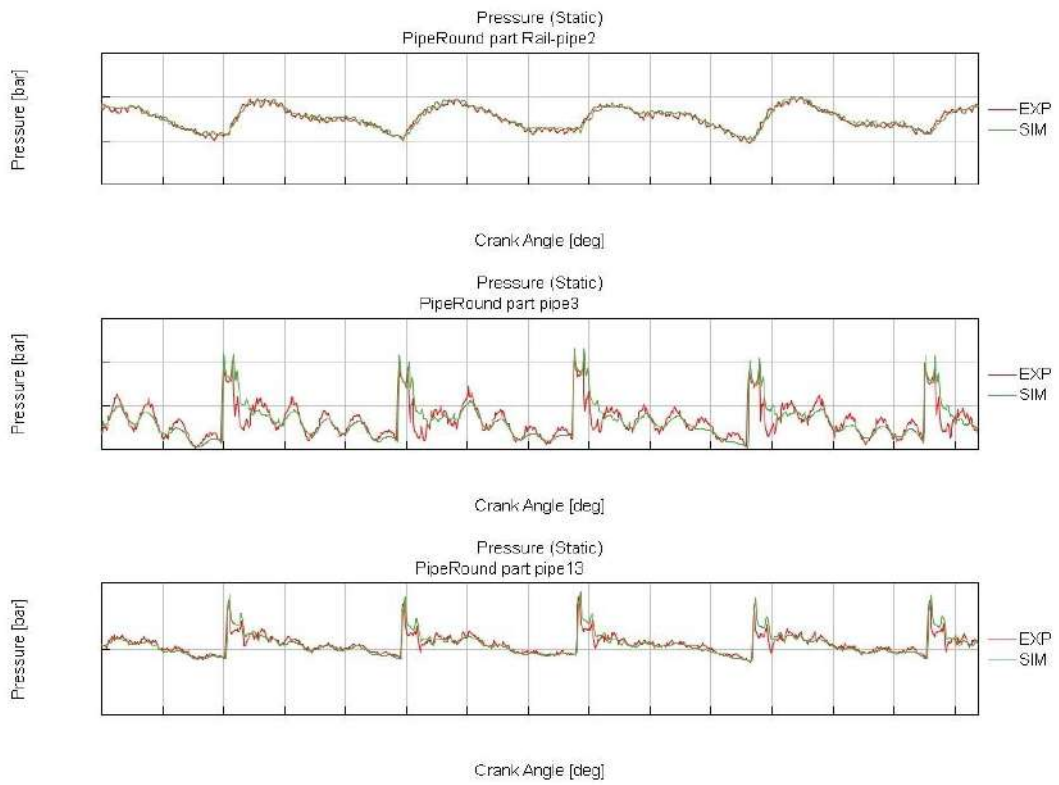


Figure 44 Pressure waves at 4000 RPM – Long pipe

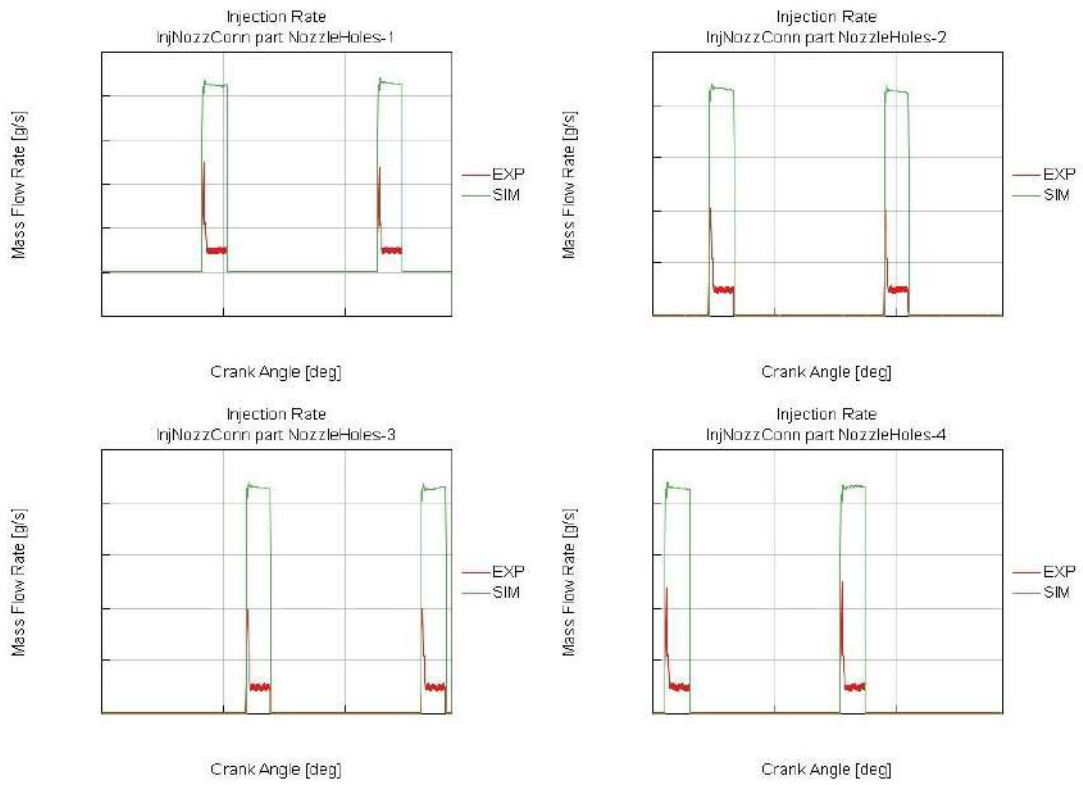


Figure 45 Mass flow rate at 4000 RPM – Short pipe

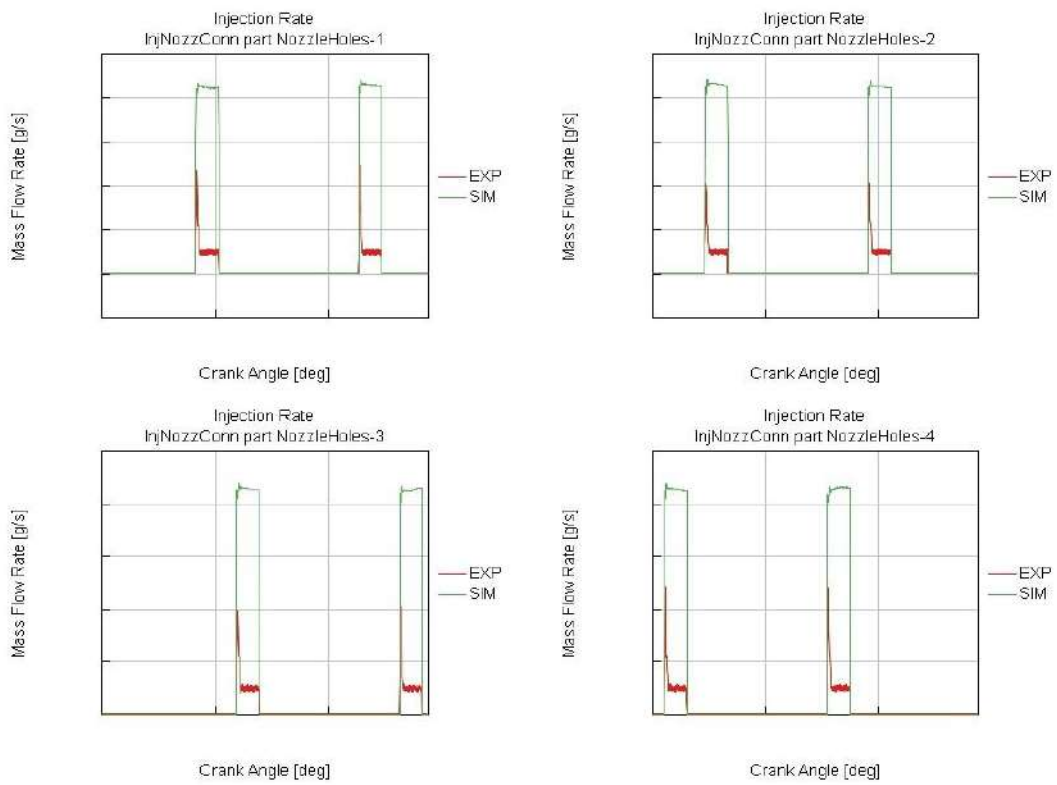


Figure 46 Mass flow rate at 4000 RPM – Long pipe



Figure 47 Pressure waves at 5000 RPM – Short pipe

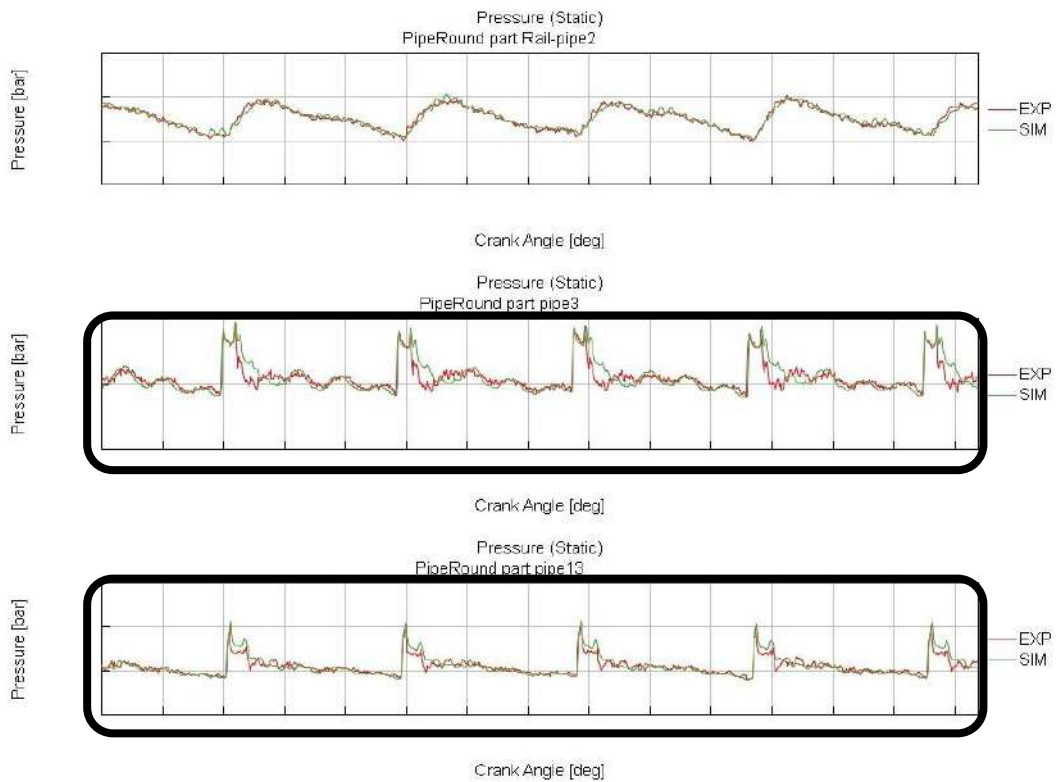


Figure 48 Pressure waves at 5000 RPM – Long pipe

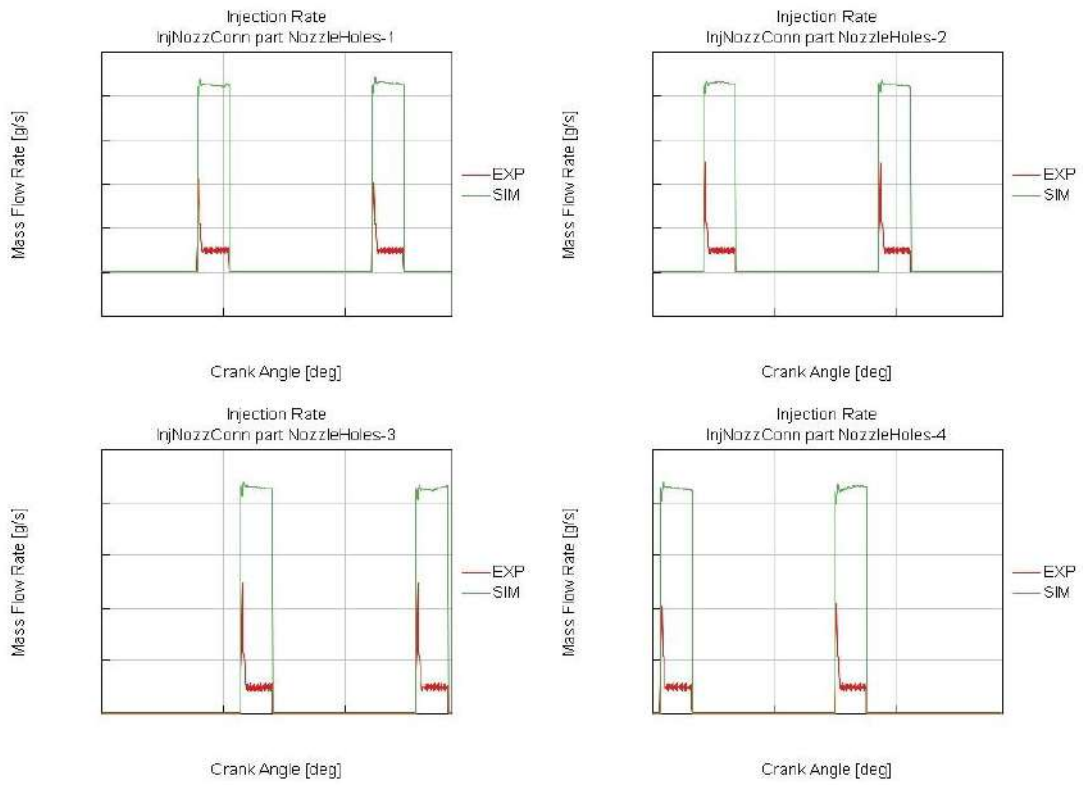


Figure 49 Mass flow rate at 5000 RPM – Short pipe

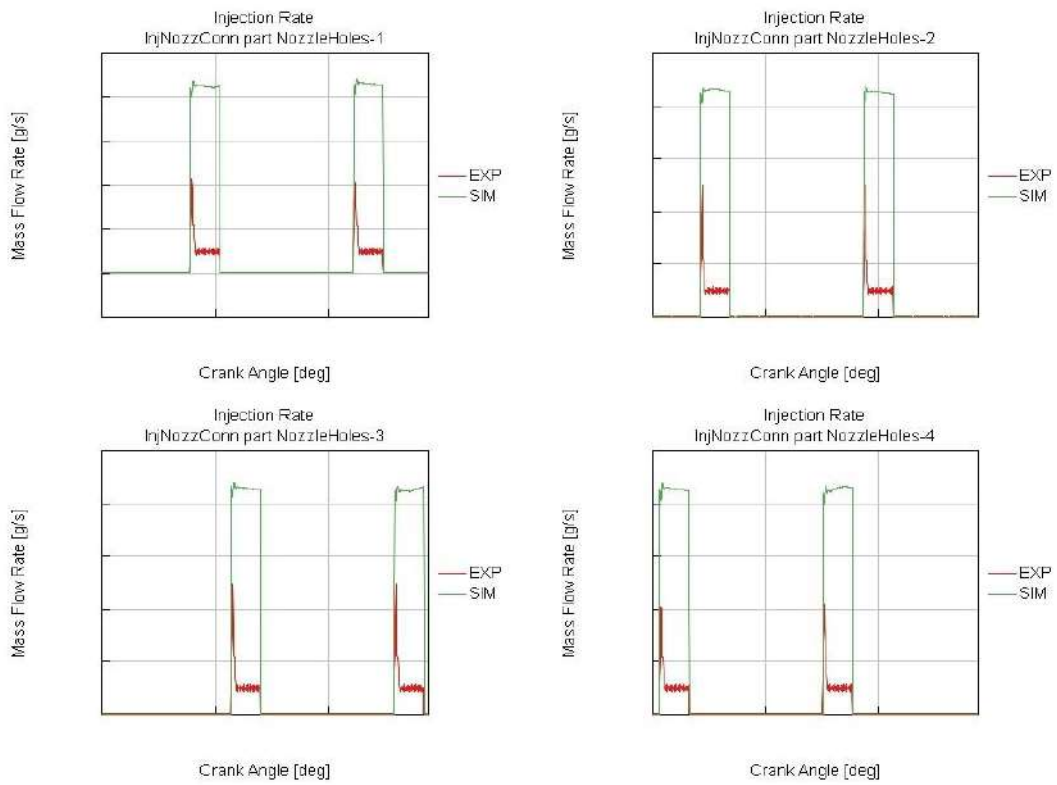


Figure 50 Mass flow rate at 5000 RPM – Long pipe

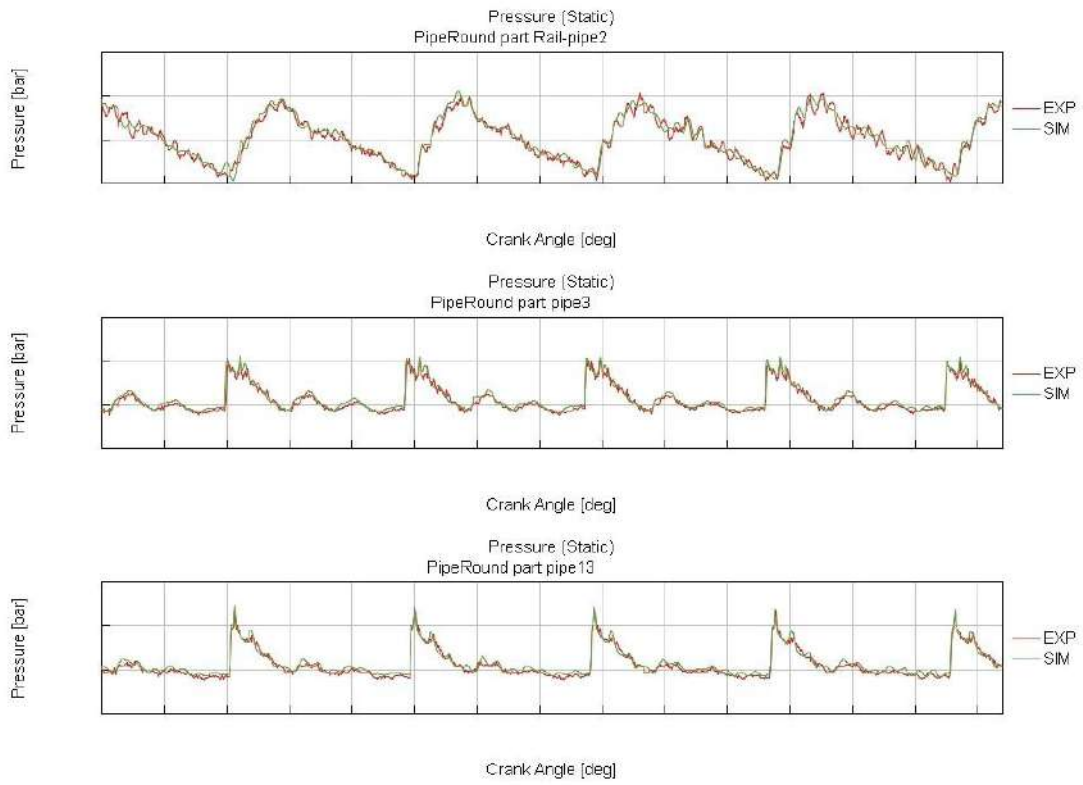


Figure 51 Pressure waves at 6000 RPM – Short pipe

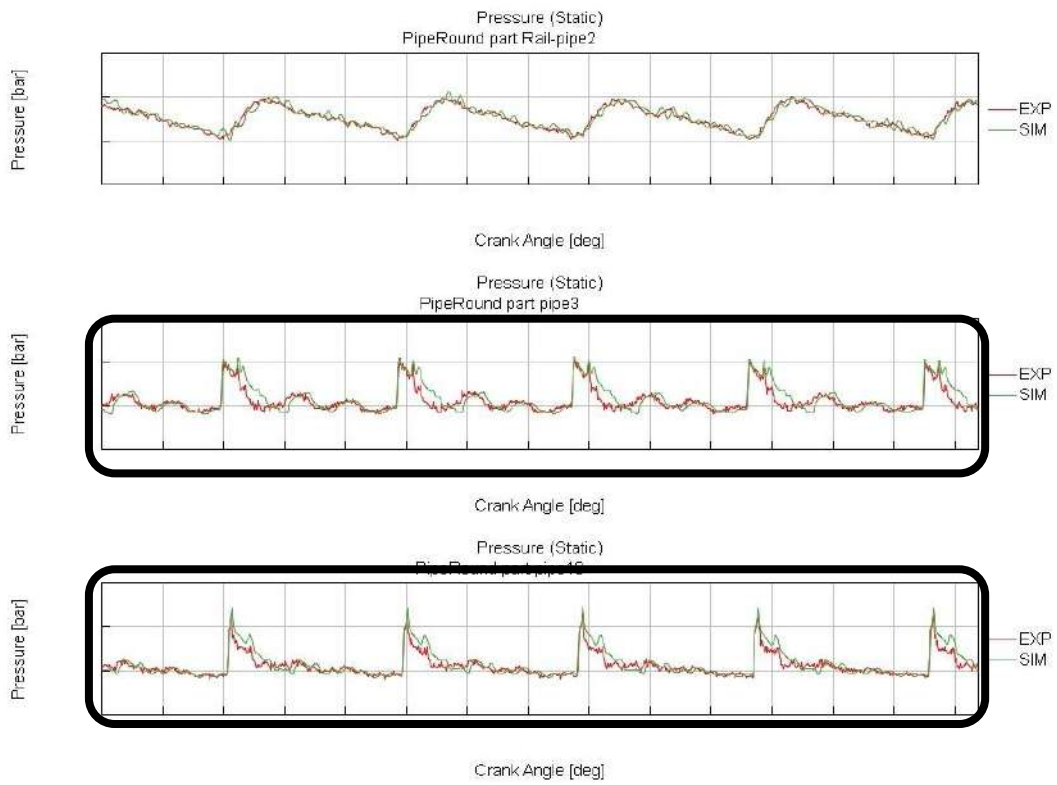


Figure 52 Pressure waves at 6000 RPM – Long pipe

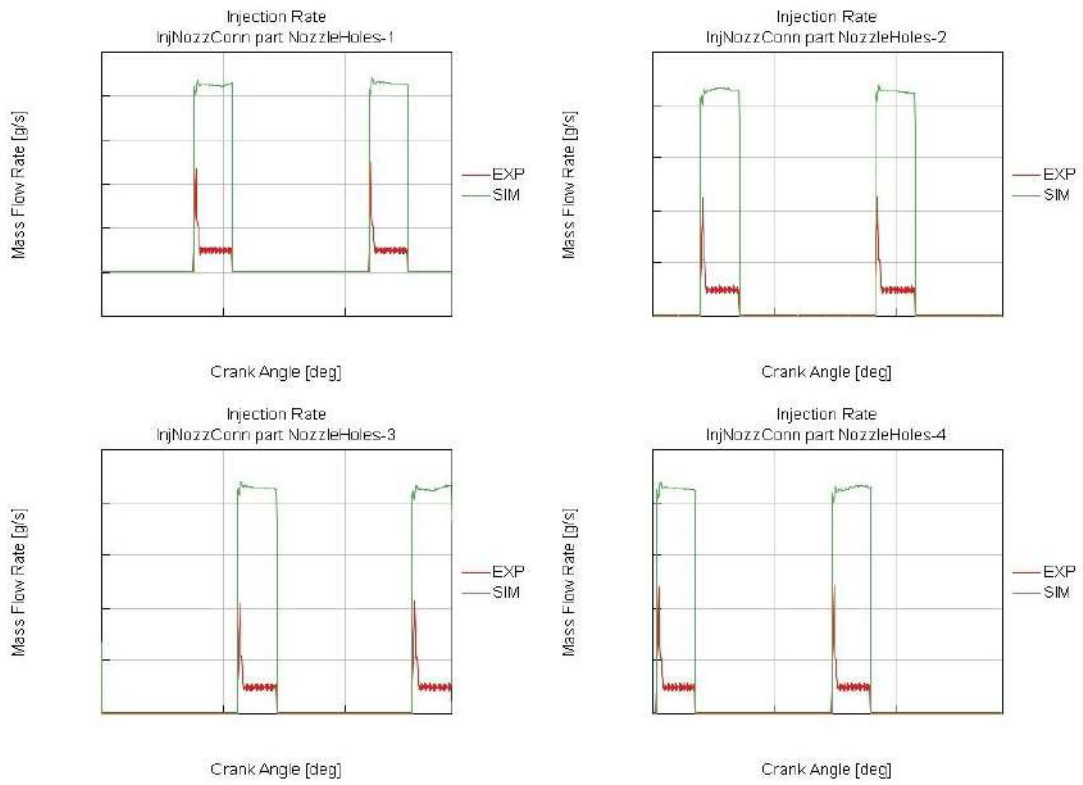


Figure 53 Mass flow rate at 6000 RPM – Short pipe

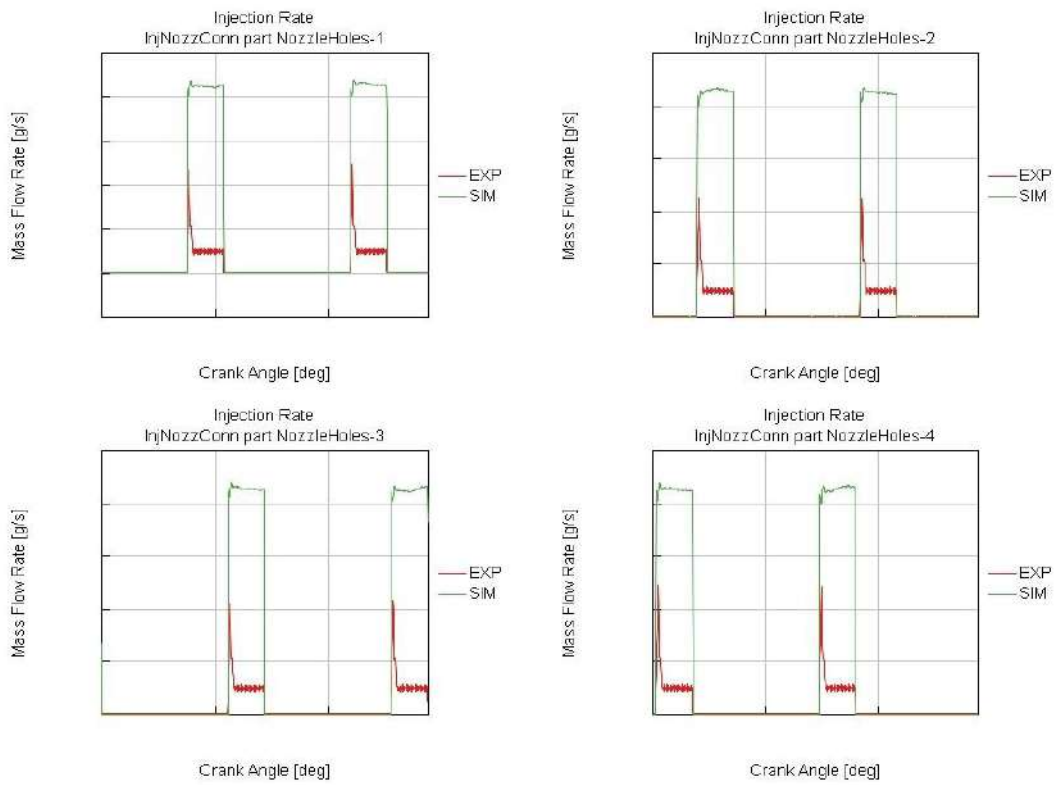


Figure 54 Mass flow rate at 6000 RPM – Long pipe

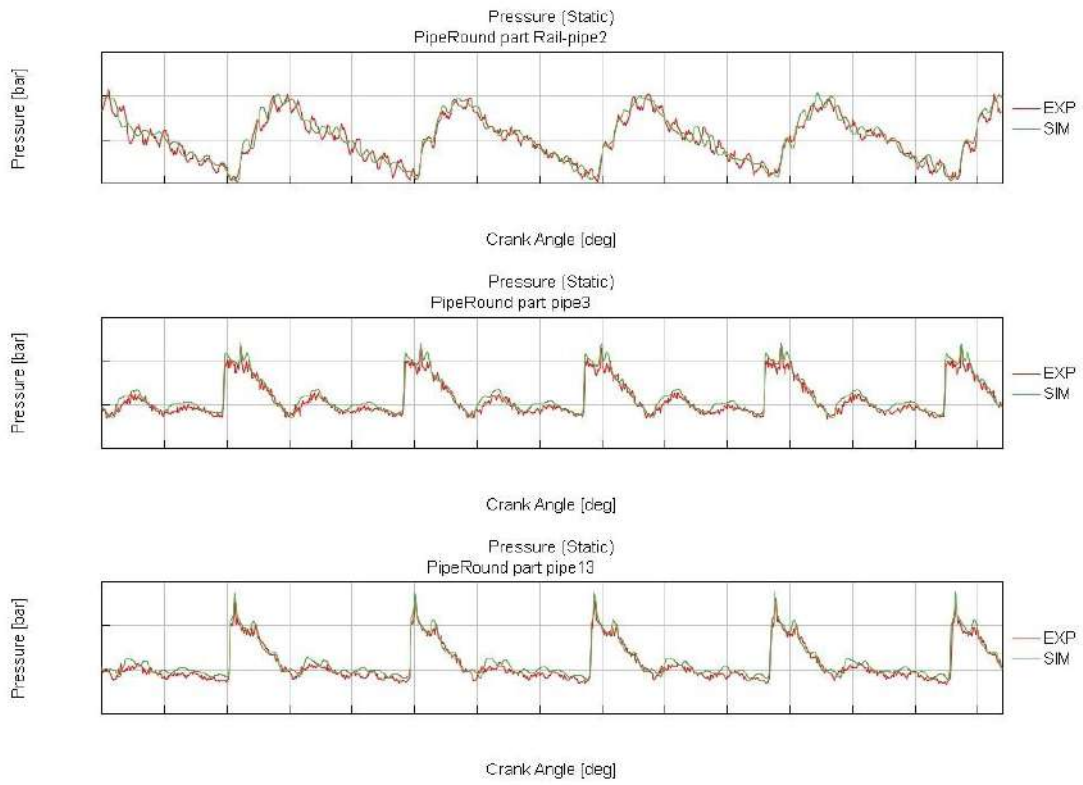


Figure 55 Pressure waves at 7000 RPM – Short pipe

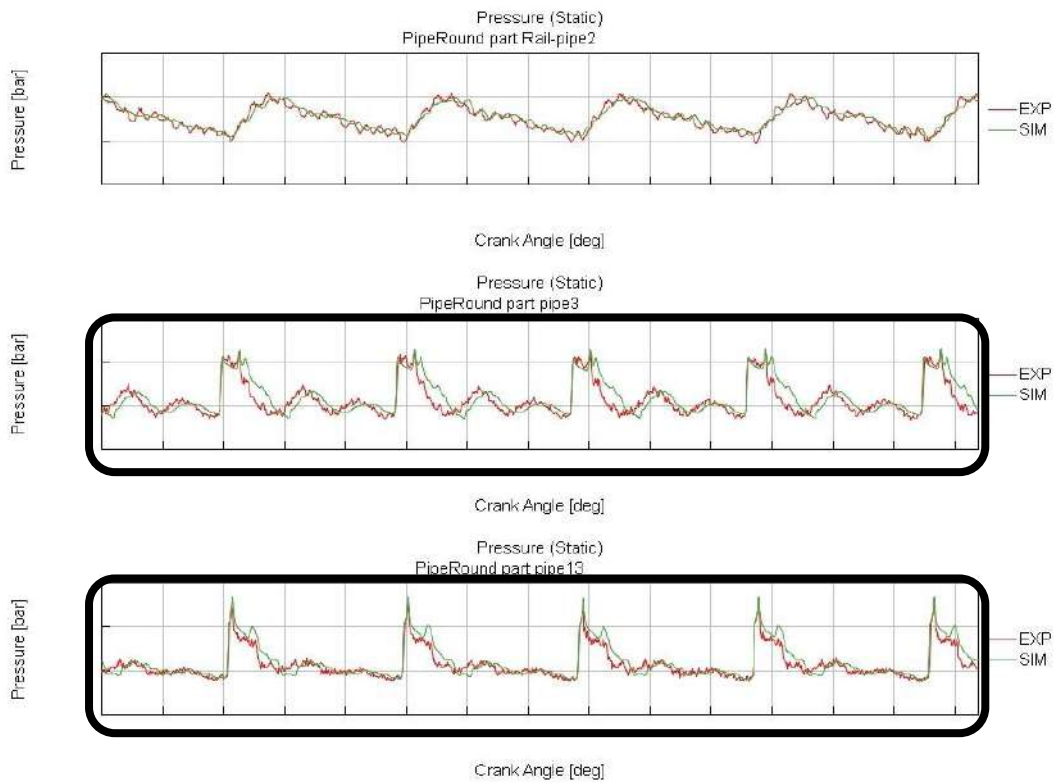


Figure 56 Pressure waves at 7000 RPM – Long pipe

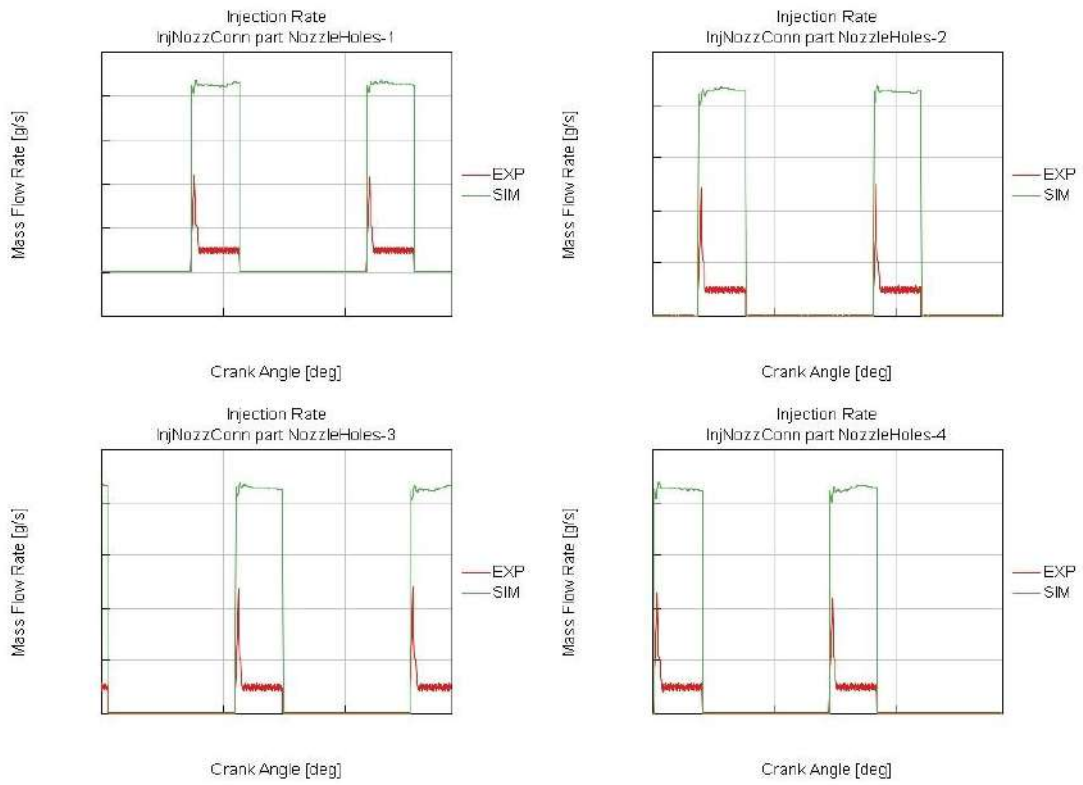


Figure 57 Mass flow rate at 7000 RPM – Short pipe

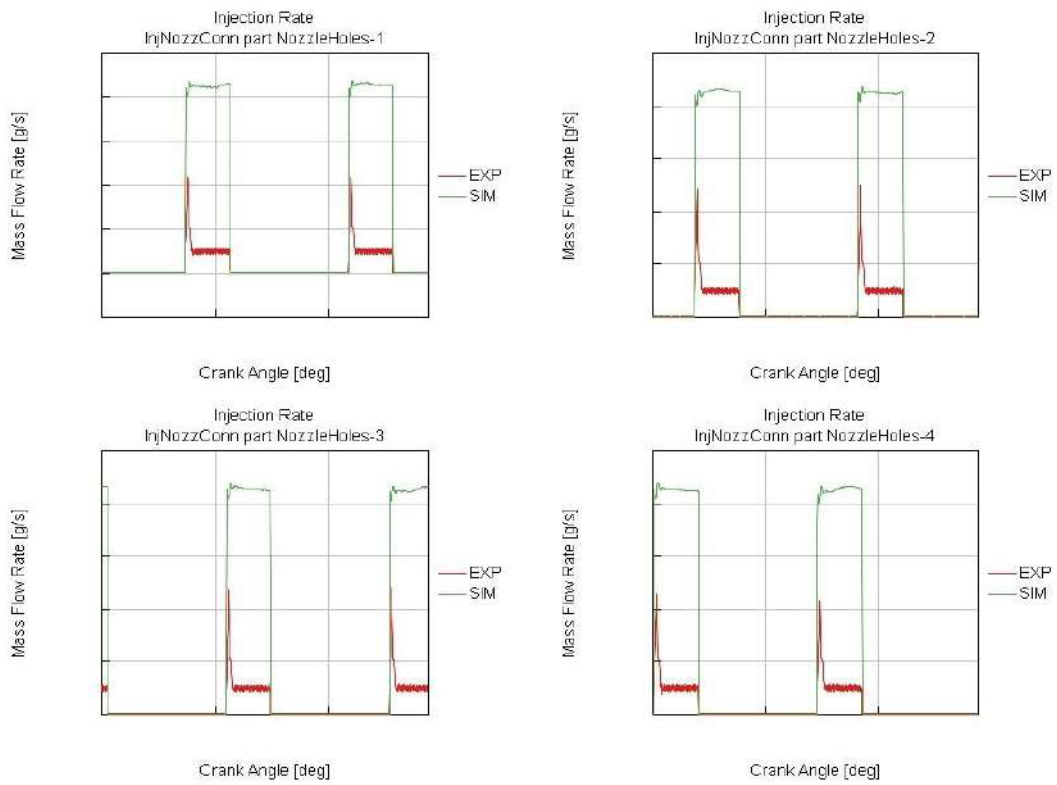


Figure 58 Mass flow rate at 7000 RPM – Long pipe

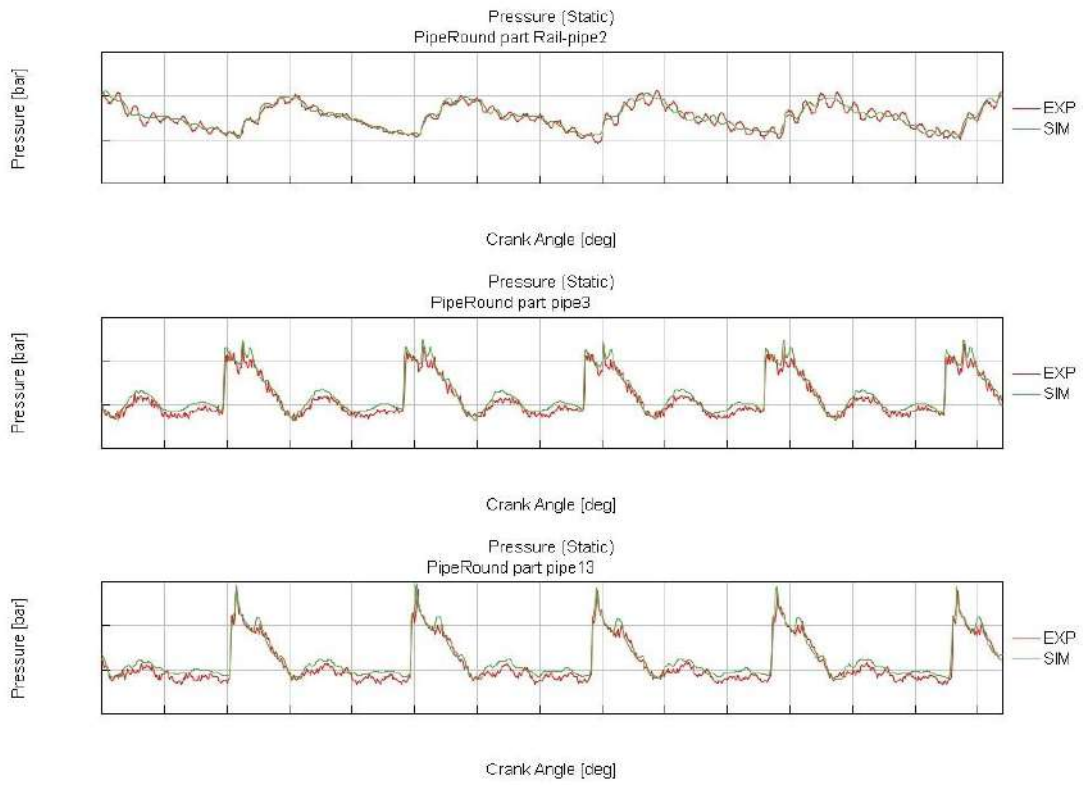


Figure 59 Pressure waves at 8000 RPM – Short pipe

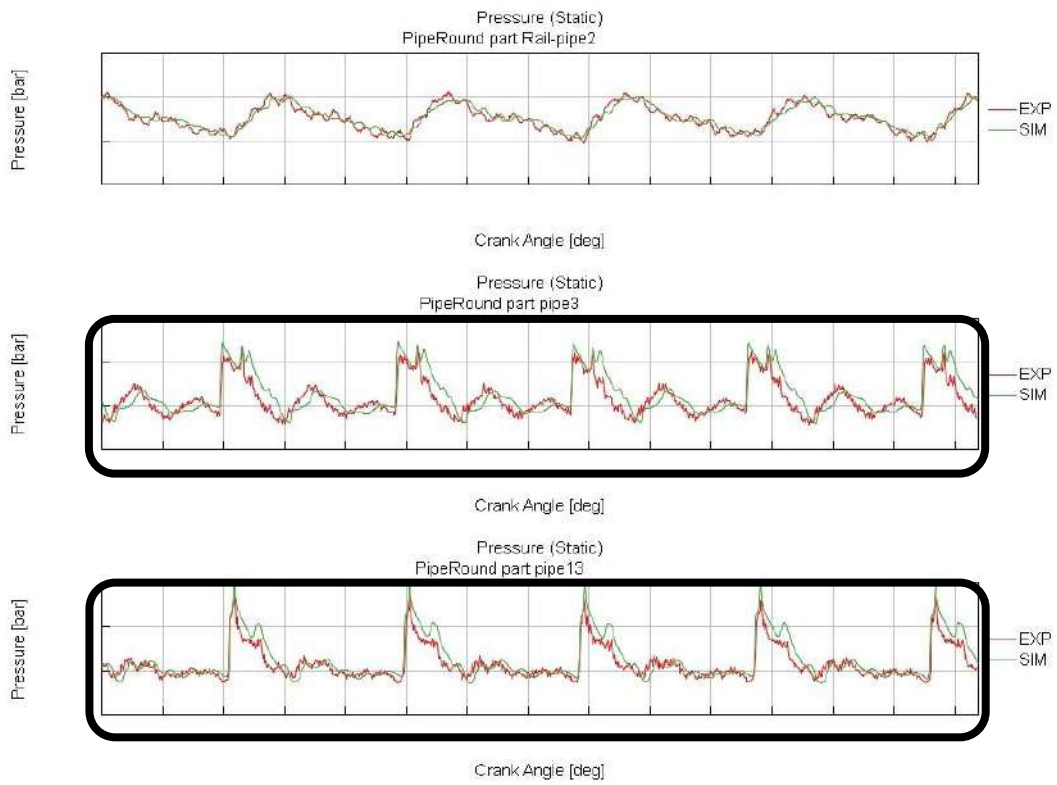


Figure 60 Pressure waves at 8000 RPM – Long pipe

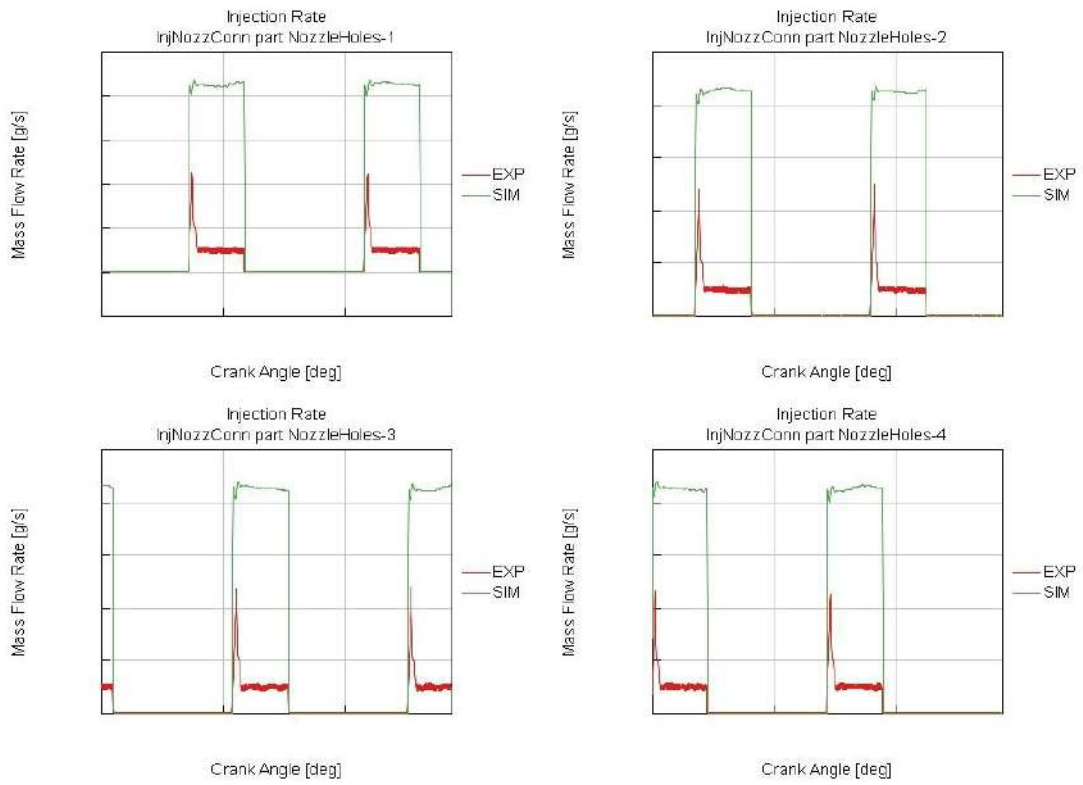


Figure 61 Mass flow rate at 8000 RPM – Short pipe

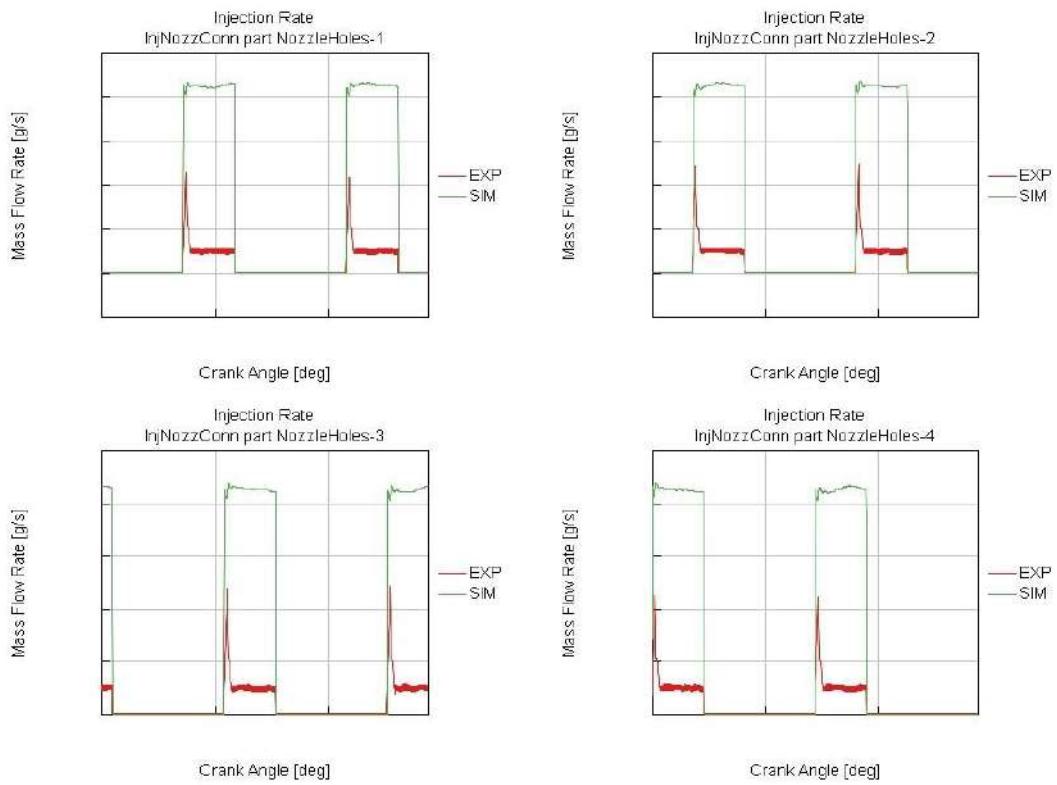


Figure 62 Mass flow rate at 8000 RPM – Long pipe

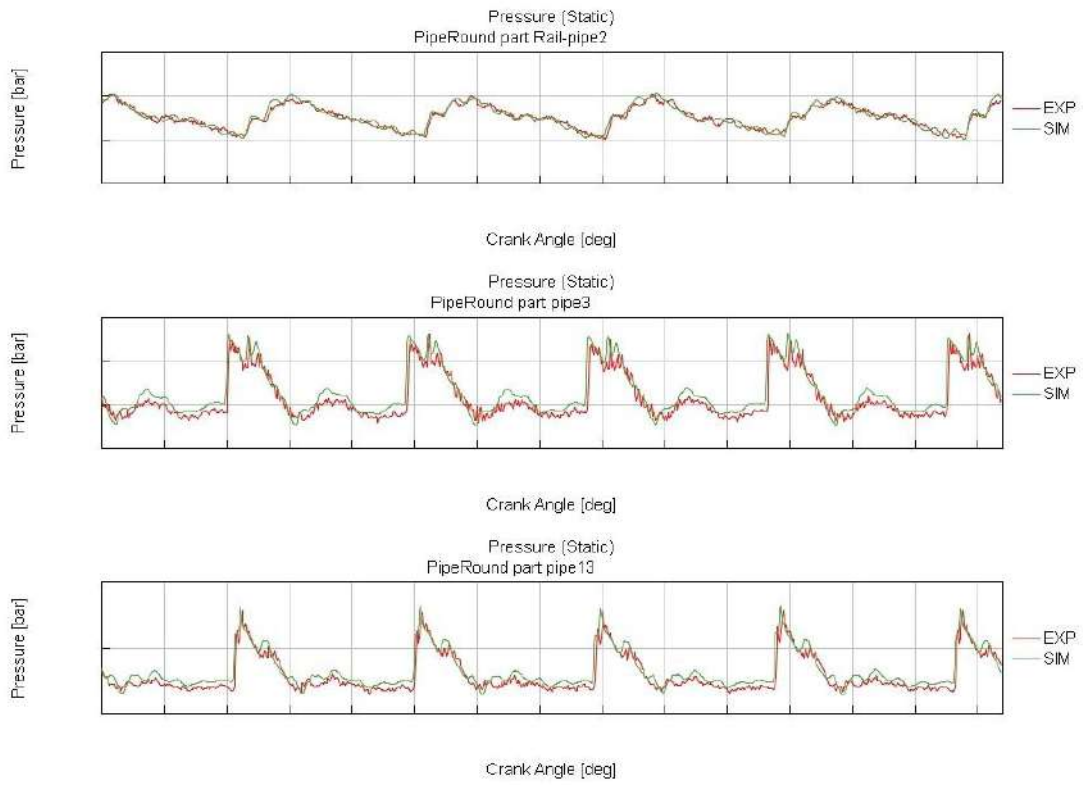


Figure 63 Pressure waves at 9000 RPM – Short pipe

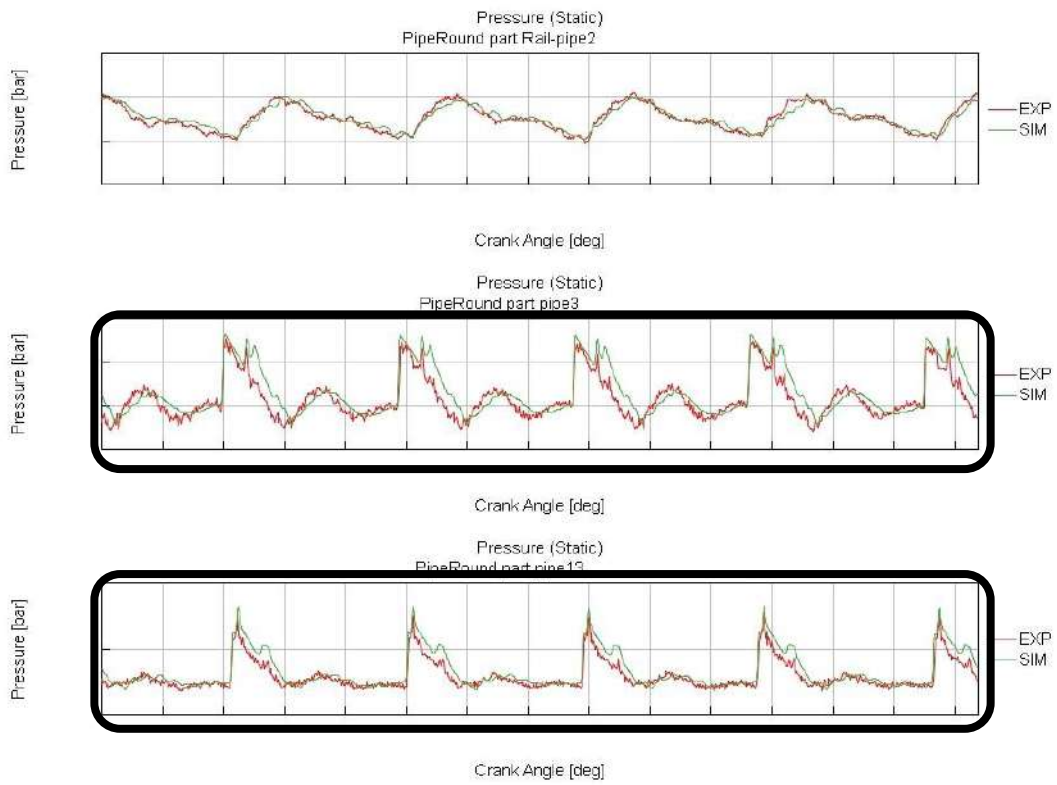


Figure 64 Pressure waves at 9000 RPM – Long pipe

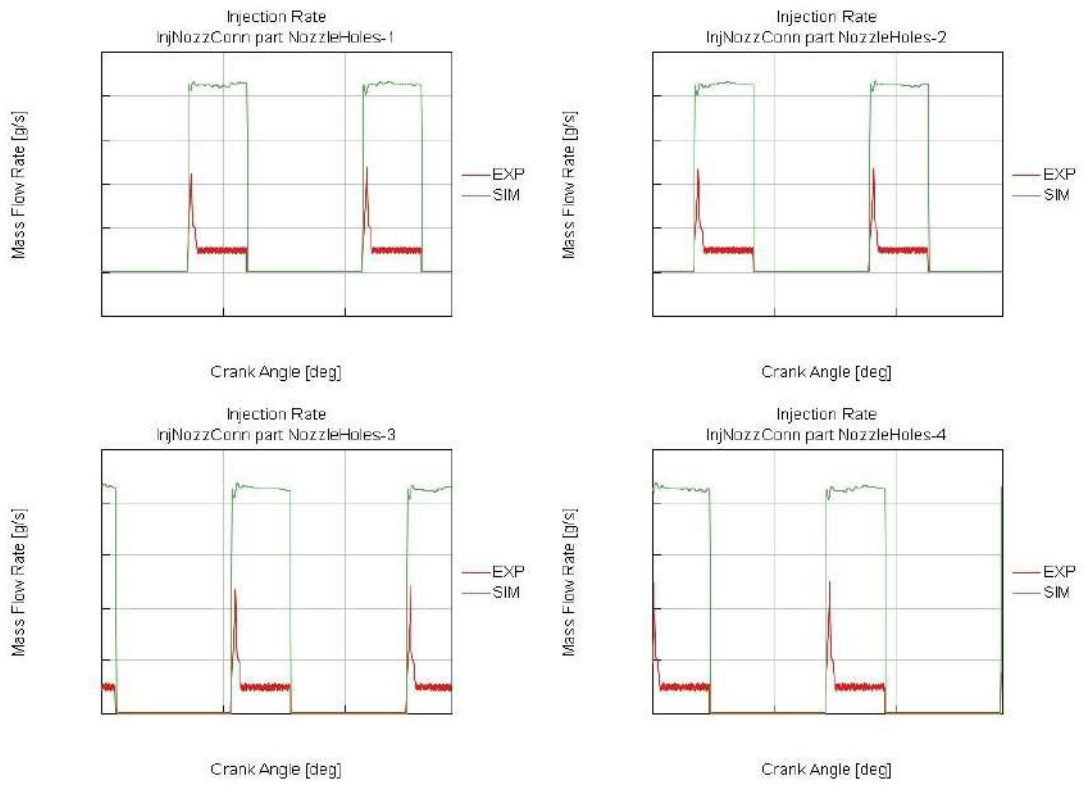


Figure 65 Mass flow rate at 9000 RPM – Short pipe

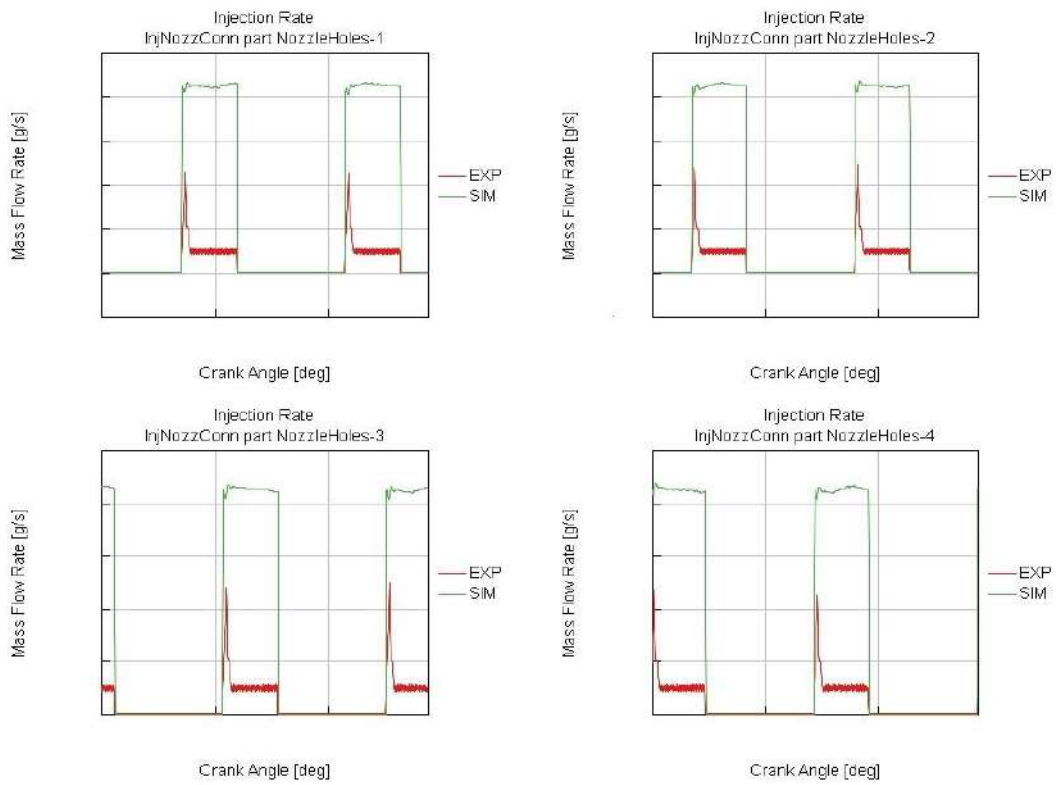


Figure 66 Mass flow rate at 9000 RPM – Long pipe

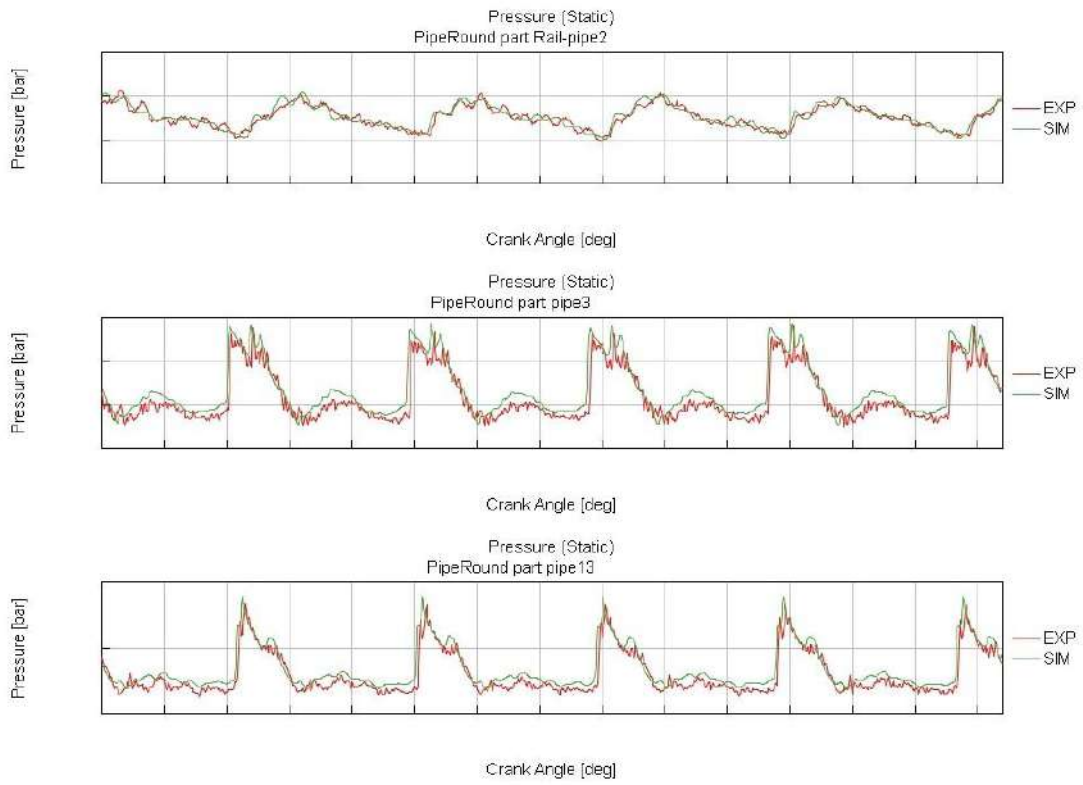


Figure 67 Pressure waves at MAX SPEED RPM – Short pipe

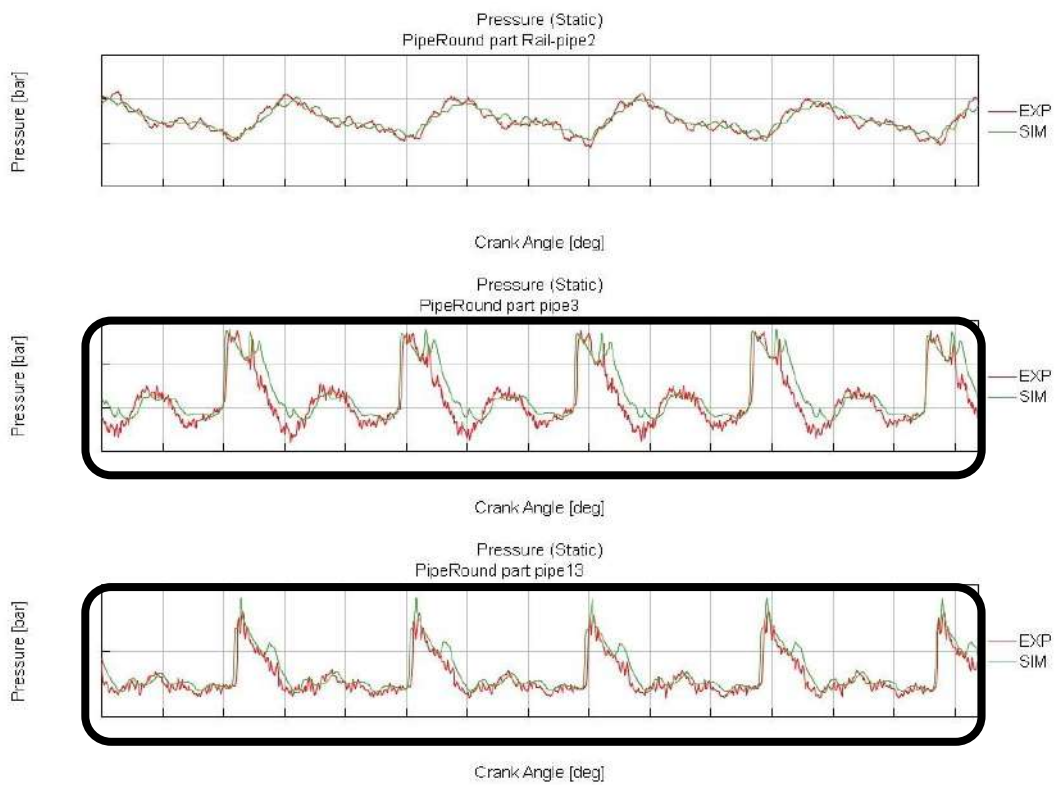


Figure 68 Pressure waves at MAX SPEED RPM – Long pipe

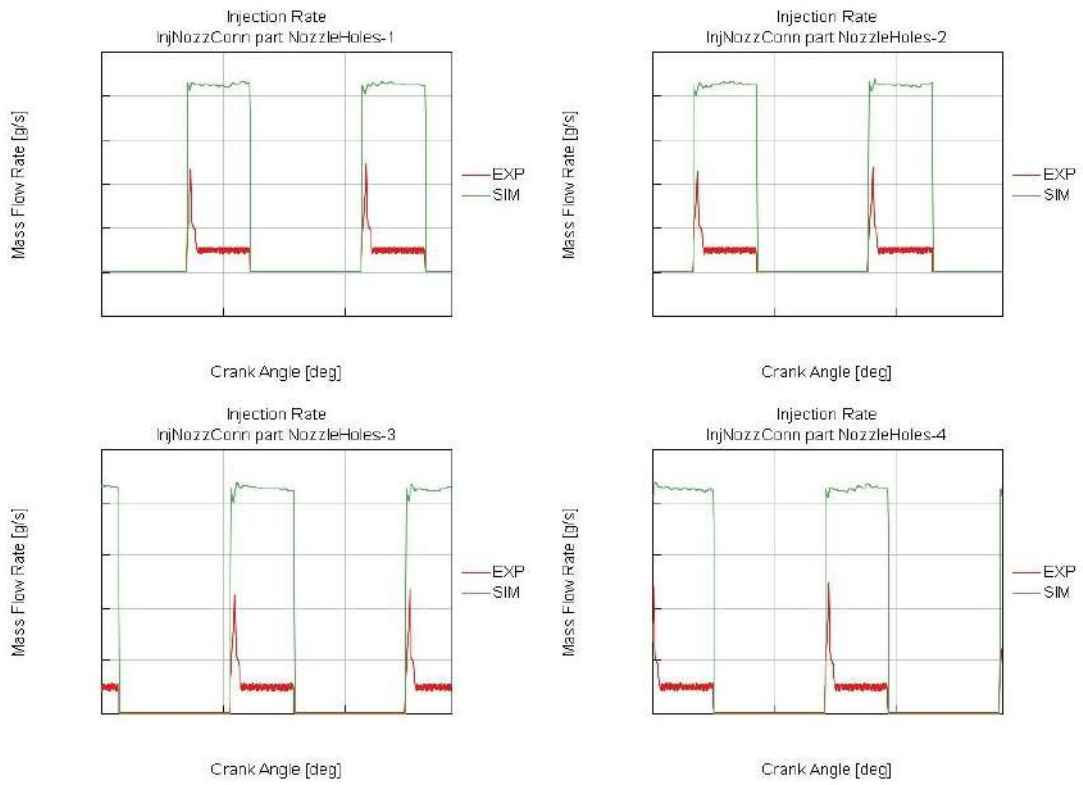


Figure 69 Mass flow rate at MAX SPEED RPM – Short pipe

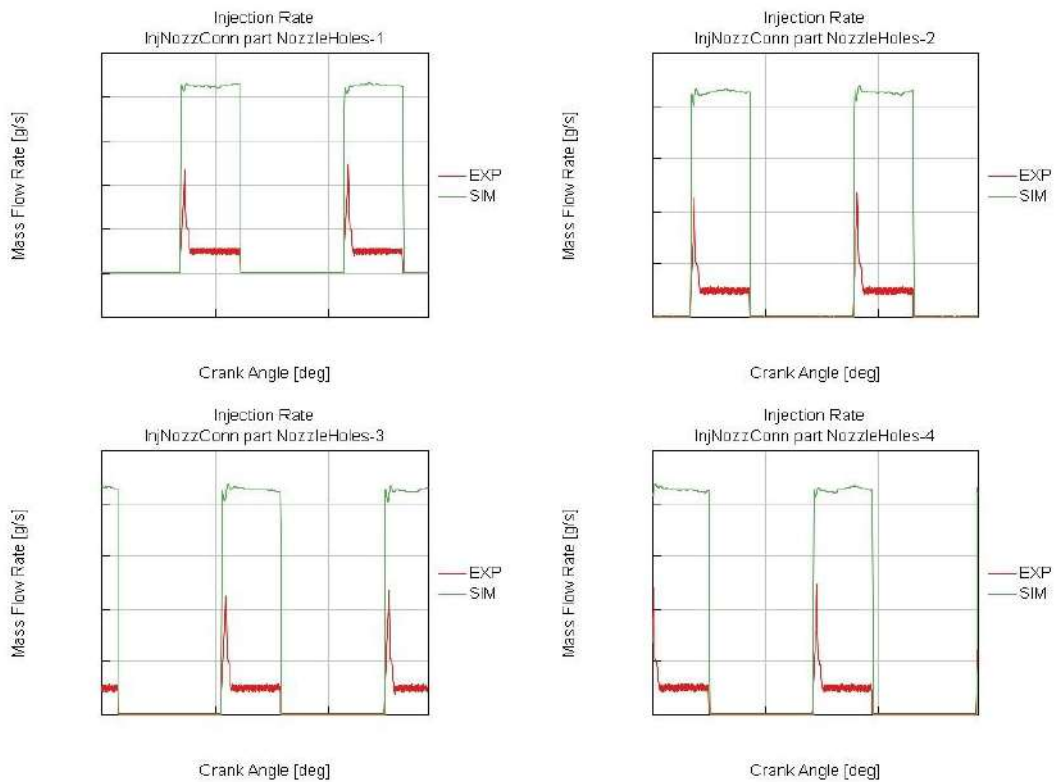


Figure 70 Mass flow rate at MAX SPEED RPM – Long pipe

5.5 Conclusions

GT-Power model manages in predicting quite reliably high and low frequency pressure waves. Also the injected mass is consistent with the one measured in the cell for all the points.

The only inconsistency regards pressure in the high pressure pipe for long pipe configurations. From 5000 rpm to maximum speed there is a delta between red curve and green curve. There is an overestimation of the model respect to experimental values in the pumping phases.

The reason can be found in the high pressure pipe geometry. Probably the effective rail diameter is a little bit out of tolerance. The simulation gives very exact results instead of experimental tests that are made on real components and for this reason not so accurate.

Finally, the model works well and it can be used for example for other points not tested or for other configurations not explored.

6

Control of the GDI pump in MIL environment

6.1 Model based design

In the software world, model-based design has appeared as the best way to meet cost, quality and time requirements.

A model is a set of equations, laws or rules describing a system behaviour, more or less accurately, according to the kind of phenomenon studied. Physical prototype can be replaced by virtual model, adjusted using experimental database to be as close as possible to reality and simulated to analyse system behaviour in all the possible scenarios.

During conception, these models will also be useful to try new features like choosing the motor type of a hybrid vehicle.

Model Based Design approach saves time during the designing phase of onboard software by testing each feature when it is developed. From the drafting of the specifications, it is possible to evaluate the feasibility of the customer's requirements. Each step of the development

benefits from this method thanks to the quick prototyping and modular solutions for simulation (hardware in the loop software and model in the loop).

Model based design approach eases system sizing by showing performance limits in early phases of the development.



Figure 71 MIL-SIL-HIL cycle

6.2 MIL, SIL and HIL

Hardware in the loop (HIL), Software in the loop (SIL) and Model in the loop (MIL) solutions allow to validate the developed solutions with simulations of real situations.

Their use accelerates design and enhances quality mastery, while reducing the appeal to real prototypes and physical tests.

Here is a short description of an “in the loop” simulation solution, in chronological order:

- **MIL:** Model in the Loop.
First, there is the necessity to develop a model of the actual plant (hardware) in a simulation environment such as GT-Power, which captures most of the important features of the hardware system. After the plant model is created, is developed the controller model (in Simulink environment) and is verified if the controller can control the plant as for the requirement. This step is called Model-in-Loop (MIL) and it tests the controller logic on the simulated model of the plant. If the controller works as desired, controller input and output should be recorded and they will be used in the later stage of verification;
- **SIL:** Software in the Loop.

Unit tests are run on the code that will be implemented into the ECU to correct errors related to system functioning (code generation validation);

- **HIL:** Hardware in the Loop.

Control laws are loaded onto a physical ECU connected to the simulation environment and sometimes to an actual mechanical part, so to check equipment implementation of control and response time (integration validation).

These phases help to test a maximum of scenarios in early development in order to reduce the average cost of tests.

6.3 Simulink software

Simulink is a graphic programming software, with blocks structure present in MATLAB, that admits the design and the simulation of mathematical models and physical systems in an interactive way.

The user interface offers a wide blocks library, some predefined and other in some way editable and customizable from the user, and it is totally integrated with the MATLAB work environment: it is indeed possible to import variables of whatever type, coming from the workspace, to generate textual output in the command window and to export simulation results through graphics, variables or mat files.

The simulations carried on in Simulink foresee the setup of a temporally interval and an integration step, that can be fixed or variable, in order to define the characteristics of the solver. The solver can in turn be selected between different characteristics provided by Simulink that differ for precision and rapidity of convergence.

6.4 Goals

The purpose of the control of the GDI pump in MIL environment is to have a modelling of the control in order to make pre-calibrations in simulation.

MIL is useful to avoid tests in the cell because it is possible to replicate what happens in the ECU on Simulink and, connecting it to the physical model, it is allowed to pre-calibrate for example PI map in advance compared to engine tests.

6.5 Control algorithm

The control algorithm aim consists in the calculation of the exact phasing of the closing inlet valve.

In order to obtain this target, it is necessary to calculate the needed flow for when the desired pressure value (using a closed-loop system) is reached and from this, thanks to the inverse pump characteristic, it is possible to define the angle before pump TDC at which there will be the closure.

A wrong definition of the closing dynamics or of the inverse modelling leads to a different flow from the one requested with an error that will increase, increasing engine speed.

6.6 Modeling phase

Simulink has been used with the purpose of modelling the control blocks of the GDI pump. This phase consisted in a translation and adaption of pre-existent models described inside a technical manual. A simplified scheme of the modelled blocks and a panoramic of the existing interactions are shown in *Figure 72*. Follows the description of each single module function.

6.6.1 Scheme of the GDI pump control model

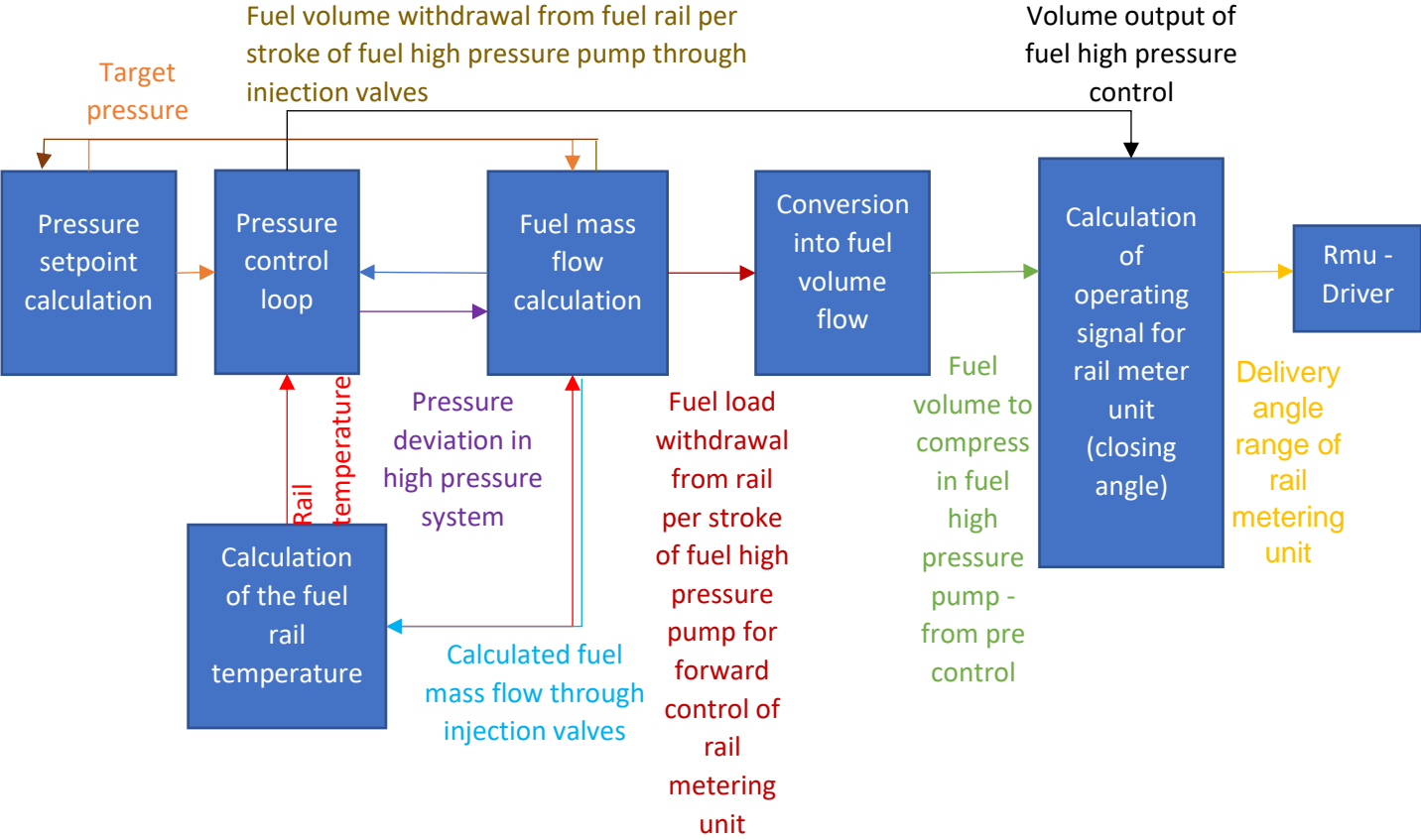


Figure 72 Scheme of the GDI pump control model

In Figure 72 a scheme of the GDI pump control model is reported highlighting models functions and interactions.

Going from left to right, there are carried out:

- pressure setpoint calculation;
- pressure control loop;
- fuel mass flow calculation;
- conversion into fuel volume flow;
- calculation of the operating signal for rail mater unit (closing angle);
- calculation of the fuel rail temperature model.

6.6.2 Fuel System Scheme

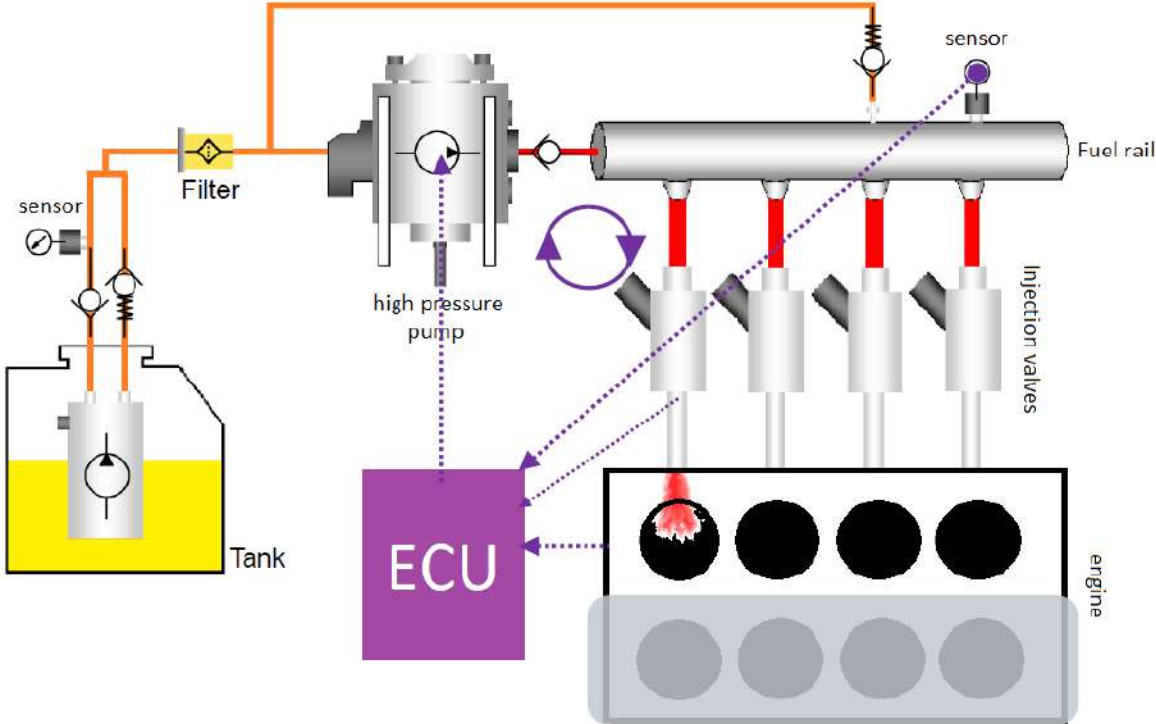


Figure 73 Fuel system scheme

In Figure 73 the entire fuel system is represented with a simplified scheme. It consists of a tank that feeds the high pressure pump, a high pressure pump, a fuel rail, injectors, cylinders and the ECU.

The ECU receives input signals like rail pressure, fuel injected, cylinder displacement and it sends the output in order to find the MSV angle at which there will be the pump inlet valve closure to pursue the desired target pressure.

6.6.3 Rail pressure target

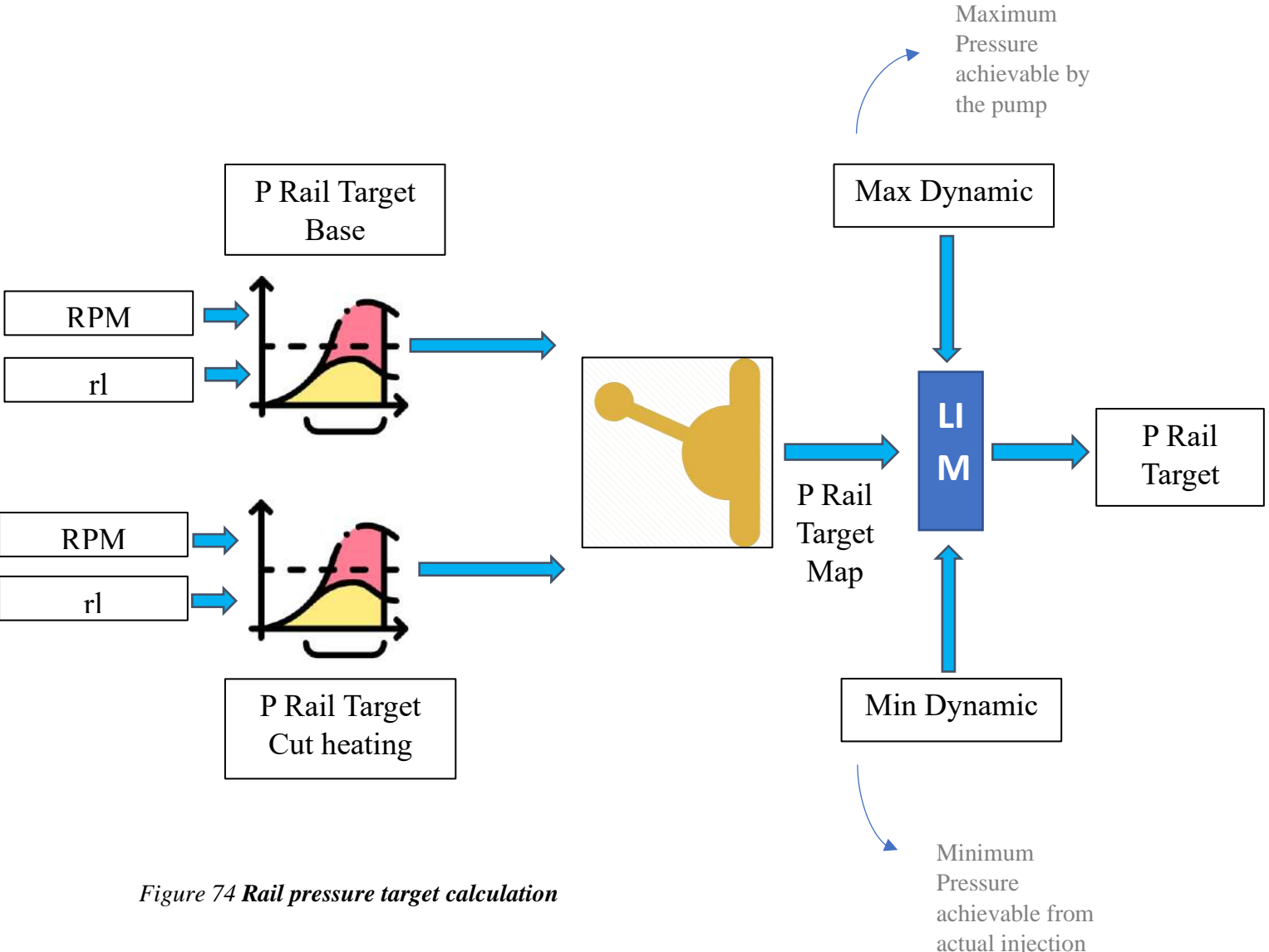


Figure 74 Rail pressure target calculation

In rail pressure target scheme, *Figure 74*, rail pressure target map is obtained from the combination of two maps: rail pressure target base map and rail pressure cut heating map both in function of speed and load. After pressure limits, the minimum achievable from actual injection and the maximum achievable by the pump, rail pressure target is obtained.

6.6.4 PI controller

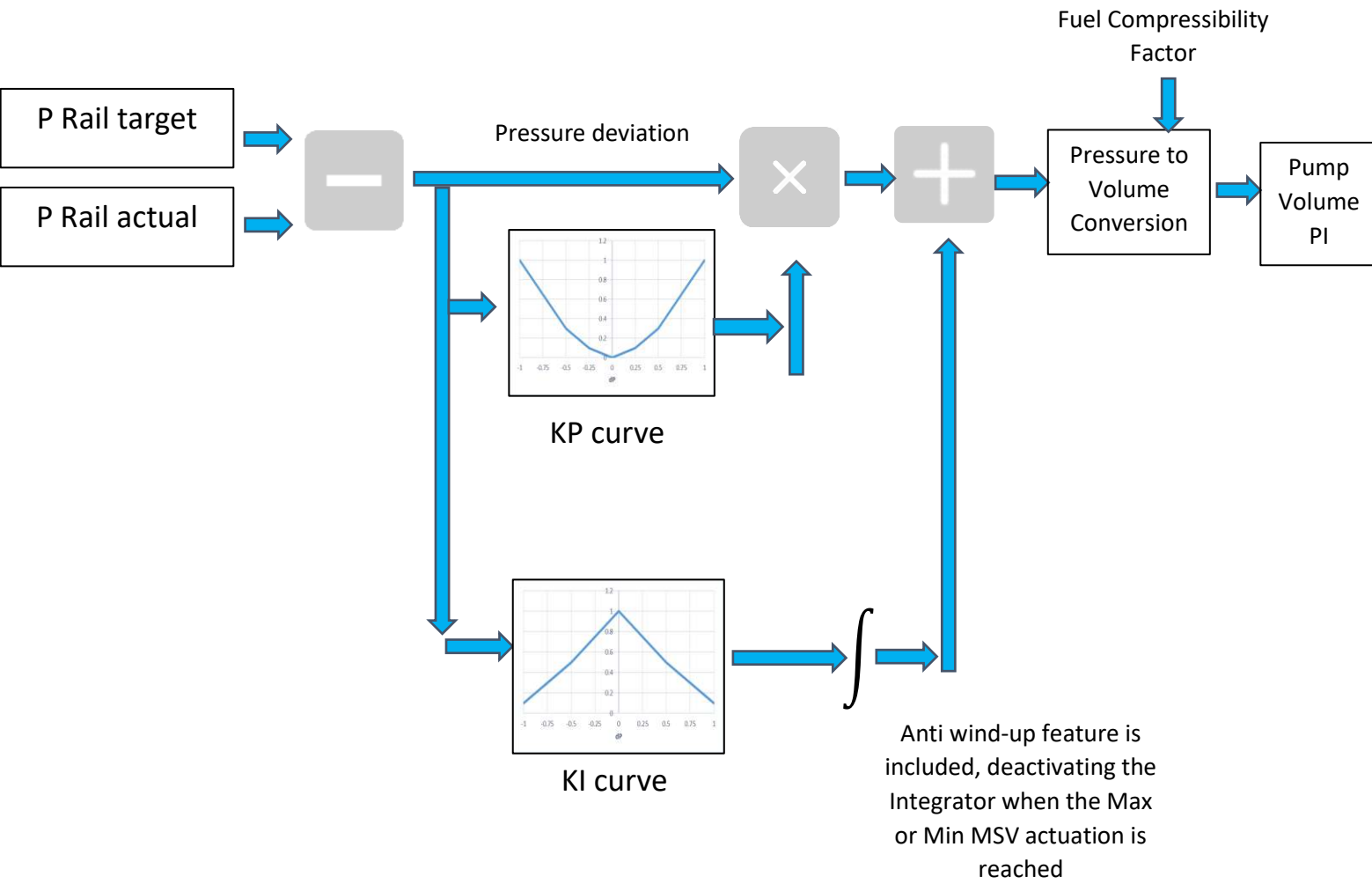


Figure 75 PI controller scheme

PI controller, *Figure 75*, is made by a proportional and integrative part. The PI input, pressure deviation, is calculable with the difference between target pressure and actual rail pressure. The given output is a volume quantity obtained after the conversion from pressure through compressibility factor.

6.6.5 Pre-control injected volume per stroke calculation

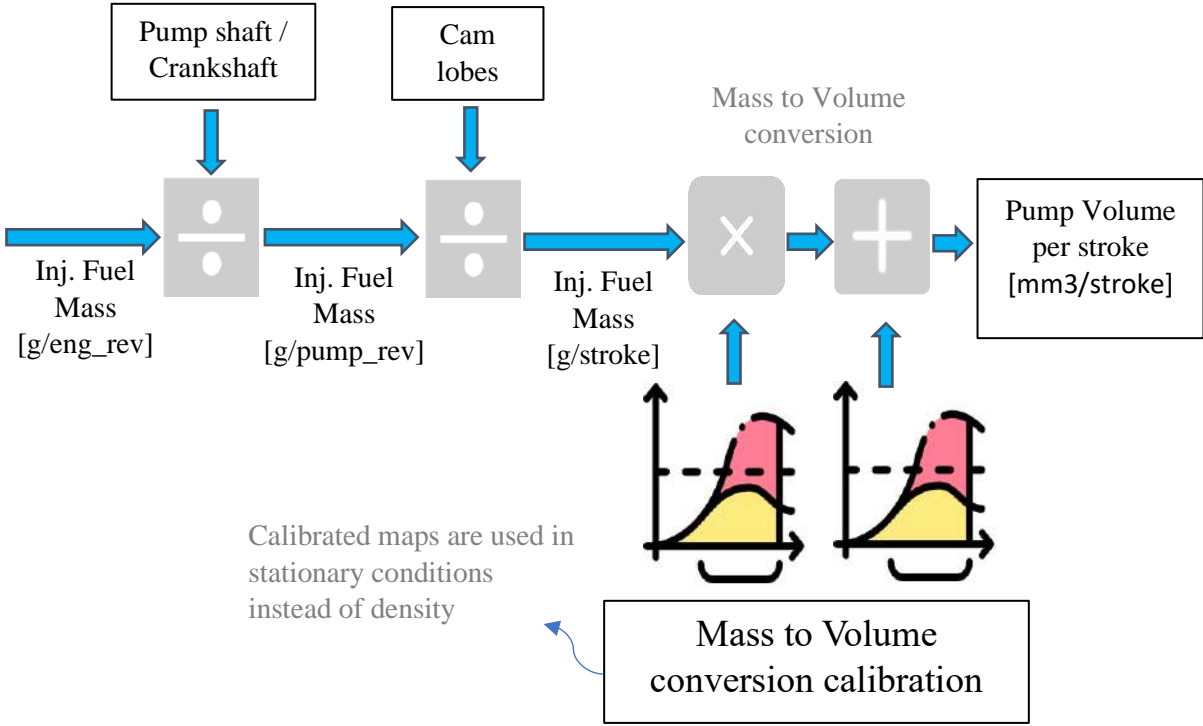


Figure 76 Pre – Control Injected Volume per stroke calculation

In Figure 76, the injected fuel mass per engine revolution is divided for the pump shaft-crankshaft ratio and for the cam lobes to obtain injected fuel mass per stroke. Hence, the conversion from mass to volume thanks to calibrated maps used in stationary conditions instead of density.

6.6.6 MSV actuator control

Control is based on the Pump Volume delivery calculation and the MSV angle, with respect to Pump TDC, is found using the pump geometries.

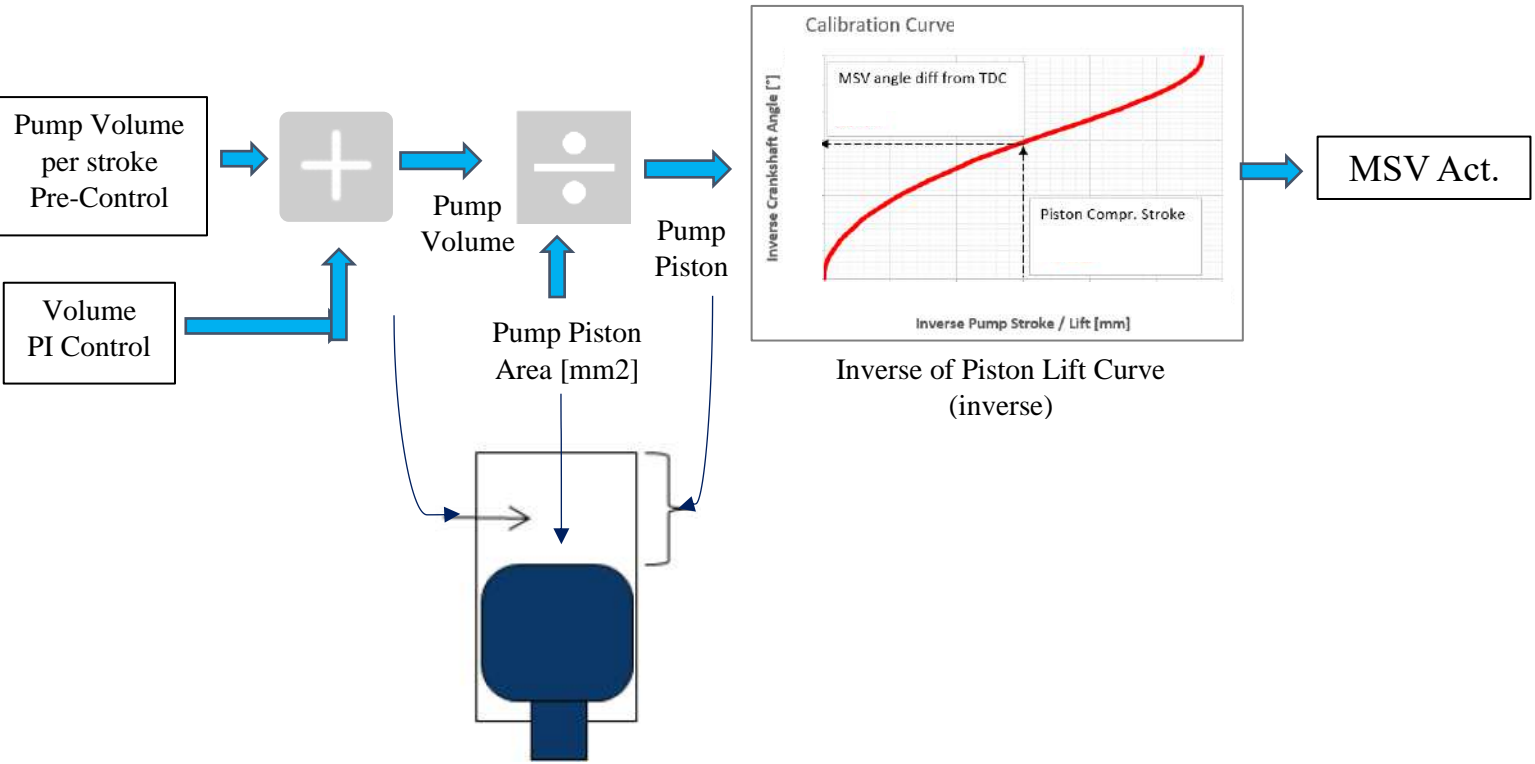


Figure 77 MSV actuator control

The final block is shown in Figure 77. Adding the pump volume per stroke given by the pre-control and the volume PI control, pump volume is calculated. After having found the pump piston, i.e. compression stroke, it is possible to extrapolate the value of the MSV angle, at which the inlet valve has to be closed before pump TDC, from the inverse of piston lift curve.

6.6.7 Fuel rail temperature model

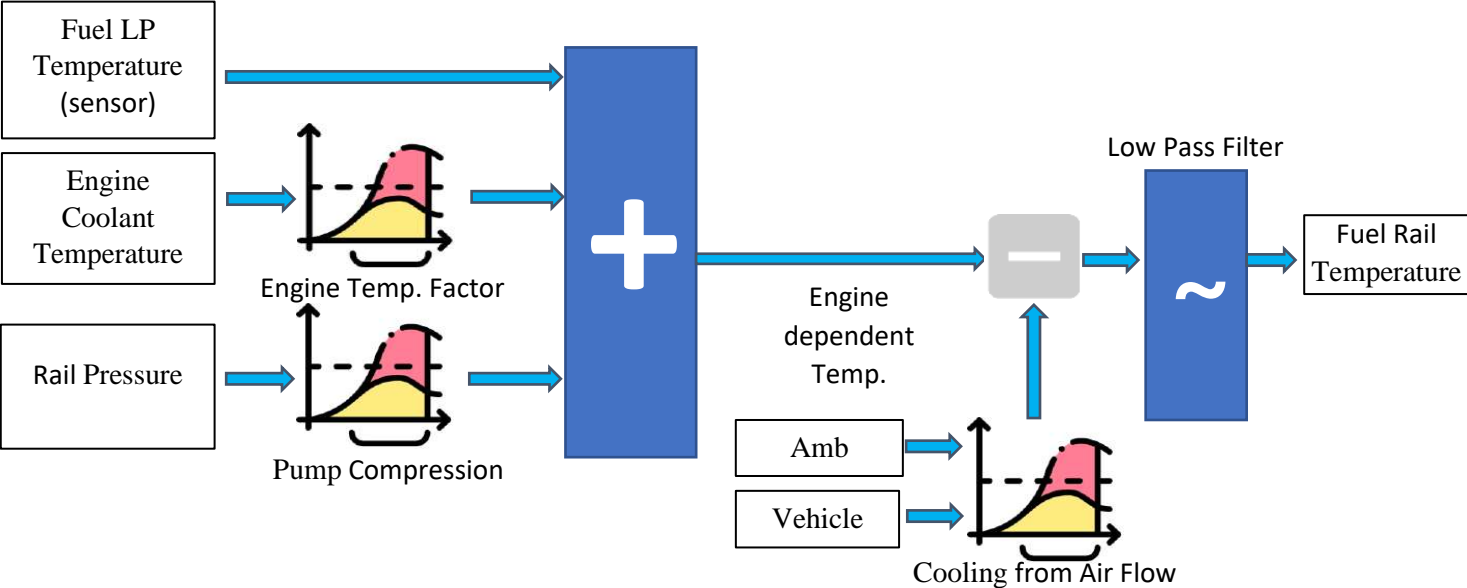


Figure 78 Fuel Rail Temperature Model

In Figure 78, fuel rail temperature is given by the sum of three contributors:

- low pressure fuel temperature measured with a sensor;
- engine coolant temperature;
- rail pressure.

Fuel rail temperature is found as the difference between engine dependent temperature and cooling from air flow.

6.7 Validation phase

Validation phase consists in verifying that all modules, alone and together, work well.

In order to do this, is necessary the use of experimental values, i.e. acquisitions, in input so to compare the outputs given by the model with the outputs coming from experimental data.

If they are superimposed the entire model is validated: it gives reliable results.

6.7.1 Results

A lot of outputs have been generated. A selection of the most important ones brought to show only three of them:

- angle before pump TDC at which there is inlet valve closure (MSV actuator control module output) ;
- Pre-control volume (Pre-control injected volume per stroke calculation module output);
- Pump volume PI (PI controller module output).

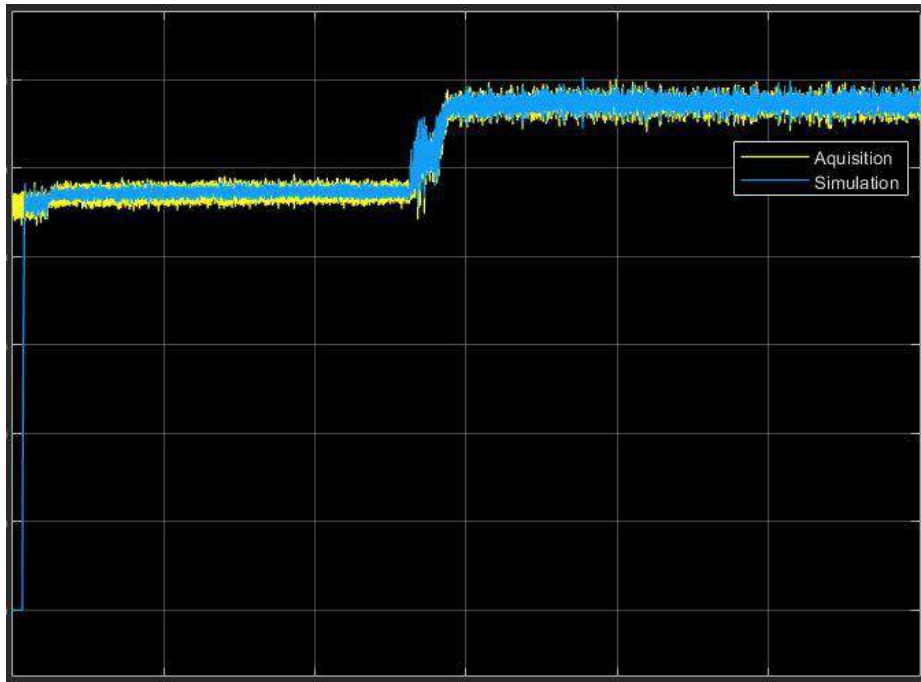


Figure 79 Angle before pump TDC at which there is inlet valve closure

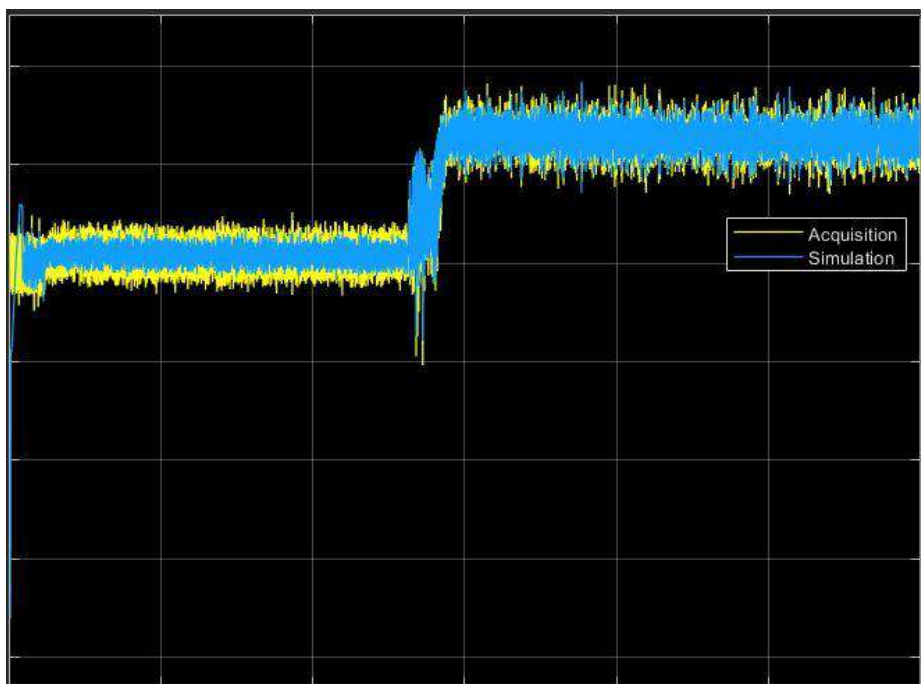


Figure 80 Pre-control volume

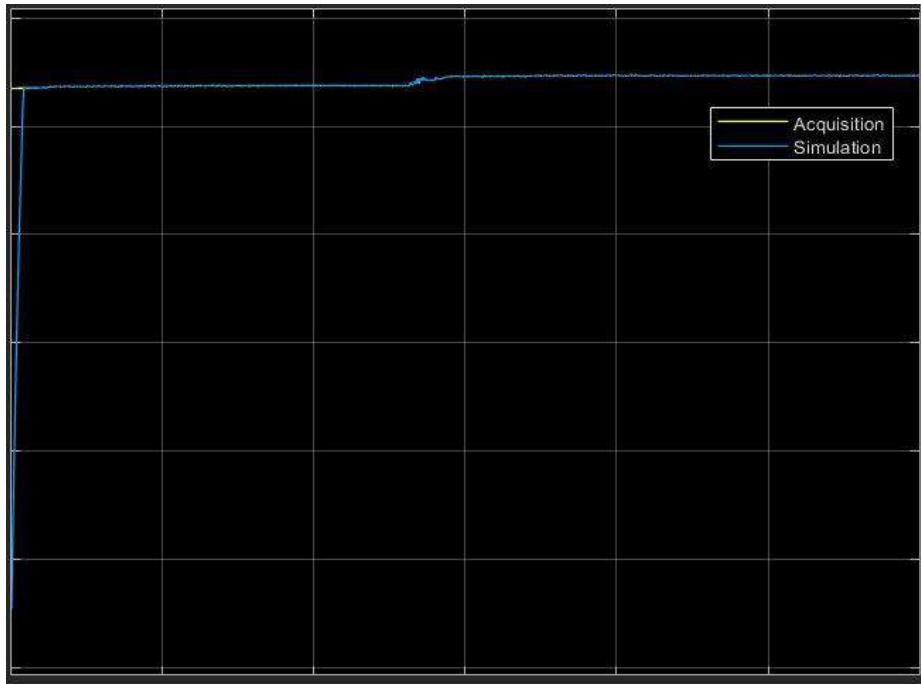


Figure 81 Pump volume PI

In *Figures 79, 80, 81*, yellow and blue lines are largely superimposed even if the PI, in particular the integrator part, does not respond exactly at what happens in the ECU. The reason can be found in the different time steps used.

6.8 Co-simulation phase in MIL environment

After the modeling and validation phases on Simulink, the control of the GDI pump in MIL environment has been done. The aim is to validate the MIL in order to be able to pre-calibrate the GDI control. Using the base calibration given by Automobili Lamborghini S.p.A., these are the results changing engine speed and load.

Each figure is made of two subplots:

1. angular rage in which the inlet valve is closed;
2. comparison between target and actual pressures paying attention on the moment in which the target is reached.

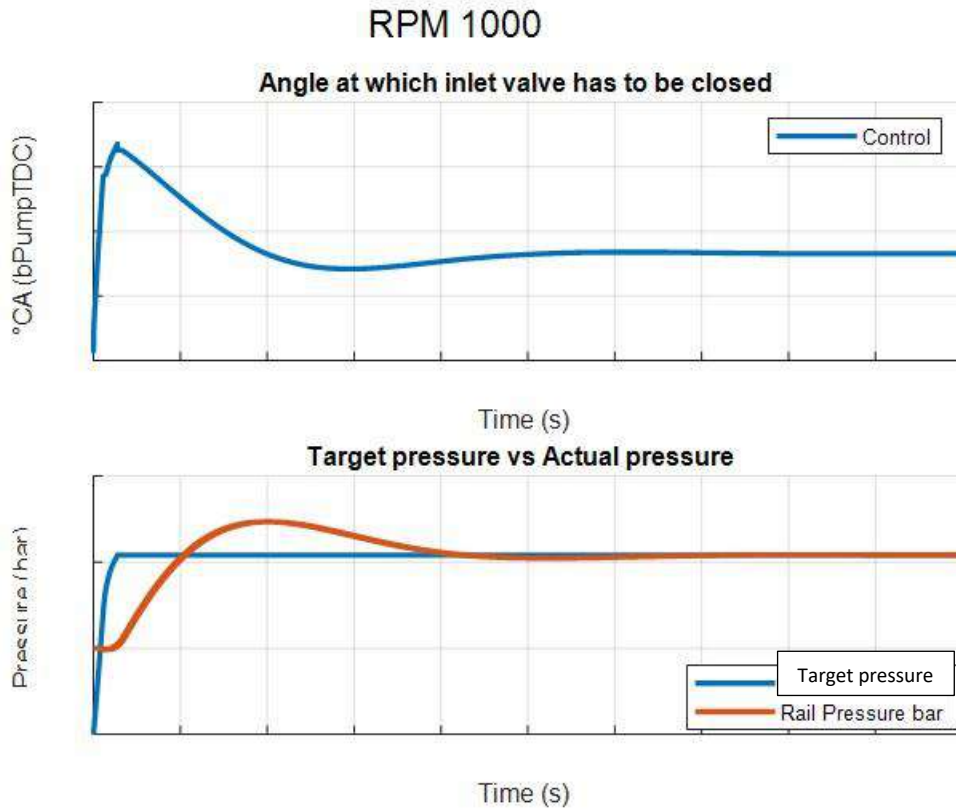


Figure 82 RPM 1000

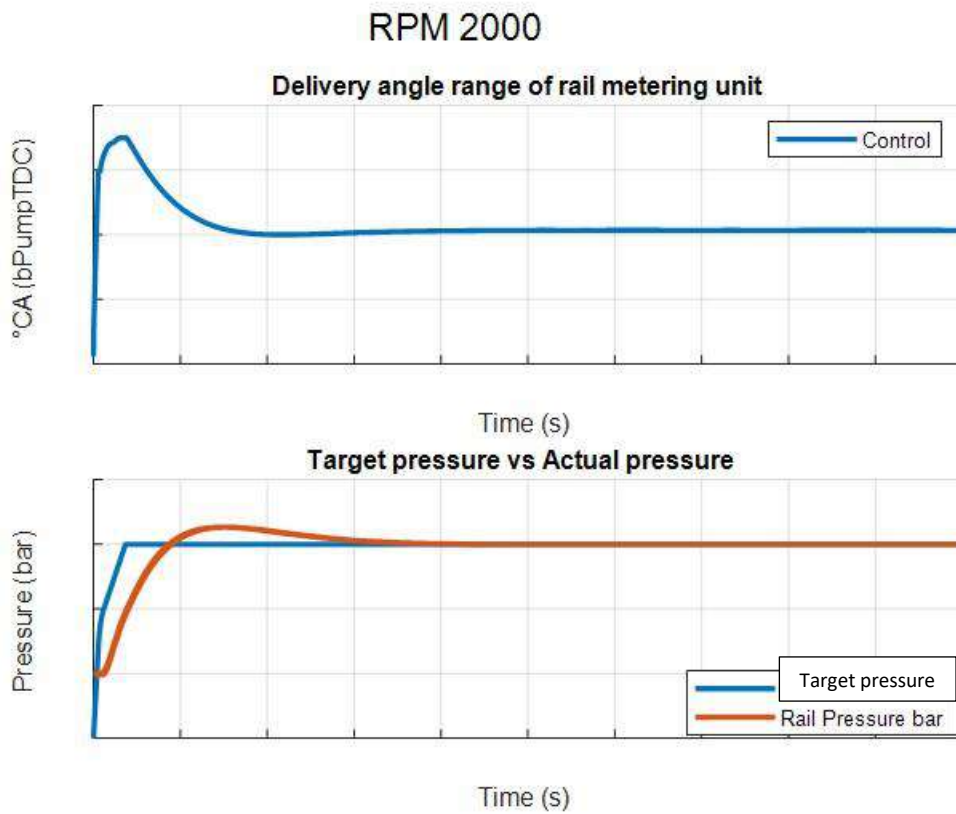


Figure 83 RPM 2000

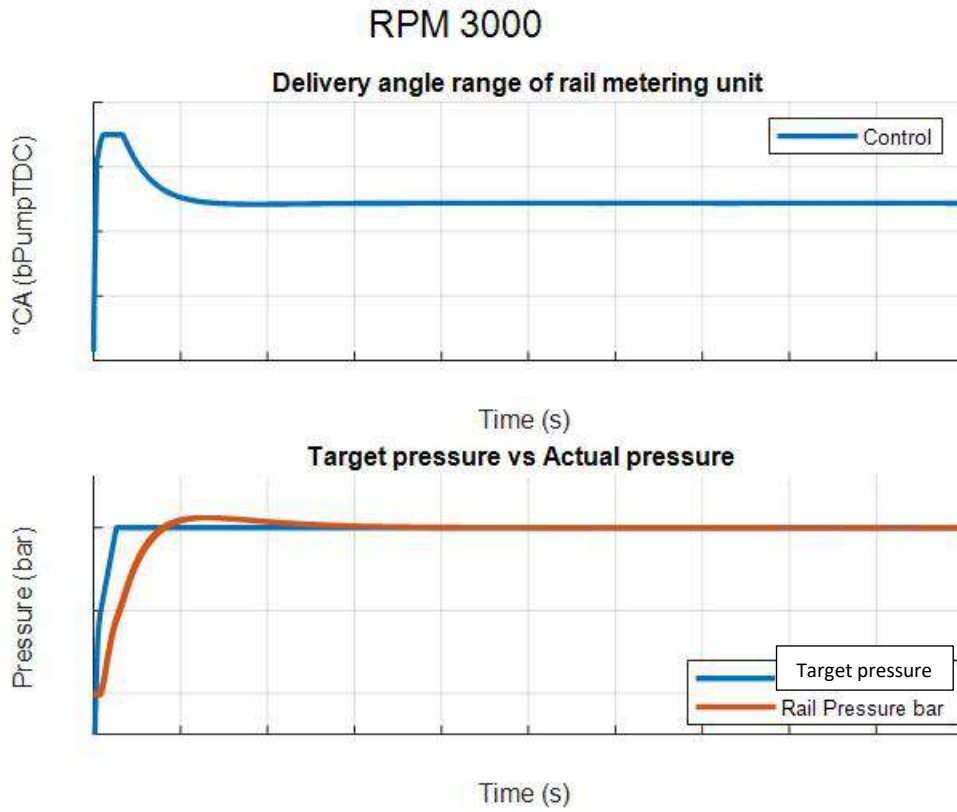


Figure 84 RPM 3000

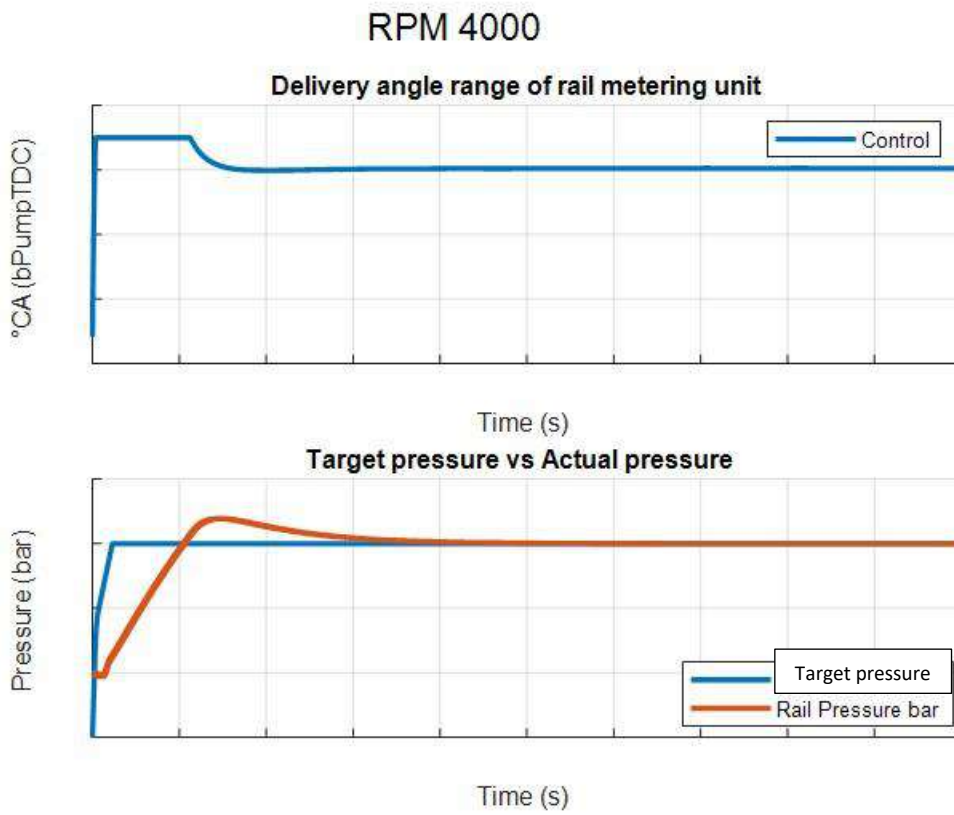


Figure 85 RPM 4000

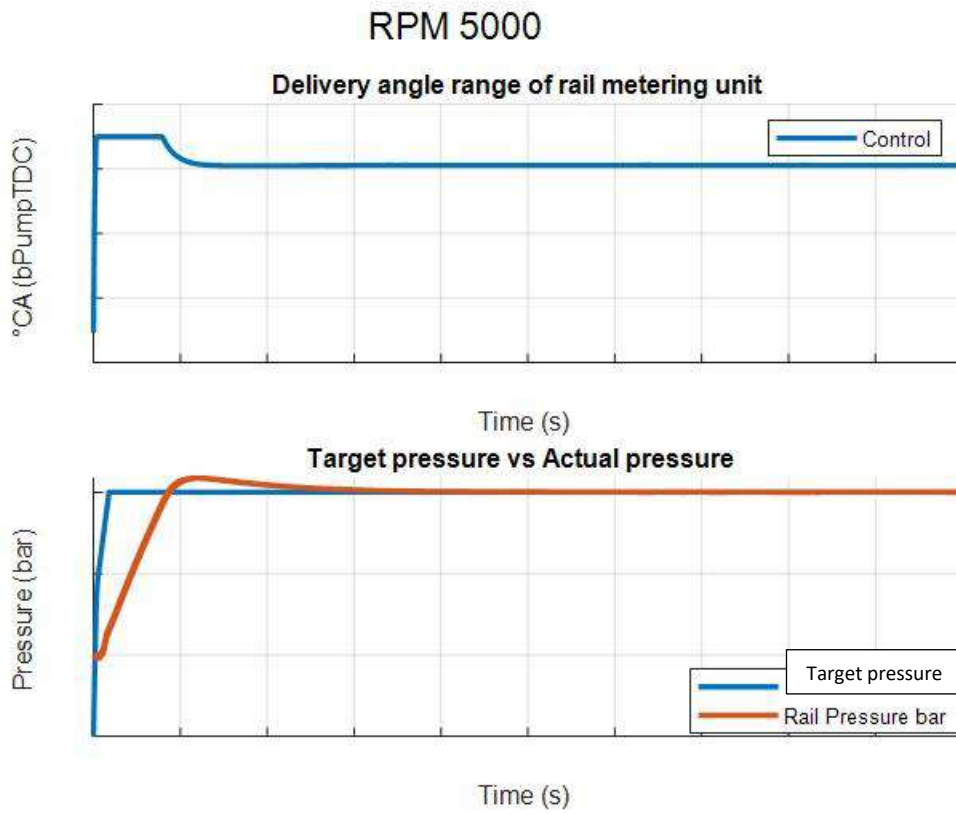


Figure 86 RPM 5000

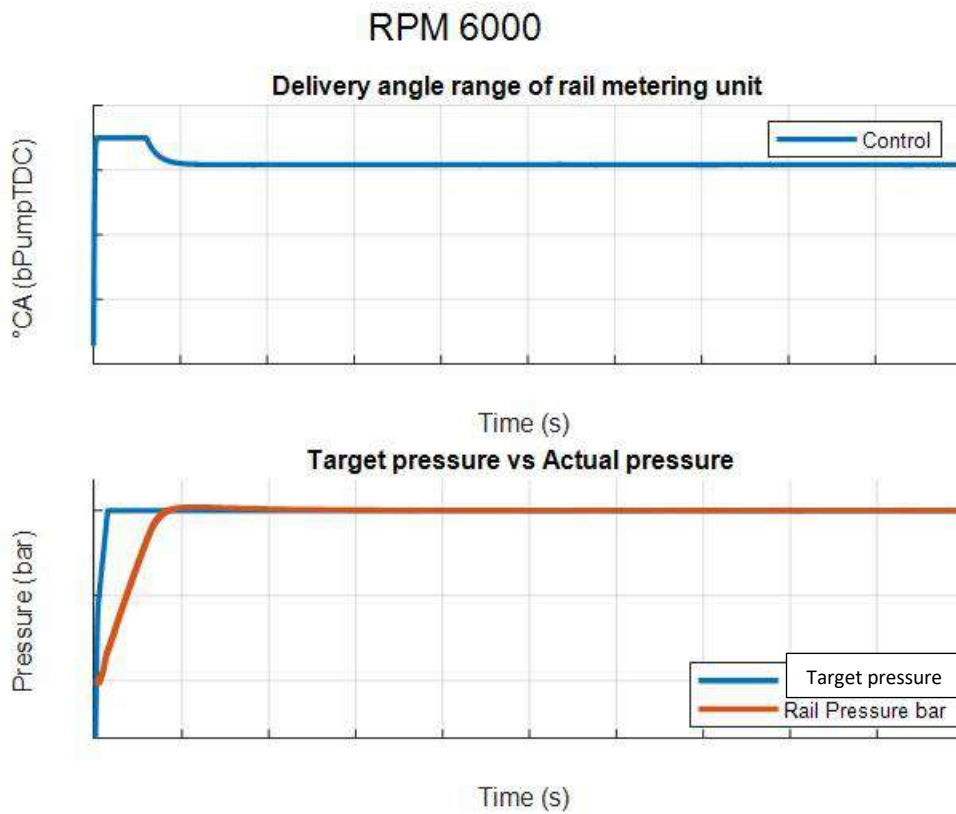


Figure 87 RPM 6000

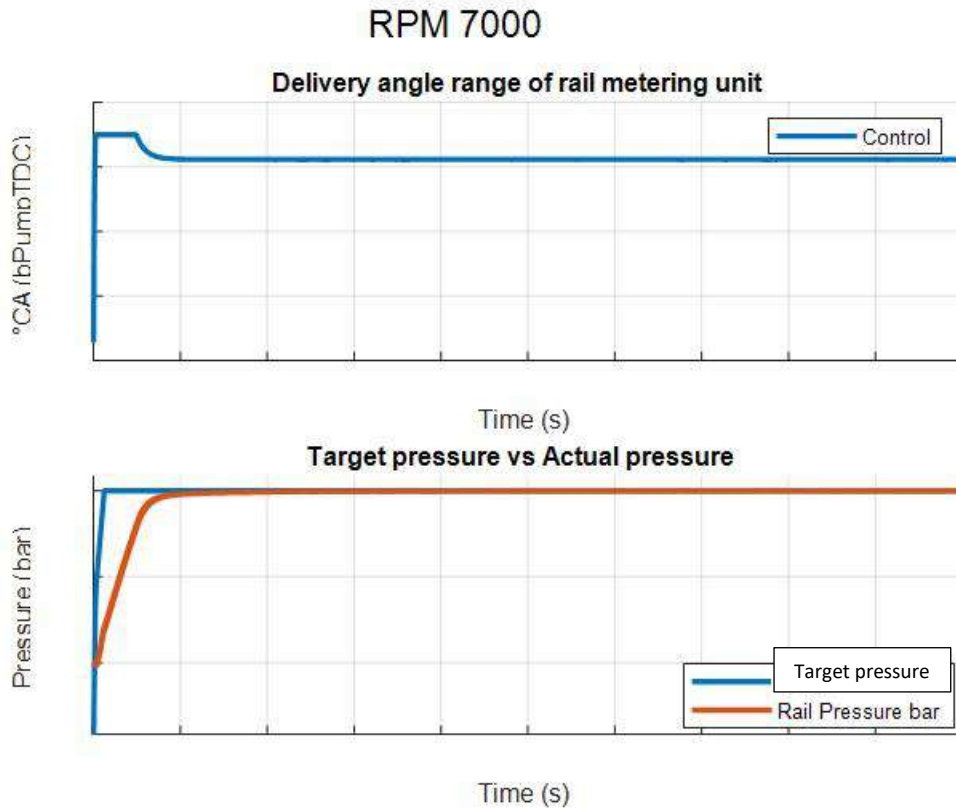


Figure 88 RPM 7000

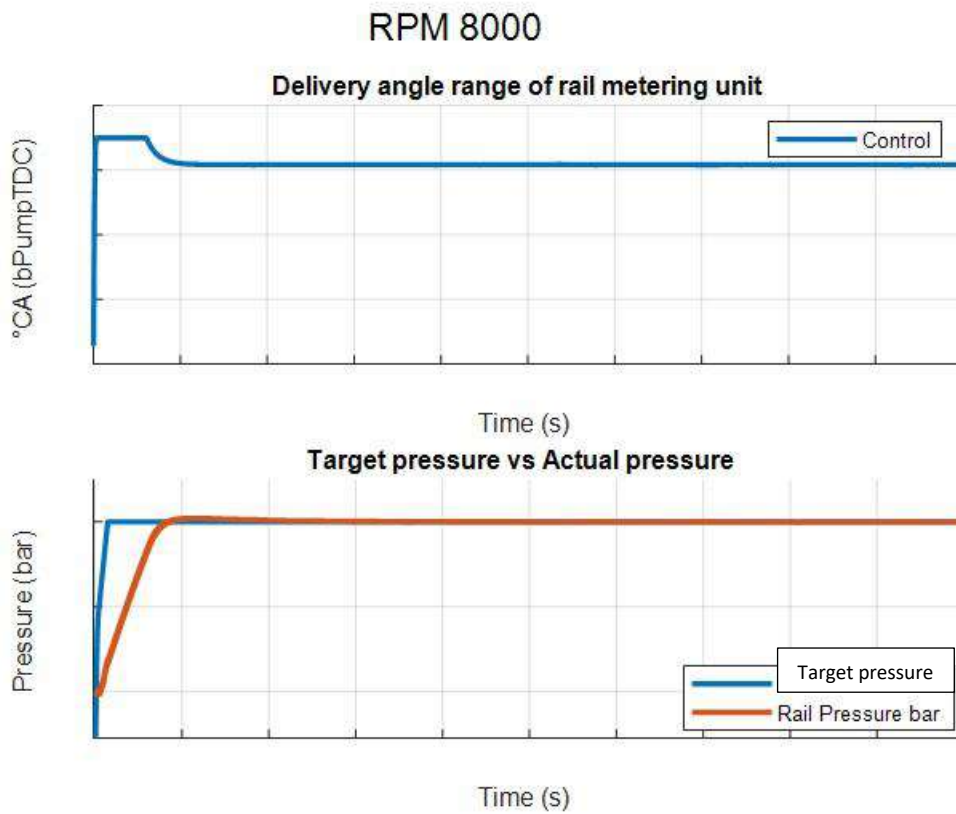


Figure 89 RPM 8000

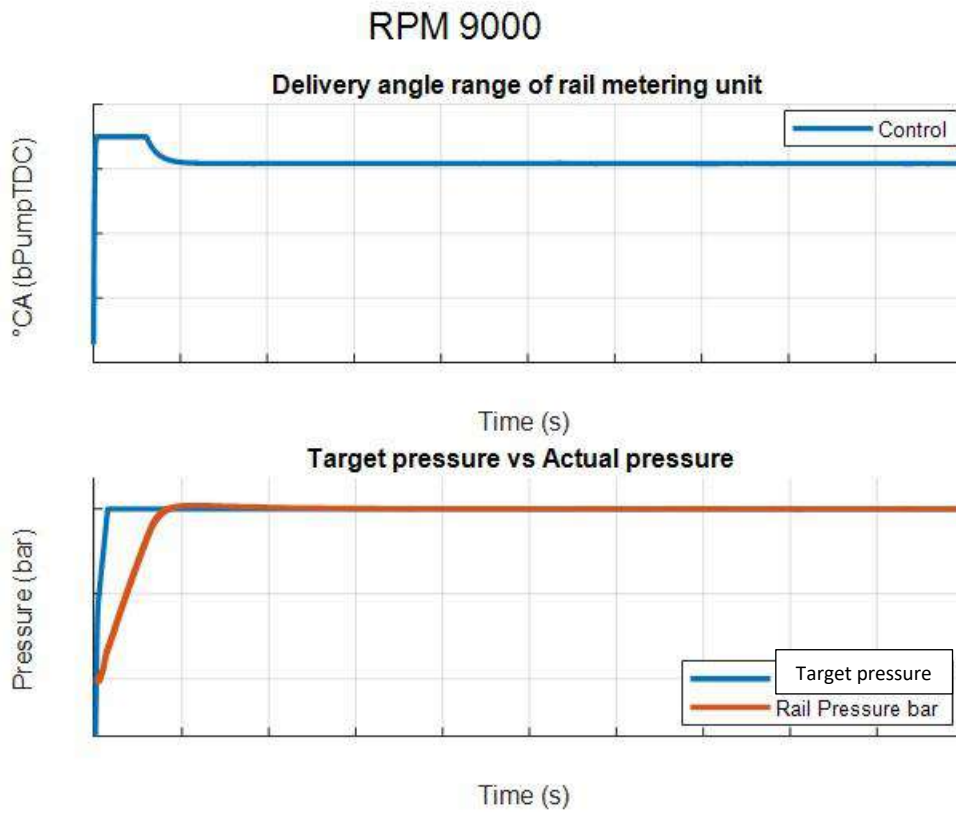


Figure 90 RPM 9000

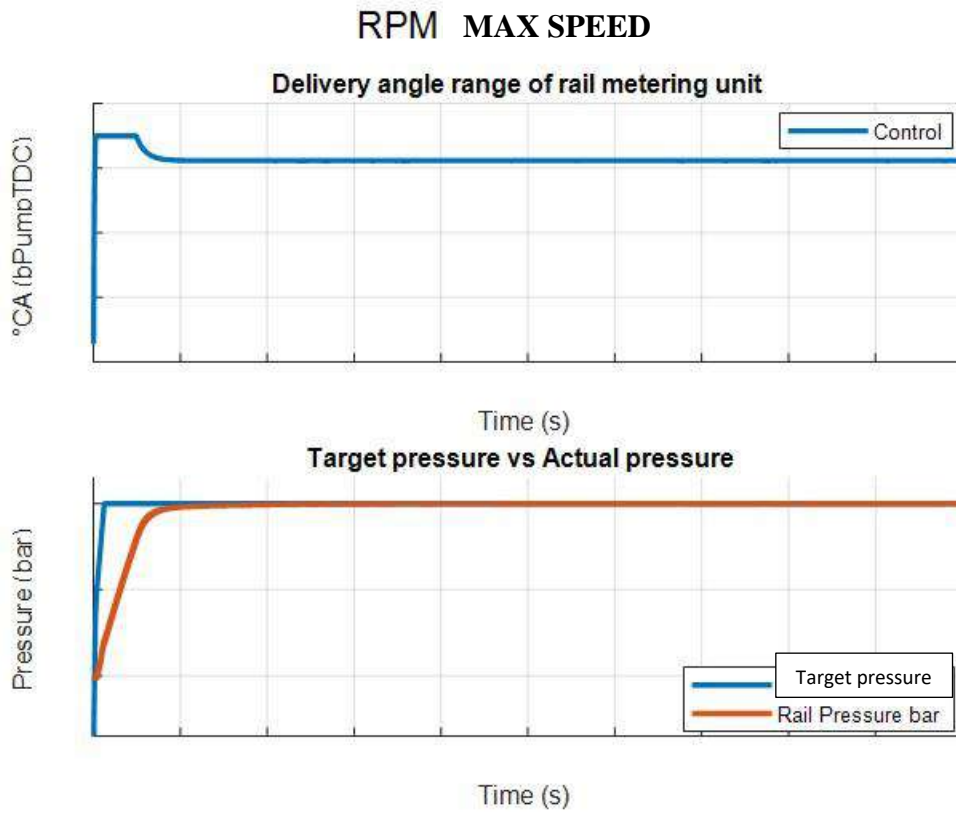


Figure 91 RPM MAX SPEED

6.9 Conclusions

Analysing the graphics it can be noticed that the controller manages in closing well the loop because the actuated pressure goes to the target. However, there are some control issues for speeds going from 1000 to 5000 rpm linked to overshoot. Overshoot is the occurrence of a signal or function exceeding its target.

As regards this problem, it can be fixed modifying the PI proportional and integrative parts making a re-calibration but this is out of the scope of this thesis.

Next goal will be PI optimization.

7

Conclusions

Starting from the set objectives, it is highlighted that:

- the best configuration, *Ref Rail + 20% – Ref Restr – Pipe Long*, has been chosen after an activity of testing and simulations on 8 different configurations taking the one with the minimum CoV;
- GT model has been validated giving a reliable physical model that can be used for testing other points or other configurations not explored;
- co-simulation has been validated giving the possibility to calibrate correctly PI map and it issues that it is necessary a re-calibration in order to avoid overshoot problem.

All the results have been satisfactory.

APPENDIX

MATLAB Scripts

%% Inputs

```
log_name='';  
excel_file_name='Export_ifiles_PQ.xlsx';  
delete(excel_file_name)  
test_ref=readtable('','PQ');  
test_ref(1,:)=[];  
export_inst_labels={'P_RAIL_A','P_RAIL_B','P_HPLINE_A','P_HPLINE_B','P_LPLINE_A'  
, 'P_FUEL_CELLA',...  
'I_INJ_A','I_INJ_B','I_INJ_C','I_INJ_D','I_PUMP',...  
'TDC_Pump','TDC_Cyl',...  
};  
export_avg_labels={'SPEED','FLOW_Cella_AVG',...  
  
'P_RAIL_A_AVG','P_RAIL_B_AVG','P_HPLINE_A_AVG','P_HPLINE_B_AVG','P_LPLI  
NE_A_AVG',...  
  
'P_RAIL_A_MX','P_RAIL_B_MX','P_HPLINE_A_MX','P_HPLINE_B_MX','P_LPLINE_A  
_MX',...  
  
'P_RAIL_A_MN','P_RAIL_B_MN','P_HPLINE_A_MN','P_HPLINE_B_MN','P_LPLINE_A  
_MN',...  
'P_FUEL_CELLA_AVG','T_FUEL_Cella_AVG','T_RAIL_A_AVG',...  
};  
rat= ;  
cycles= ;  
ang_x_ts=1;  
ang_x_length=360;  
%% load ifiles  
list_files=dir([log_name '*']);
```

```

tot_tests={list_files.name};

T_AVG=table;
T_INJ=table;

for c=tot_tests

c=char(c)

ifile=load_ifile(c,1);

test_n=str2double(c(end-2:end));

%% load Instantaneous logs

T=table;

for i =export_inst_labels

eval(['T.' char(i) '=(ifile.' char(i) '.data(:));'])

end

X_Pump=(0:ang_x_ts:height(T)-1);

T=addvars(T,X_Pump,'Before',1);

%% Sync TDC Cyl1 to 0

TDC_Cyl1=T.TDC_Cyl(1:end-0)>0.5;

TDC_GDI=T.TDC_Pump(1+0:end)>0.5;

start_pos=find(and(TDC_Cyl1,TDC_GDI),1,'first')-1;

T.X_Pump=T.X_Pump-start_pos;

T.X_Eng=T.X_Pump/rat;

T=movevars(T,'X_Eng','Before',1);

T_Out=T(T.X_Eng>=0&T.X_Eng<720*cycles,:);

corr_P_RAIL_A=(test_ref.PRail(test_n)+0*test_ref.VolFuelFlow(test_n))/mean(T_Out.P_RAIL_A);
corr_P_HPLINE_A=(test_ref.PRail(test_n)+3*test_ref.VolFuelFlow(test_n))/mean(T_Out.P_HPLINE_A);

```

```
corr_P_HPLINE_B=(test_ref.PRail(test_n)+3*test_ref.VolFuelFlow(test_n))/mean(T_Out.P_HPLINE_B);
```

```
if true
```

```
T_Out.P_RAIL_A=T_Out.P_RAIL_A*corr_P_RAIL_A;
```

```
T_Out.P_HPLINE_A=T_Out.P_HPLINE_A*corr_P_HPLINE_A;
```

```
T_Out.P_HPLINE_B=T_Out.P_HPLINE_B*corr_P_HPLINE_B;
```

```
end
```

```
eval(['TEST' num2str(test_n) '=T_Out;'])
```

```
%save excel
```

```
writetable(T_Out,excel_file_name,'Sheet',['TEST' num2str(test_n)]);
```

```
%% Check Injection Paramaters
```

```
eng_speed=mean(ifile.SPEED.data)/rat;
```

```
SOI_1_pos=find(T_Out.I_INJ_A>0.1,1,'first');
```

```
EOI_1_pos=find(T_Out.I_INJ_A>0.1,1,'last');
```

```
SOI_1=720-T_Out.X_Eng(SOI_1_pos);
```

```
EOI_1=1440-(T_Out.X_Eng(EOI_1_pos)+1);
```

```
ET_deg_1=SOI_1-EOI_1;
```

```
ET_ms_1=ET_deg_1/(eng_speed/60*360)*1000;
```

```
First_pos=find(T_Out.I_INJ_A>0.1,1,'first');
```

```
intervallo=T_Out([(1:First_pos-1)],:);
```

```
intervallo1=T_Out([(First_pos:height(T_Out))],:);
```

```
new_table1=[intervallo1;intervallo];
```

```
pos_active_injector=find(new_table1.I_INJ_A>0.1);
```

```
U=pos_active_injector(1:(numel(pos_active_injector)/2));
```

```
O=pos_active_injector(((numel(pos_active_injector)/2)+1):length(pos_active_injector));
```



```

U_1=new_table1.P_RAIL_A(U);
O_1=new_table1.P_RAIL_A(O);
U_mean=mean(U_1);
O_mean=mean(O_1);
Ptest=100;
Qstat=█;
Injvol1=sqrt(U_mean/Ptest).*Qstat.*(ET_ms_1./1000).*1000;
Injvol2=sqrt(O_mean/Ptest).*Qstat.*(ET_ms_1./1000).*1000;

%% load AVG values

T_AVG.TEST(test_n,:)=test_n;
for a=export_avg_labels
    eval(['T_AVG.' char(a) '(test_n,:)=mean(ifile.' char(a) '.data);'])
end

T_AVG.SOI(test_n,:)=SOI_1;
T_AVG.ET(test_n,:)=ET_ms_1;
T_INJ.INJ11(test_n,:)=Injvol1;
T_INJ.INJ12(test_n,:)=Injvol2;

████████████████████████████████████████████████████████████████████████████████
████████████████████████████████████████████████████████████████████████████████
████████████████████████████████████████████████████████████████████████████████
████████████████████████████████████████████████████████████████████████████████
████████████████████████████████████████████████████████████████████████████████
████████████████████████████████████████████████████████████████████████████████
████████████████████████████████████████████████████████████████████████████████

INJ=table2array(T_INJ);

```

```

std_dev=std(INJ,0,2);
Media=mean(INJ,2);
COV=std_dev./Media;
COV_percentage=COV*100;
T_AVG.COV=COV_percentage;
T_AVG.corr_P_RAIL_A(test_n,:)=corr_P_RAIL_A;
T_AVG.corr_P_HPLINE_A(test_n,:)=corr_P_HPLINE_A;
T_AVG.corr_P_HPLINE_B(test_n,:)=corr_P_HPLINE_B;
end

% clear INST_data

%save excel

writetable(T_AVG,excel_file_name,'Sheet','AVG');

%% AVERAGE AND MAXIMUM COV VALUES CALCULATION

COV_percentage1=rmmissing(COV_percentage);
COV_avg=mean(COV_percentage1);
COV_max=max(COV_percentage);

%winopen(excel_file_name)

%% REGRESSIVE PLOTS

T=readtable('█.xlsx');
T=T(T.TestN>0&T.TestN<=height(T_AVG),:);
k =find(T_AVG.TEST==0);
for i=1:numel(k)
    T.TestN(k(i))=0;

```

```

end

T=T(T.TestN>0.0,:);

Q=T_AVG(T_AVG.TEST>0,:);

%% Inputs

Ptest=100; % bar

Qstat=██████████

Injvol=sqrt((T.PRail)./Ptest).*Qstat.*((T.ET)./1000).*1000;

Volflow=(Injvol/10^6).*(T.EngRPM).*4/2;

%% Plot

% Number of revolutions

x=0:1:██████;

y=0:1:██████;

figure(1)

hold on

grid on

line(x,y)

hold on

plot(T.PumpRPM,Q.SPEED,'o','Color','r')

xlabel('TH Speed')

ylabel('AVG Speed')

title('Comparison between theoretical values of Speed and avg ones')
legend('bisector','comparative values')

% P rail

x=0:1:██████;

y=0:1:██████;

figure(2)

```

```

hold on

grid on

line(x,y)

hold on

plot(T.PRail,Q.P_RAIL_A_AVG,'o','Color','r')

xlabel('Theoretical Prail')

ylabel('AVG Prail')

title ('Comparison between theoretical values of P Rail and avg ones')

legend('bisector','comparative values')

% ET

x=0:1:█;

y=0:1:█;

figure(3)

hold on

grid on

line(x,y)

hold on

plot(T.ET,Q.ET,'o','Color','r')

xlabel('Theoretical ET')

ylabel('AVG ET')

title ('Comparison between theoretical values of ET and avg ones')

legend('bisector','comparative values')

%SOI

x=0:1:█;

y=0:1:█;

```

```

figure(4)

hold on

grid on

line(x,y)

hold on

plot(T.SOI,Q.SOI,'o','Color','r')

xlabel('Theoretical SOI')

ylabel('AVG SOI')

title ('Comparison between theoretical values of SOI and avg ones')

legend('bisector','comparative values')

% Volumetric flow

```

```

x=0:0.5:█;

```

```

y=0:0.5:█;

```

```

figure (5)

```

```

hold on

```

```

grid on

```

```

line(x,y)

```

```

hold on

```

```

plot(Volflow,Q.FLOW_Cella_AVG,'o','Color','r')

```

```

xlabel('Theoretical Volflow')

```

```

ylabel('AVG Volflow')

```

```

title ('Comparison between theoretical values of volumetric flow and avg ones')

```

```

legend('bisector','comparative values')

```

```
%% COV PLOT
```

```
T=readtable('████████████████████.xlsx');
```

```
T=T(T.TestN>0&T.TestN<=height(T_AVG),:);
```

```
k=find(T_AVG.TEST==0);
```

```
for i=1:numel(k)
```

```
T.TestN(k(i))=0;
```

```
end
```

```
T=T(T.TestN>0,:);
```

```
Q=T_AVG(T_AVG.TEST>0,:);
```

```
%% Inputs
```

```
data=(T.EngRPM T.rl COV_percentage1);
```

```
data=double(data);
```

```
data_x=data(:,1);
```

```
x_min=████;
```

```
x_max=████;
```

```
x_incr=████;
```

```
data_y=data(:,2);
```

```
y_min=█;
```

```
y_max=██;
```

```
y_incr=█;
```

```
data_z=data(:,3);
```

```
z_min=██;
```

```
z_max=███;
```

```
z_round=█;
```

```
%% Interpolation
```

```

x=x_min:x_incr:x_max;
y=y_min:y_incr:y_max;
F = scatteredInterpolant(data_x,data_y,data_z);
[X,Y]=meshgrid(x,y);
Z_raw=F(X,Y);
Z=round(min(max(Z_raw,z_min),z_max),z_round);

%% Plots
Z_res=interp2(X,Y,Z,data_x,data_y);
figure
hold on
contourf(X,Y,Z)
plot3(data_x,data_y,data_z,'or')
colorbar
hold off
axis([
caxis([
colormap jet

```

BIBLIOGRAPHY

- Lucio Postrioti, Andrea Cavicchi, Domenico Paolino, Claudio Guido, Marco Parotto, Rita Di Gioia, *An experimental and numerical analysis of pressure pulsation effects of a Gasoline Direct Injection system*;
- N. Cavina, *Appunti del corso di Motori a Combustione Interna e Propulsori Ibridi*, AA 2020-2021;
- G. M. Bianchi, *Appunti del corso di Fluidodinamica dei Motori a Combustione Interna*, AA 2020-2021.

RINGRAZIAMENTI

Vorrei ringraziare i miei genitori, Antonella e Olmer, per avermi dato la possibilità di intraprendere questo percorso e per il meraviglioso supporto dato in tutti questi anni. Mi hanno sempre sostenuto in ogni mia scelta e sono stati fondamentali nel raggiungimento di questo traguardo.

Un grande ringraziamento va al mio ragazzo Oleksandr che ha condiviso una parte del percorso di studi con me e che ha sempre creduto nelle mie capacità.

Ringrazio i miei compagni di Università in particolar modo Federica Gasparini, Daniela Bruno, Luca Lelli, Lorenzo Lovallo, Guido Zaffagnini e Ivan Berardinelli.

Ringrazio il Professore Nicolò Cavina per avermi fatto appassionare alla materia e per avermi seguito con costanza e dedizione per tutto il percorso di tirocinio e tesi.

Ringrazio gli Ingegneri Angelo Camerini, Klajdi Mustafaj e Paolo Scarpatò per avermi affiancato in questi mesi e per avermi insegnato tanto a livello lavorativo.

Ringrazio l'Ingegnere Claudio Forte per avermi guidato giorno dopo giorno e avermi fatto sentire parte della sua squadra sapendomi dare sempre i consigli giusti.

Infine ringrazio me stessa, per non aver mai mollato nonostante la fatica, i momenti di sconforto e le avversità che ci possono essere state e che con determinazione sono riuscita a superare una dopo l'altra. Questo percorso magistrale è stato difficile soprattutto per la situazione che stiamo attualmente vivendo. Nonostante i momenti bui e pesanti sono riuscita a guardare sempre in avanti perseguendo gli obiettivi che mi ero prefissata.